

THE GEOLOGY AND GEOCHEMISTRY OF THE EAST AFRICAN OROGEN IN NORTHEASTERN MOZAMBIQUE

R. BOYD AND Ø. NORDGULEN

Geological Survey of Norway, N-7491 Trondheim, Norway

email: Rognvald.Boyd@ngu.no; Oystein.Nordgulen@ngu.no

R.J. THOMAS

British Geological Survey, Keyworth, United Kingdom

email: bthomas@bgs.ac.uk

B. BINGEN, T. BJERKGÅRD, T. GRENNÉ, I. HENDERSON,

V.A. MELEZHIK, M. OFTEN, J.S. SANDSTAD, A. SOLLI, E. TVETEN

AND G. VIOLA

Geological Survey of Norway, N-7491 Trondheim, Norway

email: Bernard.Bingen@ngu.no; Terje.Bjerkard@ngu.no; Tor.Grenne@ngu.no; Iain.Henderson@ngu.no;

Victor.Melezhik@ngu.no; Morten.Often@ngu.no; Jan.Sandstad@ngu.no; Arne.Solli@ngu.no;

Einar.Tveten@ngu.no; Giulio.Viola@ngu.no

R.M. KEY AND R.A. SMITH

British Geological Survey, Edinburgh, United Kingdom

email: rmk@bgs.ac.uk; ras@bgs.ac.uk

E. GONZALEZ

Institute of Geology & Mineralogy of Spain, Madrid, Spain

email: e.gonzalez@igme.es

L.J. HOLLICK

British Geological Survey, Exeter, United Kingdom

email: lhollick@bgs.ac.uk

J. JACOBS

Department of Earth Sciences, University of Bergen, Norway.

email: joachim.jacobs@geo.uib.no

D. JAMAL

University Eduardo Mondlane, Maputo, Mozambique

email: daud.jamal@uem.mz

G. MOTUZA

Department of Geology & Mineralogy, University of Vilnius, Lithuania

email: Gediminas.Motuza@gf.vu.lt

W. BAUER

Aziana Exploration, Antananarivo, Madagascar

email: bauer.geol@web.de

E. DAUDI, P. FEITIO, V. MANHICA, A. MONIZ AND D. ROSSE

National Directorate of Geology, Maputo, Mozambique

email: edaudi@tvcabo.co.mz

Please provide email address for all authors

© 2010 March Geological Society of South Africa

ABSTRACT

The geology of northeastern Mozambique has been remapped at 1:250 000 scale. Proterozoic rocks, which make up the bulk of the area, form a number of gneiss complexes defined on the basis of their lithologies, metamorphic grade, structures, tectonic relationships and ages. The gneiss complexes, which contain both ortho- and paragneisses, range from Palaeo- to Neoproterozoic in age, and were juxtaposed along tectonic contacts during the late Neoproterozoic to Cambrian Pan-African Orogeny. In this paper we describe the geological evolution of the terranes north of the Lurio Belt, a major tectonic boundary which separates the complexes described in this paper from the Nampula Complex to the south. The Marrupa, Nairoto and Meluco Complexes are dominated by orthogneisses of felsic to intermediate compositions. Granulitic rocks, including charnockites, are present in the Unango, M'Sawize, Xixano and Ocua Complexes (the last forms the centre of the Lurio Belt). The Neoproterozoic Geci and Txitonga Groups are dominated by metasupracrustal rocks at low metamorphic grades and have been tectonically juxtaposed with the Unango Complex. Geochemical data integrate and support a model of terrain assembly in northeast Mozambique, which is largely published and mainly derived from our new geochronological, lithostratigraphic and structural work. This model shows the contrast between the mainly felsic lower tectonostratigraphic levels (Unango, Marrupa, Nairoto and Meluco Complexes) and the significantly more juvenile overlying complexes (Xixano, Muquia, M'Sawize, Lalama and Montepuez Complexes), which were all assembled during the Cambrian Pan-African orogeny. The juxtaposed terranes were stitched by several suites of Cambrian late- to post-tectonic granitoids.

Introduction

Northeast Mozambique offers an important transect across the southern part of the East African Orogen (EAO; Figure 1), from its Palaeoproterozoic basement along the shore of Lake Niassa to the Indian Ocean coastal plain. It lies at a critical junction between the north-south trending "Mozambique Belt" (e.g. Holmes, 1951) and the east-west trending Zambezi-Irumide Belts. The broad geology of this region is known from studies carried out by the Bureau de Recherches Géologiques et Minières (BRGM) in the early 1970s and 1980s (e.g. Jourde and Wolff, 1974). Teams from the former Soviet Union and several Eastern European countries studied selected areas in the 1980s, and a photo-geological survey focussing on mineral resources was carried out by Hunting Geology and Geophysics Ltd (1984). More detailed work in certain parts of the country was carried out by other teams (e.g. Aquater, 1983 a-f; Costa et al., 1983; 1992). The BRGM work included geophysical and geochemical studies of priority mineralised areas and geological mapping which was compiled at 1:250 000 scale. This key work, synthesized by Pinna et al. (1993), which covered the area north of 17°S and east of 34°E, relied on Rb-Sr whole-rock geochronological data and formed the basis for a lithostratigraphic scheme upon which the 1:1 000 000 scale geological map of Mozambique (Pinna and Marteau, 1987) and later syntheses were based (Saachi et al., 1984; Lächelt 1993; Lächelt and Daudi, 1999; Marques et al. 2000, Kröner, 2001; Marques, 2002, Lächelt 2004; Thomas et al., 2006; Grantham et al., 2008). Jamal (2005) reported U-Pb zircon data on a number of units and this study is an important recent contribution to understanding the geology of the eastern part of the area.

A new reconnaissance mapping project aimed at producing 1: 250 000 scale geological maps of the whole of Mozambique was undertaken in the period 2002 to 2007, in cooperation with the National Directorate of Geology of Mozambique (DNG). The ca. 260 000 km²

area of northeast Mozambique delineated in Figure 1 was mapped by the "Norconsult Consortium", a consortium of the Geological Survey of Norway and the British Geological Survey, headed by the Norwegian company Norconsult and aided by the Mozambican engineering company, Eteng Lda.. In addition to geological mapping, the project included structural, geochemical, petrological and geochronological studies, and an inventory of mineral resources. The results were reported in Norconsult Consortium (2007 a; b).

In this paper we summarise the results of this mapping project, focussing on the field, petrographic and whole-rock geochemical data and on contrasts between the resulting findings and earlier interpretations (Pinna et al., 1993). The paper describes the area north of the Lurio Belt – the area immediately to the south, the Nampula Complex, was mapped partly by the Norconsult Consortium and partly by the Council for Geoscience (CGS) of South Africa. Details of the Nampula Complex will be published elsewhere. Here we describe the main lithostratigraphic units recognised and propose a revised tectonostratigraphic model of the crustal architecture of this important segment of the East African Orogen. Geochemical data are presented with the aim of providing an overview of the geochemistry of the crust in northeastern Mozambique. The samples were collected in order to characterize the major and trace element composition of exposed rock units, and not to support process-oriented geochemical research. Structural, geochronological and other thematic data are published elsewhere (Engvik et al., 2007; Melezik et al., 2006; 2008; Viola et al., 2008; Bingen et al., 2009; Bjerksgård et al., 2009). These articles represent an integral part of our study and were fundamental in proposing the model discussed: the reader is referred to those publications for more details. The objective of this paper is thus to summarise the tectonostratigraphic scheme for northeastern Mozambique adopted in the new maps and to discuss this in relation to previous models mainly that of Pinna et al. (1993).

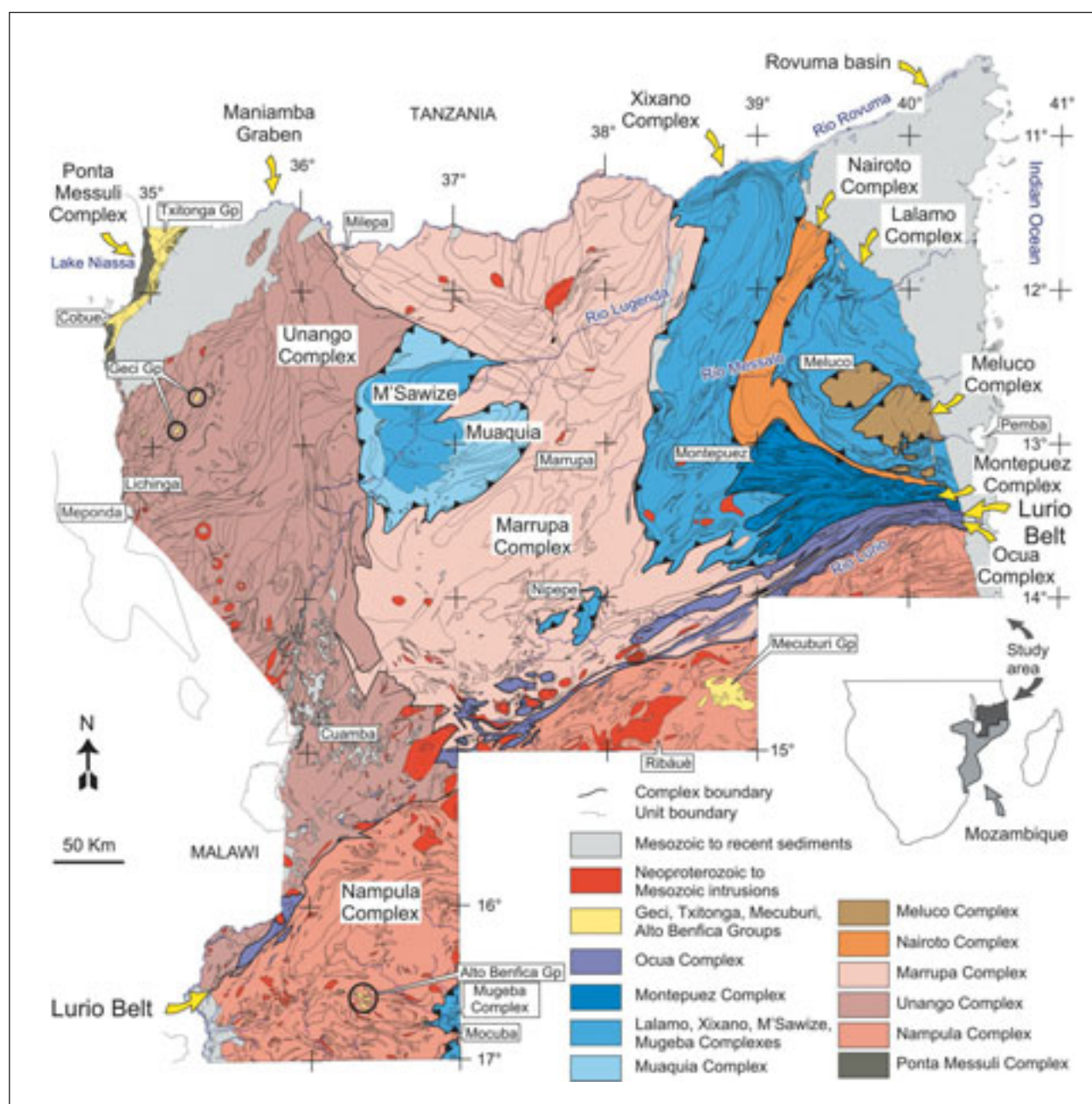


Figure 1. Sketch map of the main geological units in northeast Mozambique based on compilations at 1:250 000 scale. This paper describes the geology of the area north of the Lurio Belt (north of the Nampula Complex). Thick lines mark the boundaries between Complexes and thin lines the boundaries of individual rock units from the 1:250 000 map. The main thrust contact separating the mainly felsic lower tectonostratigraphic complexes (rose colours) from the overlying more juvenile complexes probably formed outboard of the Congo-Tanzania Craton foreland (blue colours) is decorated by saw-teeth.

Geological setting of northeastern Mozambique

The crystalline basement of northeastern Mozambique is overlain by Permo-Jurassic Karoo sedimentary rocks, mainly along the northeasterly to southwesterly trending Maniamba graben in the northwest of the study area, and by Jurassic-Neogene sediments of the Rovuma Basin in the coastal area (Figure 1). The crust exposed between these basins is mainly made up of Precambrian (Palaeo- to Neoproterozoic) to Cambrian high-grade

gneisses and Neoproterozoic to Cambrian intrusive plutonic rocks. It includes a prominent, east-northeasterly to west-southwesterly trending Pan-African shear zone, known as the Lurio Belt (Figure 1). The 25 to 30 km wide, north-northwesterly dipping Lurio Belt extends over 600 km across the study area. It is expressed by a strong zone of flattening in the east, which grades laterally into a complex zone of anastomosing shear zones and folds towards the southwest (Viola et al., 2008).

Table 1. Lithostratigraphy of the Unango Complex. Bold font indicates the dominant component in a compositional range.

UNANGO COMPLEX LITHOSTRATIGRAPHY			
INTRUSIVE ORTHOGNEISSES			
Unit	Compositional range	Mineralogy	Notes
Ultramafic rocks	Serpentinised peridotite, pyroxenite, metagabbro	Olivine (serpentine)-cpx-opx ± plagioclase	Small pods and lenses, especially along Unango-Nampula Complex boundary
Biotite-hornblende orthogneiss, metagabbro (Meponda Gneiss) (Figure 2a)	Gabbro-granodiorite-granite	Quartz-2 feldspars-hbl-biotite	Highly deformed, foliated to banded, partly migmatitic
Metagabbro	Gabbro	Cpx-opx-plagioclase ± biotite ± quartz ± titanite	Foliated, but ophitic texture preserved
Partly migmatitic charnockitic orthogneiss	Charnockite	Quartz-2 feldspars-hbl ± opx ± garnet	Strong gneissosity, with mafic schlieren
Syenitic orthogneiss	Syenite	Kspar-plagioclase-biotite-magnetite ± quartz ±	Possible igneous layering present
Feldspar-phryric charnockitic orthogneiss (Figure 2d)	Monzogranite	Quartz-K-spar (phenocrysts)-plagioclase-hbl ± opx ± garnet	Opx only as relicts, rimmed by biotite, hornblende and garnet-plagioclase
Granodiorite orthogneiss (Chiconono orthogneiss) (Figure 2c)	Monzodiorite- granodiorite - monzogranite	Quartz-2 feldspars-biotite ± hbl ± rare garnet ± magnetite (+ pyroxene in charnockite)	Retrogressed to greenschist. Intrusions polyphase, coeval
Enderbite to charnockitic granofels (Lichinga Gneiss) (Figure 2b)	Enderbite -mangerite- charnockite	Quartz-2 feldspars-opx-cpx-biotite ± magnetite (+ pyroxene in charnockite)	Equigranular, locally migmatitic
Granitic to granodioritic migmatitic orthogneiss	Quartz diorite -granodiorite - granite	Quartz-2 feldspars-biotite ± hbl ± garnet ± ilmenite ± titanite	Very heterogeneous, migmatitic, relict granulite facies assemblages
Granitic to granodioritic orthogneiss	Diorite- granodiorite -granite-syenite-charnockite	Quartz-2 feldspars-biotite ± hbl ± garnet ± magnetite (+ pyroxene in charnockite)	Major belts, locally augen gneiss, mylonitic and/or migmatitic, pyroxene pegmatite phase seen
OLDER SUPRACRUSTAL ROCKS			
Unit	Minor lithologies	Mineralogy	Notes
Quartzite		Quartz-muscovite ± kyanite	Minor lithology - may represent paleoregolith
Quartz-feldspar gneiss, quartzite	Magnetite quartzite	Quartz (up tp 75%) + feldspar ± magnetite porphyroblasts	Clear paragneiss sequence, granulite facies textures
Biotite gneiss, partly mylonitic		Quartz-plagioclase-biotite ± garnet	Bands up to 10km wide, locally migmatitic
Banded migmatite gneiss	Calc-silicate gneiss, mafic granulite	Quartz-feldspar-biotite-hbl ± 2 px ± garnet ± magnetite	Granulite facies, locally migmatitic. Occurs as pods and lenses
Hornblende gneiss		Quartz-feldspar-hbl (epidote) -biotite	Amphibolite grade retrogressed to greenschist
Banded mafic granulitic gneiss	Felsic gneiss, quartzite	Garnet-hbl-biotite ± pyroxene± graphite	Granulite vestiges in amphibolite

Nomenclature and analytical methods

The new mapping, supported by geophysical data and U-Pb zircon geochronology, required the development of a new tectonostratigraphic scheme in northeastern Mozambique, because the available nomenclature proposed by Pinna et al. (1993) suffers from two main fundamental shortcomings:

1. It makes extensive use of the lithostratigraphic terms “Group” and “Supergroup” for rocks that are not only strongly deformed and subject to high-grade metamorphism, but also of mixed, igneous and metasedimentary parentage;
2. The lithotectonic units as defined in Pinna et al. (1993), cross the Lurio Belt, which is now regarded as a first-order tectonic zone (terrane boundary) (Viola et al., 2008). In addition, the distribution, correlation and geographic extent of many of units recognized by Pinna et al. (1993) have been substantially revised during the current survey.

In this work, the Proterozoic rocks are divided, instead of groups and supergroups, into a number of gneiss “complexes” on the basis of lithostratigraphy, metamorphic grade, structure, tectonic relationships and age (Figure 1). The terminology employed is based on the definitions contained in *The Mozambique Code of Stratigraphic Terminology and Nomenclature* (Direcção Nacional de Geologia, 2001). The complex metamorphic and structural development of most of the regional-scale geological units in the area described, necessitates the use of the lithodemic terms “suite” and “complex” rather than standard lithostratigraphic terms such as “group” as no “relationship to the original stratification” is preserved. The term “Complex” is defined as follows: “...characterized by structural complexity and/or lithological diversity.” All the regional-scale high-grade basement units lying tectonostratigraphically below the exposed Neoproterozoic metasedimentary sequences (Txitonga and Geci Groups) conform to this definition. The complexes are the equivalent of “terranes” in a tectonostratigraphic sense. In the following sections, the complexes are described in order of observed ascending tectonostratigraphic level and age.

Grenvillian-aged orogenic events, straddling the boundary between the Mesoproterozoic and Neoproterozoic, are referred to as “Kibaran”, “Irumide/Irumidian” and “Namaquan” in various parts of Africa. In Mozambique, the terms “Mozambican” (Pinna et al., 1993) or “Lurian” Orogeny (Jourde and Wolff, 1974) have been used to cover this orogenic cycle. These two terms are abandoned here as the metamorphism in the “Mozambique Belt” and “Lurio Belt” can be demonstrated to be mainly late-Neoproterozoic to Cambrian (e.g. Bingen et al., 2009). The Irumide/Irumidian orogeny, well described in the Irumide Belt of Zambia along the margin of the Congo-Tanzania Craton (DeWaele et al., 2006), is the most appropriate name to refer to Grenvillian-aged orogenic events in northeastern Mozambique. Subsequent to

Mesoproterozoic events, the “Pan-African” orogeny is a broad term to describe the protracted Neoproterozoic to Cambrian orogeny in Africa. High-grade metamorphism attributed to this orogeny in eastern and southern Africa ranges from ca. 800 to 470 Ma (compilation in Meert, 2003). Three main frequency maxima of tectonic activity are apparent in the data, at ca. 760 to 730 Ma, 660 to 610 Ma and 570 to 530 Ma, respectively. The third of these events is referred to as the “Kuunga orogeny” by Meert (2003).

Whole-rock geochemical analyses are reported in this publication. They are tabulated in Appendix 1 (or data repository attached to this article). Representative samples of the main magmatic suites and orthogneiss units of all mapped complexes were selected. They were analysed for major and trace elements using standard XRF techniques at the Geological Survey of Norway, Trondheim. Analyses were completed on a Philips X-ray Spectrometer PW 1480 with a Rh X-ray tube. Determination of major elements is performed on samples fused with $\text{Li}_2\text{B}_4\text{O}_7$ to glass beads, and trace elements on pressed pellets.

Since the 1970s, around 20 different classification schemes have been proposed for granitoids (see review in Barbarin, 1990), but no genetic scheme has gained universal acceptance. This reflects the hidden complexity resulting from a number of processes that can generate granitic magmas, resulting in their apparently simple mineral assemblages (e.g. see Introduction in Frost et al., 2001).

To describe the geochemistry of the magmatic rocks in the study area, we combine the use of the genetic S-I-M-A-system with the basically non-genetic and non-tectonic classification proposed by Frost et al. (2001). Although the original concepts of S- and I-types are no longer valid, the terms are still commonly in use, and convey, in a simple manner, the overall geochemical properties of the rocks. The classification of Frost et al. (2001) is useful in the sense that it reflects the major chemical features relevant to granite mineralogy: silica, Fe-number ($\text{FeO}^{\text{tot}}/(\text{FeO}^{\text{tot}} + \text{MgO})$), the modified alkalime index MALI ($\text{Na}_2\text{O} + \text{K}_2\text{O} - \text{CaO}$) and Alumina Saturation Index ASI.

Palaeoproterozoic foreland: Ponta Messuli Complex

The Ponta Messuli Complex, which forms a small part of the foreland to the East African Orogen, is exposed along the shores of Lake Niassa, northwest of the Maniamba graben (Figure 1). It consists of partly migmatitic amphibolite- to granulite-facies orthogneiss, with minor amphibolite. It has been shown to be the oldest unit in northeastern Mozambique, giving a Palaeoproterozoic metamorphic age of 1950 ± 15 Ma, and characterized by the presence of detrital zircons older than 2074 ± 11 Ma (Bingen et al., 2009). Sm/Nd model ages indicate that Archaean material was involved in the formation of the complex (Saranga et al., DNG manuscript). The Ponta Messuli Complex is only weakly affected by Neoproterozoic-Cambrian (Pan-African)

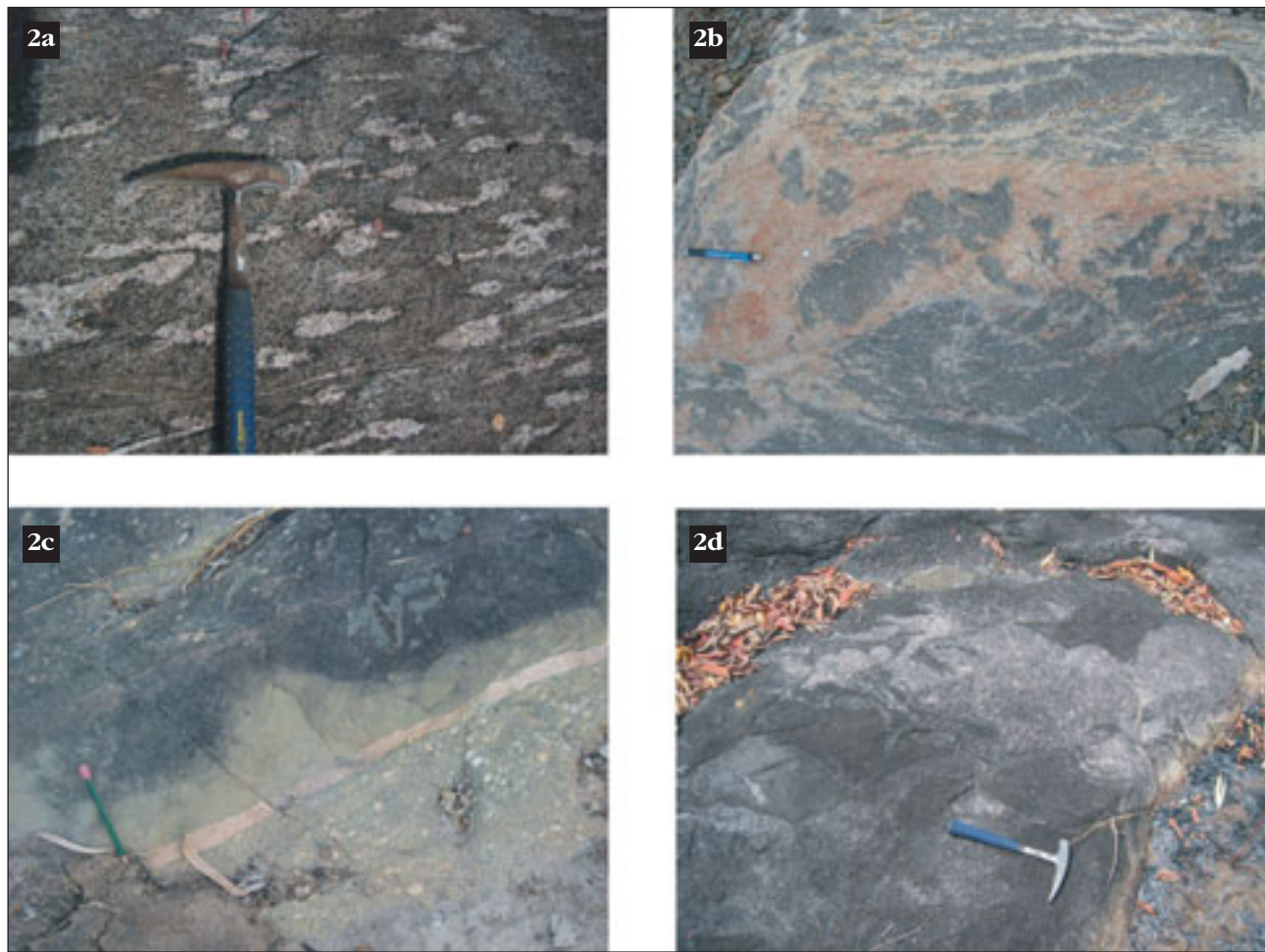


Figure 2. Unango Complex lithologies: (a) Patchy leucosomes in biotite-hornblende gneiss. (UTM 36S 737573, 8509000); (b) Migmatitic, enderbitic gneiss. Note early migmatitic banding (mesosome) truncated by later neosome. In quarry on road from Lichinga to Unango (UTM 36S, 738603, 8551456); (c) Composite monzogranitic (pink) and quartz monzodioritic (fine-grained greenish) dyke in porphyritic granodiorite. (UTM 36S 798033, 8573363); (d) Magma mingling of monzo-granite (light grey) and quartz monzo-diorite (dark grey). Monzogranite north-northwest of the Chiconono granodiorite. (UTM 36S 791805, 8655799).

metamorphism (Norconsult, 2007a; Viola et al., 2008). It is interpreted as a part of the Palaeoproterozoic foreland of the Pan-African East African Orogen (as shown, i.a. by Burke et al., 2003).

Mesoproterozoic Unango Complex

The Unango Complex forms most of the western part of Niassa Province and corresponds largely to the “Unango Group” of Pinna et al. (1993). It is exposed to the southeast of the Maniamba graben, and extends between the Tanzanian and Malawian borders (Figure 1). In the east, the Unango Complex is overthrust by the Marrupa Complex from the east and is overlain by a nappe sheet consisting of the Muaquia and M’Sawize Complexes (Figure 1). In the south, the Unango Complex is juxtaposed against the Nampula Complex along the Lurio Belt. The contact consists of a plexus of very poorly exposed, steep, east-northeasterly trending, anastomosing, shear zones of as yet unresolved kinematics, which is clearly seen on high-resolution aeromagnetic images.

The complex is dominated by intermediate to felsic orthogneiss, partly at granulite grade and partly to completely retrogressed. Migmatisation of variable character is extensive. High-grade paragneisses locally predominate in the west, along the border with Malawi. The relative age relationship between the orthogneiss and supracrustal rocks cannot be established from field observations as many of the units in the complex are bounded by anastomosing shear zones.

Supracrustal gneisses (including paragneisses) in the Unango Complex

The Unango Complex includes isolated pods, lenses and bands of supracrustal gneiss of varied composition, typically enclosed within the voluminous intrusive orthogneiss. They include silicic rocks with undoubtedly sedimentary protoliths and various intermediate to basic layered gneisses of more debatable origin, which may have a mixed volcano-sedimentary parentage. Many gneisses of the latter type show granulite-facies assemblages. The most significant units which

were mapped at 1: 250 000 scale are outlined in Table 1.

Rocks with clear sedimentary protoliths include "semipelitic" gneisses and migmatites, composed of interbanded felsic, garnetiferous biotite gneisses and sparse quartzites with darker hornblende gneisses, locally with graphite, outcropping, for example south of Lichinga, and called the Chala gneiss (e.g. Bloomfield et al. 1966; Andreoli 1984; Kröner et al. 2001). Other sequences contain rare bands of calc-silicate gneiss. Some quartzitic paragneiss units contain euhedral porphyroblasts of magnetite up to 1 cm in diameter. These rocks contain up to 75% quartz + K-feldspar in an equilibrium texture, testifying to a quartz-arenite parentage (magnetite-quartzite). Minor muscovite-kyanite quartzites are also recorded near Lichinga.

Vestiges of typical granulite-facies characteristics such as dark feldspar and a clotted distribution of mafic minerals (e.g. McGregor and Friend, 1997) are found, testifying to the generally comparatively anhydrous nature of the Unango Complex. This is borne out by the presence of higher grade, granulite-facies assemblages within the supracrustal units, including mafic gneisses commonly containing orthopyroxene ± clinopyroxene and felsic gneisses, also containing orthopyroxene. Migmatisation is variable, but locally intense, manifested as layer-parallel, stromatic leucosomes and several generations of crosscutting leucocratic veins. More diffuse nebulitic migmatites also occur, along with agmatites containing angular blocks of palaeosome in lower strain zones and rocks with a high degree of anatexis, resulting in diatexitic gneisses. Between the northern and southern parts of the Unango Complex there is a wedge of partly migmatitic biotite-hornblende gneiss (*Meponda Gneiss*) (Figure 2a), cut by anastomosing shear zones, within some of which thin lenses of ultramafic rock and of quartzite can be found.

Orthogneisses in the Unango Complex

Many of the orthogneiss suites of the Unango Complex are charnockitic (*sensu lato*). For example, the *Lichinga Gneiss* is an enderbitic to charnockitic granofels, which is partly migmatitic and which forms a major component in the complex north of Lichinga. The enderbites are typically homogeneous, equigranular rocks with a polygonal texture, composed of clinopyroxene, orthopyroxene, plagioclase and hornblende, with quartz that is locally blue in colour: their composition is, in general, monzodioritic. Rocks with a higher content of K-feldspar can be classified as mangerite (orthopyroxene-bearing monzonite) and, with higher quartz, charnockite (orthopyroxene-bearing granite). Red (high-Ti) biotite is always present, usually as a minor component and magnetite is the typical accessory phase. Retrogression and low-temperature deformation features occur locally. Natural outcrops tend to appear fairly homogeneous, but quarries show great heterogeneity, often with a high degree of migmatisation, with different

types and phases of migmatite, including agmatites, (Figure 2b).

Some units (e.g. *charnockitic gneiss, feldspar-phyric*) are charnockites *sensu stricto*, with hornblende-biotite monzogranite composition and porphyroblastic with twinned K-feldspar augen and megacrysts up to 5 cm in size. Mafic mineral aggregates form clots including relict, altered orthopyroxene. In the Cuamba area, partly migmatitic charnockitic gneisses are equigranular and have a prominent gneissosity on a scale of 0.1 to 10 cm, with mafic seams as well as quartz-feldspar- and quartz-rich bands.

The *Chiconono Gneiss*, a feldspar-phyric granodioritic to monzonitic orthogneiss (Figure 2c), differs from the units described above, in showing a mineral paragenesis indicating greenschist facies over large areas. This unit shows a polyphase character with internal relationships including: (a) monzogranite xenoliths and veins and (b) composite monzogranitic and more mafic dykes, without chilled margins, in the granodiorite (Figure 2d). These age relationships imply that the various components of the igneous complex were emplaced broadly at the same time. Typical granitic to granodioritic gneisses occur south of Metangula and north of Lichinga, with augen gneisses developed in high-strain zones (e.g. in the Milanje area).

The monzogranitic orthogneisses are quartz-feldspathic, biotite-bearing and locally show iron mineralisation. Migmatisation is widespread, locally in two episodes, one pre- or syn-foliation and one post-foliation. Magnetite is common, in some localities in coarse pegmatite veins. These rocks are widely distributed throughout the Unango Complex, being also present farther south, in the Insaca-Guruè area, where charnockitic facies are also developed (characterized by white-weathering plagioclase mesocrysts up to 1 cm long on weathered surfaces). Foliation is invariably strong and locally proto-myloitic, with ribbon quartz. Granular to layered mafic enclaves and schlieren containing biotite, hornblende and locally pyroxenes are common.

Table 2. Geochemical compositional ranges for the main lithological groups in the Unango Complex.

Unango Complex				
main rock types	SiO ₂	K ₂ O	Mg#	N
Granite	65.9 – 78.4	3.0 – 6.2	0.01 – 0.30	39
Granodiorite	60.4 – 70.3	1.6 – 5.1	0.15 – 0.50	24
Syenite, quartz				
syenite	56.7 – 66.3	4.4 – 8.2	0.03 – 0.35	11
Monzodiorite,				
monzonite,				
q-monzonite	47.6 – 59.9	1.4 – 7.7	0.07 – 0.49	30
Gabbro, diorite,				
quartz-diorite	41.5 – 58.9	0.2 – 2.3	0.41 – 0.73	13
Amphibolite	43.1 – 46.3	0.8 – 1.0	0.46 – 0.51	3
Dykes	49.1 – 63.4	2.2 – 3.9	0.02 – 0.46	4

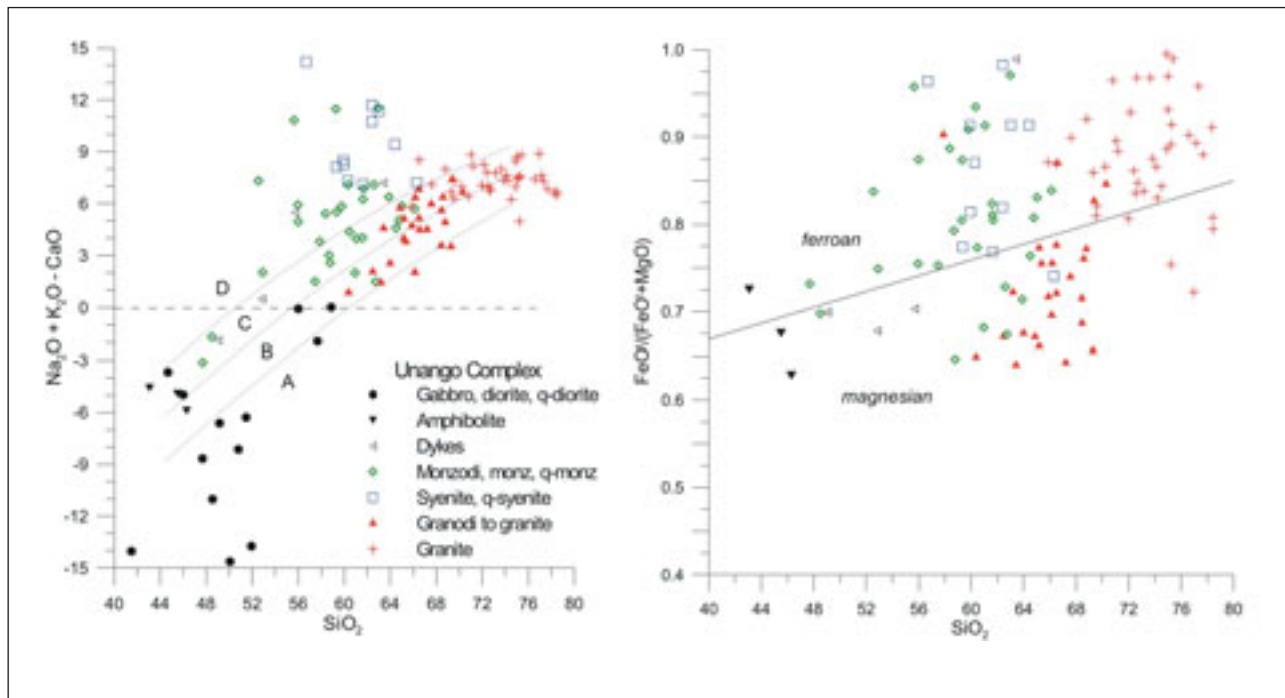


Figure 3. Modified alkali-lime index (left) plotted against SiO_2 (weight %) for rocks of the Unango Complex. The lines subdivide between calcic (**A**), calc-alkaline (**B**), alkali-calcic (**C**) and shoshonitic (**D**) rocks. Classification diagram (right) showing the subdivision of the rocks in magnesian (below) and ferroan (above). Granodioritic and more mafic rocks plot almost entirely to the magnesian field. A large proportion of monzonitic and syenitic rocks are ferroan. Diagrams from Frost et al. (2001)

Pale-weathering albite syenite orthogneisses form a small lithological unit north of Lago Ciuta on the border with Malawi. The rocks are mostly medium to coarse-grained and banded, composed of interlocking granofelsic feldspar with minor mafic minerals, biotite and magnetite. The syenite contains thin mafic layers with dark pyroxene-rich layers up to several dm thick, intercalated with feldspathic bands, which range in thickness from 1 cm to 1 m. The mafic layers occur in groups, locally showing discordances, which possibly represent primary igneous layering.

The *Meponda Gneiss* is biotite-hornblende gneiss, which occupies a large area around Meponda. These rocks are generally highly deformed, foliated, folded and banded, with variations in the content of mafic and felsic minerals, defining the layering from cm to tens of metres in scale. Extensive horizons of metagabbro/mafic gneiss are present in the biotite gneiss, along with lenses and layers of granitic to granodioritic orthogneiss within this unit.

The Unango Complex contains minor bodies of mafic to ultramafic rock with igneous protoliths. Metagabbro is found west and northwest of the main road from Lichinga to Meponda. These rocks are typically fine- to medium-grained, with a weak foliation along the contacts with surrounding charnockitic gneisses, and with original ophitic textures commonly preserved. The rocks consist of clinopyroxene, orthopyroxene and plagioclase as major components, locally with amphibole in porphyroblasts up to 1 to 2 cm

long, with accessory biotite, quartz, K-feldspar and titanite. Such rocks also occur as small, deformed pods and lenses in the southernmost part of the Unango

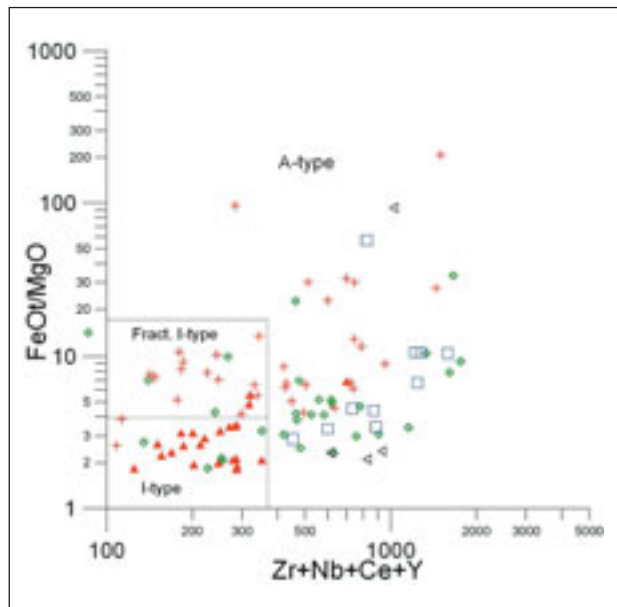


Figure 4. Total FeO/MgO vs $\text{Zr} + \text{Nb} + \text{Ce} + \text{Y}$ (ppm), Unango Complex. Legend as in Figure 3. Granodiorites are classified as I-type rocks, whereas granites plot as fractionated I-type and A-type. Monzonitic rocks are mainly A-type. Syenitic rocks and acid dykes are uniformly A-type. Diagram from Whalen et al. (1987).

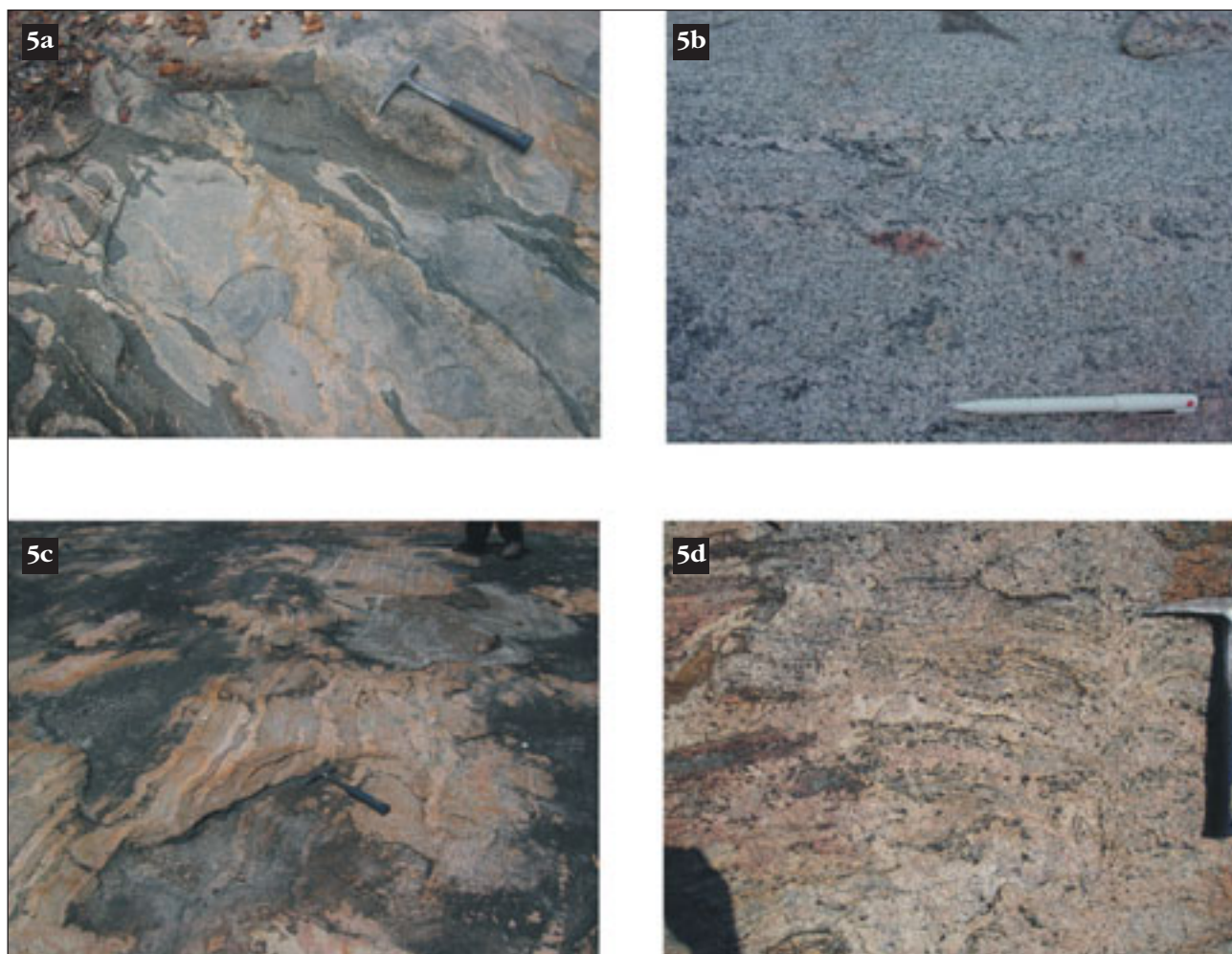


Figure 5. *Marrupa Complex lithologies:* (a) Migmatitic grey gneisses with disrupted mafic bands as well as two neosome phases. (UTM 37S, 267147 8362019); (b) Homogeneous facies of leucocratic hornblende-bearing granitic orthogneiss. Note heterogranular nature and characteristic dark speckled hornblende. (UTM 37S 326698 8383148). (c) Migmatitic, biotite-bearing, granodioritic gneiss with cm-dm thick leucocratic quartz-feldspar leucosomes. (UTM 37S 363766 8568146); (d) Amphibole-bearing diatexite. Note the very high proportion of diffuse, coarse-grained granitic leucosome (black spots are amphiboles), and darker palaeosome remnants of biotite-hornblende. (UTM 37S 331968 8431497).

Complex close to the border with Malawi. These are mainly coarse-grained, dark-grey metagabbros, though the status of some of the more banded amphibolites with which they are commonly associated is less certain.

In addition to metagabbros, ultramafic lenses are found, usually clearly associated with shear zones. Small lenses occur in major shear zones south and east of Lichinga, while more varied lithologies, in most cases also clearly linked to shear zones, are found to the south, in the region of the Lurio Belt (Nampula-Unango Complex boundary) which is marked by a series of northeasterly trending anastomosing shear zones. The westernmost of these, entirely within the Unango Complex in the Milanje area, is associated with a line of poorly exposed tectonic pods and slivers of ultramafic-mafic rocks made up of a mixed assemblage of serpentinised peridotite and pyroxenite with subordinate melagabbro.

Orthogneisses from the Unango Complex yielded U-Pb zircon intrusion ages between 1062 ± 13 and 949 ± 11 Ma (Bingen et al., 2009). The northwestern part of the Unango Complex is dominated by charnockitic to enderbitic rocks with variably retrogressed granulite-facies paragneisses. U-Pb data on zircon rims demonstrate that this metamorphism has an average age of 955 ± 9 Ma (Bingen et al., 2009). Some shear-bounded slices of granitic to granodioritic orthogneiss in the northeastern parts of the complex appear not to have exceeded amphibolite grade. They are typically strongly migmatised, suggesting high volatile activity. The area south of Lichinga is dominated by migmatised felsic to intermediate orthogneisses with a less obvious granulite-facies prehistory. U-Pb data on zircon and monazite indicate that the Pan-African metamorphic overprint, dated between 569 ± 9 and 527 ± 8 Ma (Bingen et al., 2009), becomes dominant in the area south of Lichinga.

Table 3: Lithostratigraphy of the Marrupa Complex. Bold font indicates the dominant component in a compositional range.

MARRUPA COMPLEX LITHOSTRATIGRAPHY				
INTRUSIVE ORTHOGNEISES				
Unit	Compositional range	Mineralogy		Notes
Alkali Syenite (Matondawela)	Syenite	K- Na feldspars- \pm serperine-magnetite-andradite \pm nepheline \pm titanite \pm zircon		Enriched in Nb, Zr
Syenite)		Quartz-2 feldspars \pm biotite		
Mylonitic granite	Granite			Occurs in major shear zones on contacts with Unango and Muquia Complexes
Serpentinine				Two lenses up to 20m thick + loose boulders; fragments of a larger complex.
Granitic banded orthogneiss				Variable migmatization.
Quartz-feldspar-hornblende migmatic gneiss (Figure 5b)	Tonalite- granodiorite -granite	Quartz-2 feldspars-biotite \pm hbl \pm garnet \pm magnetite		Strongly folded, commonly moderately migmatised locally banded
Amphibole-bearing granite diatexite (Figure 5d)	Tonalite- granodiorite- granite	Quartz-2 feldspars-biotite \pm hbl \pm magnetite		>50% granitic leucosome, containing pods and schlieren of mafic palacosome
Granodioritic banded migmatic orthogneiss (Figure 5c)	Tonalite- granodiorite -granite	Quartz-2 feldspars-biotite \pm hbl \pm magnetite		Cm-dm-scale banding due to early phase of migmatization. Local augen texture.
Tonalitic banded migmatic orthogneiss	Tonalite	Quartz-plagioclase-biotite \pm K-spar \pm hbl \pm garnet \pm magnetite \pm titanite		Layers and lenses of amphibolite and calcsilicate rock. Two phases of migmatization.
OLDER SUPRARUSTAL ROCKS				
Unit	Minor lithologies	Mineralogy		Notes
Amphibolitic gneiss	Felsic bands	Hbl-px-plagioclase \pm quartz		
Quartz-rich paragneiss	Mafic bands	Quartz-plagioclase \pm garnet \pm top \pm cpx \pm hbl		
Migmatitic leucogneiss	Amphibolite, coarse-grained pegmatite	\pm biotite		Early stromatic migmatisation postdated by later, diffuse phase
Quartz-feldspar leucogneiss	Amphibolite	Quartz-2 feldspars \pm biotite \pm magnetite \pm ilmenite		Locally migmatitic. Mafic pods and schlieren
Quartz-feldspar gneiss/paragneiss				Possibly both metasedimentary and metavolcanic components
Migmatitic grey gneiss (Figure 5a)		Quartz-2 feldspars- biotite		Up to 25% pygmatically folded leucosome

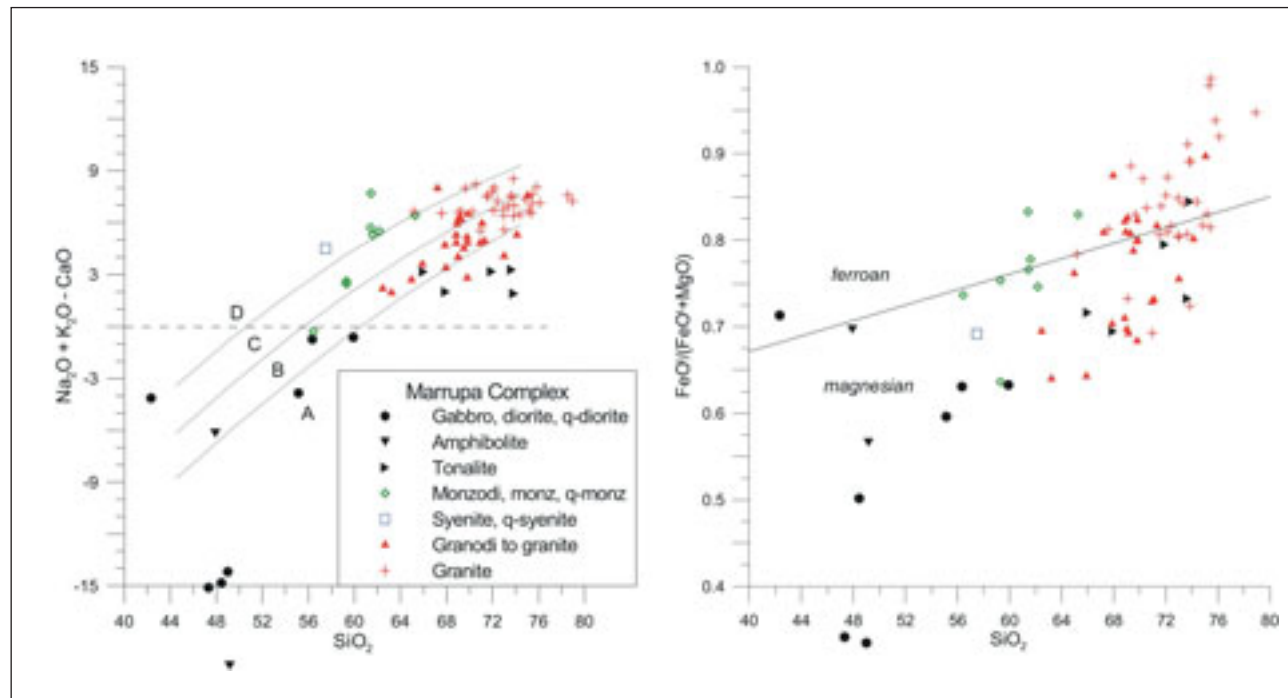


Figure 6. Modified alkali-lime index (left) plotted against SiO_2 for rocks of the Marrupa Complex. The lines subdivide between calcic (**A**), calc-alkaline (**B**), alkali-calcic (**C**) and shoshonitic (**D**) rocks. The monzonitic rocks and syenite have moderately high contents of alkalis and plot in the alkali-calcic to shoshonitic fields. Note the calcic and magnesian nature of the tonalitic samples. Classification diagram (right) showing the subdivision of the rocks in magnesian (below) and ferroan (above). Diagrams from Frost et al. (2001).

Geochimistry of the Unango Complex

The mafic rocks of the Unango Complex, including gabbro, diorite and amphibolite, are metaluminous, low-to medium-K calc-alkaline rocks, with substantial variation in Mg# (>0.4) (Table 2). Compared to the more evolved rocks, these are present in subordinate amount. A conspicuous feature of the complex is the absence of tonalite and low- to medium-K granodiorite. In contrast, there are abundant intermediate monzodioritic to monzonitic rocks. These rocks are alkali-calcic to shoshonitic, and a considerable proportion of the samples are ferroan (Figure 3). The group exhibits significant variation in minor and trace element contents. A number of samples have very high contents

of e.g. Sr, Zr and Ba. Note that the samples of dykes are alkali-calcic and ferroan and plot close to the monzonitic rocks in most diagrams.

Granodioritic rocks are generally metaluminous to weakly peraluminous and high-K calc-alkaline with Mg# at 0.15 to 0.50. The rocks are generally more evolved than the monzodioritic to monzonitic rocks, and have lower contents of K_2O and total alkalis, and higher CaO at similar SiO_2 values. Using the classification of Frost et al. (2001), the rocks are calc-alkaline to alkali-calcic and mainly magnesian although a few samples stand apart having a clearly ferroan signature (Figure 3). The trace elements are characterized by moderate contents of LREE and HFS-elements. The rocks have moderate to fairly high contents of Sr (<600 ppm) and moderate to low Zr, whereas the contents of Rb and Ba vary considerably. Trace-element contents are consistent with normal I-type composition although one sample with anomalously high Zr content (sample 31223, UTM 36S 814130, 8481778) plots in the A-type field (Figure 4). The granites (ss) form a diverse group of high-K calc-alkaline rocks with notable variation in Mg# (0.01–0.30). The rocks are metaluminous to weakly peraluminous with alumina saturation index ranging from 0.92 to 1.13. The majority of the rocks are ferroan (Figure 3). Trace-element contents are variable and a great proportion of the samples have moderate to low contents of LIL (e.g. Rb, Sr, Ba) and HFS elements. About 50% of the samples have elevated contents of Zr and/or light rare earth (LRE) elements and plot in the A-type

Table 4. Geochemical compositional ranges for the main lithological groups in the Marrupa Complex.

Marrupa Complex	SiO_2	K_2O	Mg#	N
Granite	65.2 – 78.9	3.8 – 6.1	0.09 – 0.44	33
Granodiorite	62.5 – 71.3	2.1 – 5.2	0.27 – 0.50	25
Syenite, quartz				
syenite	57.5	6.4	0.44	1
Monzodiorite,				
monzonite,				
q-monzonite	56.4 – 65.3	2.9 – 5.7	0.26 – 0.50	7
Tonalite	66.0 – 73.9	0.9 – 1.7	0.25 – 0.44	5
Gabbro, diorite,				
quartz-diorite	42.3 – 59.9	0.2 – 2.1	0.42 – 0.78	7
Amphibolite	47.9 – 49.2	0.3 – 0.6	0.44 – 0.58	2

field of Figure 4. The remaining samples plot in the field of fractionated I-type granites consistent with the ferroan nature of the rocks.

The rocks classified as syenites and quartz syenites are shoshonitic and mainly ferroan (Figure 3) with very high contents of alkalis and low CaO. The rocks display variable contents of TiO₂ and P₂O₅, but the spread in these elements is less pronounced than for the monzonitic rocks. The LIL and HFS elements also show great variation in abundance. As for the monzonitic rocks, several samples have strongly elevated contents of e.g. Sr, Zr and Ba. The compositionally distinct groups are quite well illustrated in Figure 4. The diagram shows that the granodioritic rocks plot mainly in the field of I-type granites, about 50% of the granites have compositions similar to fractionated I-type rocks, whereas other granites plot in the A-type field together with syenitic rocks. Note that the monzodioritic to monzonitic rocks plot in the fields of both the fractionated I-type and the A-type granites. Dyke rocks have consistently high contents of HFS-elements and plot in the A-type field.

Marrupa Complex

The Marrupa Complex lies east of the Unango Complex and is terminated in the south by the Lurio Belt (Figure 1). It corresponds largely to the "Marrupa antiform" or "Marrupa Group" of Pinna & Marteau (1987) and Pinna et al. (1993), which they correlated

with their "Nampula Group", south of the Lurio Belt. The complex (Table 3) is dominated by felsic to intermediate orthogneisses (Figures 5a, b, c). Mafic orthogneisses are subordinate, and paragneisses of sedimentary origin are much less common than in the Nampula and Unango Complexes (see Table 4). The gneisses vary from homogeneous and rather fine-grained (Figure 5b), to more coarse-grained, and include banded and migmatitic varieties (Figures 5c, d) with biotite-hornblende-bearing assemblages indicative of amphibolite facies metamorphism. The intrusion age of the orthogneiss ranges from 1026 ± 9 to 946 ± 11 Ma (7 samples; Norconsult 2007a; Bingen et al., 2009) and timing of metamorphism is constrained by U-Pb dates on zircon rims and monazite at 555 ± 11 Ma (average of five samples, Bingen et al., 2009).

Geochronology of the Marrupa Complex

The mafic rocks, together with tonalitic rocks, make up a group of essentially low-K calcic to calc-alkaline, magnesian rocks (Table 4, Figure 6). Metaluminous tonalites and more mafic rocks make up about 15% of the samples. Monzodioritic to monzonitic rocks are represented by a few samples, and only one sample of syenitic composition was taken. These rocks are alkali-calcic to shoshonitic and straddle the boundary between magnesian and ferroan (Figure 6). Weakly peraluminous granites and granodiorites are clearly the predominant rocks in the complex. The granodiorites appear to make up two subgroups. One group consists essentially of magnesian medium-K calc-alkaline rocks, and the other includes magnesian to ferroan, high-K calc-alkaline rocks.

The trace-element contents for the rocks are highly variable for many elements. The Sr contents illustrate this quite well, showing a wide range of values for all rock groups. The mafic to intermediate rocks including tonalites have fairly low contents of Rb, Ba and Zr as well as LREE. As expected, the magnesian granodiorites have lower Rb contents than other granodiorites; however, the range in Rb and Ba contents is substantial for these rocks. In general, the trace-element contents are consistent with the main components and suggest that the Marrupa Complex comprises different rock types including normal and fractionated I-type granites in addition to rocks with a clear A-type affinity (Figure 7).

Nairoto Complex

The Nairoto Complex is exposed in the northeastern part of the mapped area and is dominated by felsic orthogneisses. From near Mueda to Montepuez (Figure 1) the complex strikes north-northeast to south-southwest and has a width of 15 to 30 km (Figure 1). North of Montepuez there is a major fold, with an axial plane trending north-northeast to south-southwest that rotates the southeastern extension of the unit to a west-northwest to east-southeast trend, forming a 10 to 15 km wide belt which extends towards Mecufi where it is overlain by the Rovuma Basin.

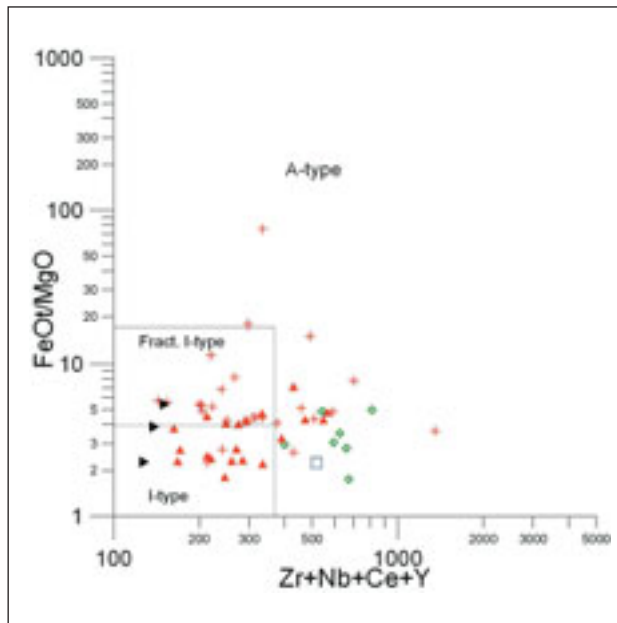


Figure 7. Total FeO/MgO vs Zr+Nb+Ce+Y (ppm) for rocks of the Marrupa Complex. Legend as in Figure 6. The tonalitic and magnesian granodioritic rocks plot mainly in the field of I-type granite although some granodiorites are in the A-type field. The granites plot in all the fields of the diagram, however, about 30% of the granites plot in the A-type field together with monzonitic and syenitic rocks. Diagram from Whalen et al. (1987).

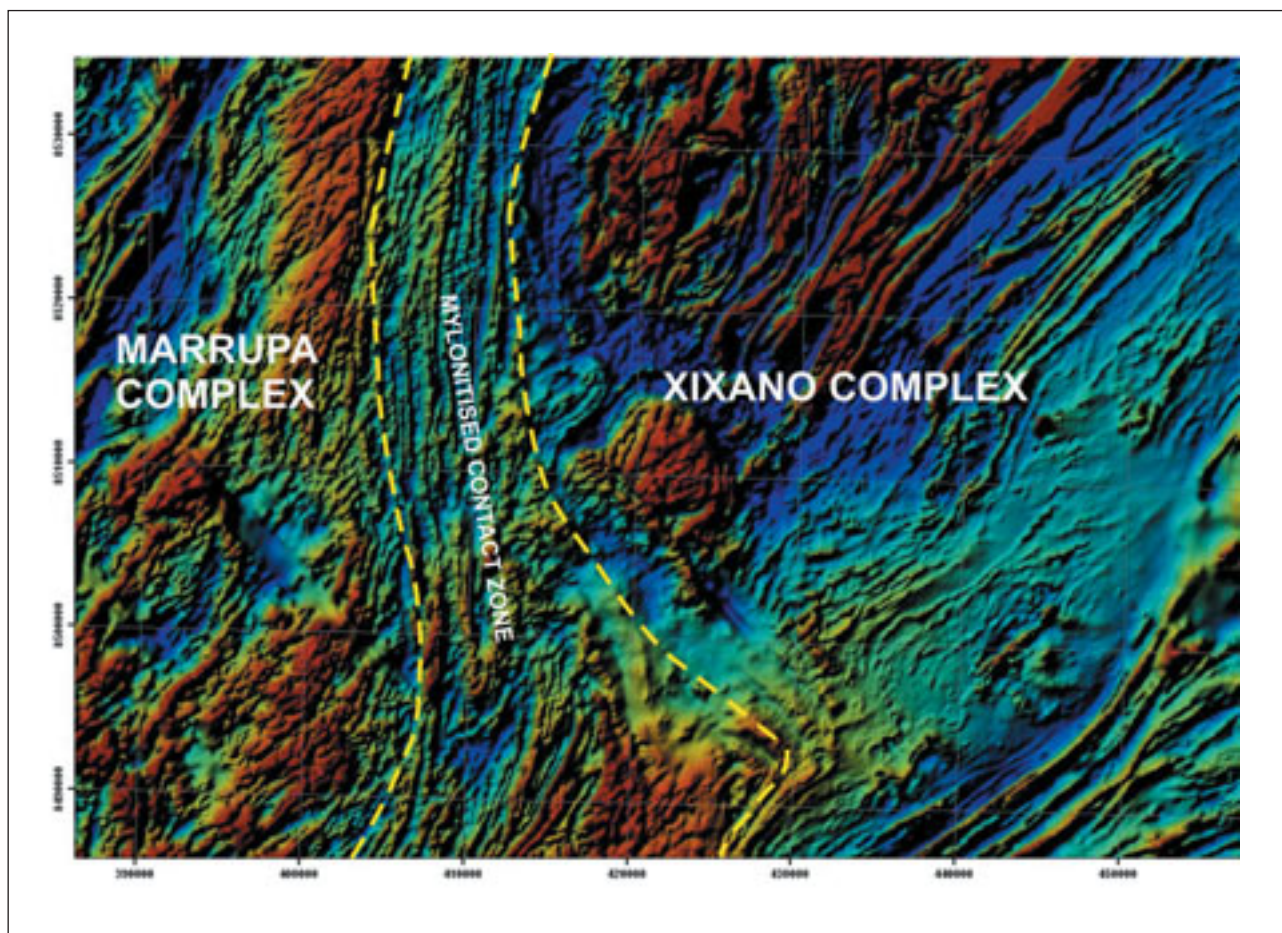


Figure 8. Aeromagnetic map showing the contact zone between the Marrupa and Xixano Complexes. A ~10 km wide zone of sheared rock occurs at the contact on which Xixano Complex meta-supracrustal rocks are tectonically juxtaposed with the Marrupa Complex.

The complex thus comprises an arc-shaped belt wrapped around the Lalamo Complex, the contacts with which are clearly tectonic. The orthogneisses that form the complex are commonly magnetite-bearing, and the belt shows pronounced positive aeromagnetic anomalies.

The term Nairoto was introduced by Pinna et al. (1993) who gave the unit group status even though they realized that its components were mainly metamorphosed intrusive rocks. They correlated the Nairoto Complex with the Meluco and Marrupa Complexes (our usages) as part of a basement mega-unit (their Nampula Supergroup) onto which their Chiure Group was thrust. Geochronological data reported by Jamal et al. (2005) are compatible with the correlation between the Nairoto and Marrupa Complexes. The Nairoto Complex consists predominantly of locally migmatised felsic orthogneisses. These rocks are calc-alkaline, with predominantly granodioritic and tonalitic compositions and minor granitic components, and can be classified as normal I-type granitoids. There are no indications that the metamorphic grade exceeded amphibolite facies.

Variations in migmatisation and composition are seen clearly in east-west profiles north and south of Rio

Messalo (Figure 1). All textural variations from granitic gneiss with a weak foliation, to multiply-folded migmatites are seen. The typical granitoid gneiss is well foliated, fine- to medium-grained and contains biotite. Pegmatitic veins and patches are common. Irregular biotite-rich lenses, inclusions and bands commonly occur in the migmatitic granitic gneiss and migmatites. The orthogneiss contains thin lenses of fine-grained ($\leq 1\text{mm}$), granular, greyish-white to red meta-arkose with a weak foliation, generally defined by biotite. The typical granitic migmatite is banded, and is locally intensely folded.

Meluco Complex

The Meluco Complex occurs in two large, oval, dome-like structures (measuring 30 x 50 km and 45 x 60 km) southeast of Meluco (Figure 1). The main part of the Meluco Complex was earlier called the Meluco Group, and was, together with other high-grade orthogneiss units, assigned to the Nampula Supergroup (Pinna and Marteau, 1987). These high-grade units were interpreted by Jourde and Wolff (1974) as an old migmatitic basement, considered to have been extensively reworked by the ca. 1000 Ma "Lurian Orogeny". According to Pinna et al. (1993), the Meluco Group

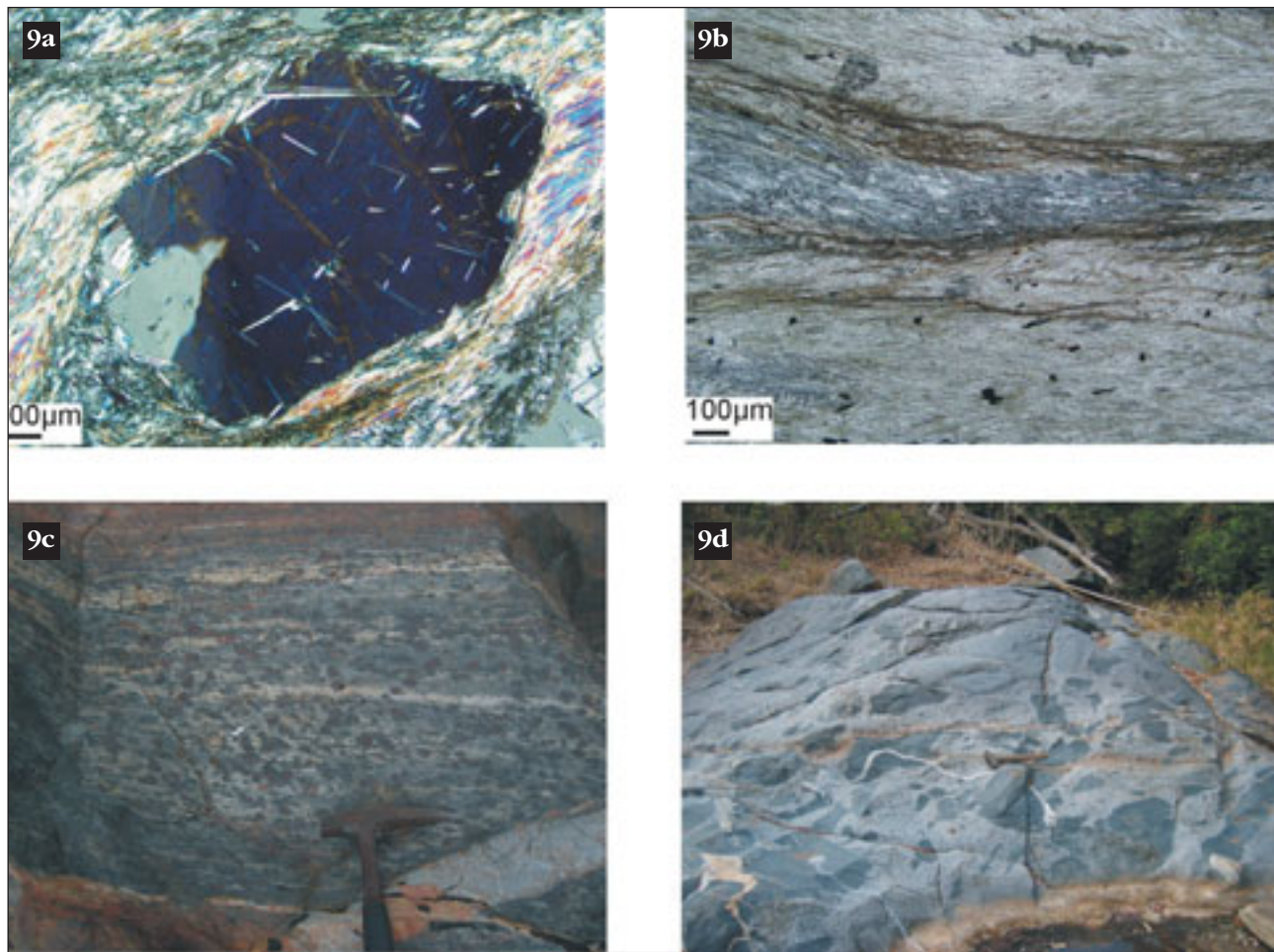


Figure 9. Xixano Complex lithologies: (a) Quartz mica schist, showing quartz porphyroclasts with unoriented needles of sillimanite, relics of a high-grade event, and (b) Chlorite-rich shears in a muscovitic groundmass testifying to greenschist-facies overprinting on focused shear planes. (UTM 37S 470800, 8503702); (c) Banded amphibolitic gneiss with garnets up to 1 to 2 cm in diameter. (UTM 37S 442660, 8733158); (d) Xenoliths of meta-gabbro in quartz diorite (UTM 37S 459212, 8658780).

represents polyphase batholiths emplaced in the deep part of a mature island arc or active continental margin. The Meluco Complex consists of granitic to granodioritic orthogneisses, with subordinate tonalitic gneiss. The complex and convoluted magnetic and radiometric signatures of the complex are characterised by a rather irregular, folded pattern, in contrast to the supracrustal rocks in the surrounding Lalamo Complex, which define a clearly banded pattern that wraps around the Meluco Complex in a concentric fashion. The thesis that the Meluco Complex is a basement for the supracrustal rocks is therefore plausible, but unproven. The contact with the Lalamo Complex, at the only locality where it has been observed (UTM 37S 557097, 8612382), is a thrust, with the rocks of the Lalamo Complex thrust over the Meluco Complex in a "top-to-the-south" sense. Granitic gneiss from the eastern dome yields an intrusion age of 946 ± 12 Ma (Norconsult 2007a). An equivalent age is obtained from one sample of the western dome (Jamal, 2005). Four samples of granodioritic/granitic gneiss from the Meluco Complex

have been analysed by XRF, and indicate a high-K calc-alkaline character for the complex; they can be classified as fractionated I-type granitoids.

The gneisses are coarse-grained, with generally quartz-rich assemblages that include plagioclase, K-feldspar, biotite and hornblende \pm red garnet and opaque minerals. The migmatic textures vary from stromatic to coarser fabrics with sharply defined, thicker neosome layers up to tens of cm in thickness, to multi-phase, complex migmatites with disrupted mafic bands invaded by granitic partial-melt patches and with mafic (restite) lenses surrounded by rock rich in granitic neosome veins and patches. The gneissosity becomes diffuse where there is extensive partial melting. There are also thick (>10 m) granite sheets concordant with the gneissosity.

Xixano Complex

The Xixano Complex is characterized by a highly distinctive, mainly weak radiometric signature on new high-resolution airborne geophysical data which has

Table 5. Lithostratigraphy of the Xixano Complex. Bold font indicates the dominant component in a compositional range.

XIXANO COMPLEX LITHOSTRATIGRAPHY

INTRUSIVE ORTHOGNEISSES

Unit	Compositional range	Mineralogy	Notes
Mylonite	Tonalite-granite (quartzite)	Quartz-2 feldspars-biotite	Intense deformation (stretching ratios up to 30:1)
Monte Mapancane granite	Granodiorite-granite	Quartz-2 feldspars-biotite ± hbl ± magnetite	Less deformed than other orthogneisses.
Granitic-granodioritic gneiss Suite) (Figure 9d)	Gabbro-diorite-tonalite	Amphiboles-cpx-plagioclase-biotite±quartz±garnet	Wide variation in textures/retrogression; local augen texture. ?Younger than other orthogneisses. Highly variable, also locally, incl. gabbro pegmatite.
Metagabbro	Gabbro	Hbl-cpx-plagioclase±quartz±biotite±K-spars±garnet±pyrrhotite	Locally scapolitised and carbonatised; fine-grained pyrrhotite is common; Cu, Ni contents are low.
Amphibolitic gneiss (Figure 9c)	Gabbro-tonalite	Actinolite-plagioclase±chlorite±quartz±garnet	Varied protoliths and degrees of metamorphism/retrogression
Mangeritic gneiss Charnockitic rocks	Tonalite Tonalite- granodiorite - granite	Hbl-plagioclase-biotite±K-spars Quartz-2 feldspars-hbl ± opx±cpx ± garnet±micas±chlorite	Commonly retrograded to hornblende gneiss Commonly banded and locally retrograded
SUPRACRUSTAL ROCKS			
Unit	Minor lithologies	Mineralogy	Notes
Marble, variably dolomitic	Marble	Calcite-dolomite + variety of trace minerals	Many lenses and horizons, up to >50 km long.
Quartzite	Meta-sandstone	Quartz±2 feldspars±biotite± muscovite	Thin tectonic slivers
Quartz-mica gneiss (Figure 9 a,b)	Schistose varieties, quartz-rich paragneisses, amphibolite	Quartz-2 feldspars-muscovite±biotite±fuchsite±garnet±graphite±sillimanite	Potential for graphite
Biotite gneiss	Quartz-feldspar gneiss, amphibolitic gneiss	Quartz-2 feldspars-biotite	Heterogeneous paragneiss
Metarhyolite	Rhyodacite	Quartz-2 feldspars-muscovite±chlorite	Tectonically dissected lenses
Quartz-feldspar gneiss		Quartz-2 feldspars-biotite-garnet	Two phases of migmatite

facilitated its recognition as a new tectonostratigraphic unit (Norconsult 2007b; Viola et al., 2008). It extends to the south-southwest from the Tanzanian border, east of Rio Lugenda to the Lurio Belt. The Xixano Complex overlies the Marrupa Complex, including two newly recognized tectonic outliers (a large, north-south-trending klippe near Nipepe and a smaller one to the west, Figure 1) (Viola et al., 2008). The complex includes parts of the Chiure and Morrola Groups, as defined by Pinna and Marteau (1987), who attributed them to the Chiure and Lurio Supergroups respectively. The contact between the Xixano Complex and the Marrupa Complex in the west is a major shear zone, interpreted as a thrust (Figure 8, Viola et al., 2008) that

Table 6. Geochemical compositional ranges for the main lithological groups constituting the Xixano Complex.

Xixano Complex	SiO ₂	K ₂ O	Mg#	N
Granite	68.8 - 77.7	3.9 - 5.7	0.03 - 0.48	11
Granodiorite	69.7 - 72.7	2.5 - 4.5	0.22 - 0.33	3
Monzodiorite, monzonite,				
Quartz monzonite	49.8	2.0	0.49	1
Tonalite	57.8 - 72.1	0.2 - 1.3	0.21 - 0.52	8
Gabbro, diorite, quartz-diorite	41.2 - 50.4	0.1 - 0.3	0.4 - 0.72	8
Amphibolite	43.9 - 60.2	0.1 - 0.4	0.22 - 0.72	4
Metavolcanic rocks	51.1 - 76.4	0.1 - 0.4	0.22 - 0.72	7

was subsequently folded against the Lurio Belt in the south. The shear-zone contact with the Montepuez Complex in the east is also strongly folded. A major shear zone also separates the Xixano Complex from the Nairobi Complex in the east.

The Xixano Complex (Table 5) includes a variety of metasupracrustal rocks (Figures 9a, b) enveloping predominantly mafic igneous rocks and granulites (Figures 9c, d) that form the core of a regional north-northeast to south-southwest-trending synform. The paragneisses include mica gneiss and schist, quartz-feldspar gneiss, metasandstone, quartzite and marble. Felsic orthogneisses occur with the paragneisses, mainly in northern and eastern areas. The metamorphic grade in the paragneiss is dominantly amphibolite facies, although granulite-facies rocks are locally preserved within tectonic lenses.

The oldest dated rock in the Xixano Complex is a weakly deformed metarhyolite, which is interlayered in the metasupracrustal rocks and which gives a reliable extrusion age of 818 ± 10 Ma (Norconsult 2007a). Marble horizons, also interlayered with supracrustal rocks, have apparent deposition ages, as estimated by chemostratigraphic methods, of 850 to 750 Ma in the north of the Xixano Complex and ca. 740 Ma in the south (Melezhik et al., 2008). A meta-igneous granulite (enderbite) yielded a younger intrusion age of 744 ± 11 Ma (Norconsult 2007a). Available geochronology thus demonstrates that the bulk of the Xixano Complex is

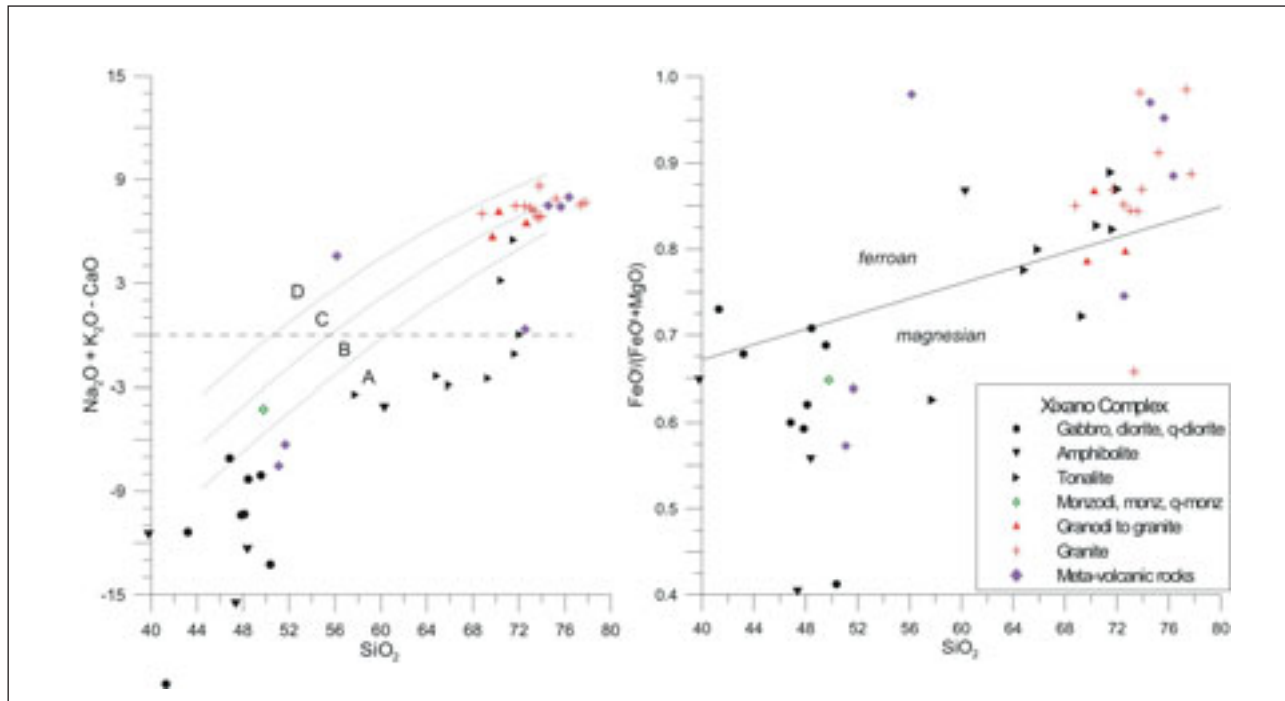


Figure 10. Modified alkali-lime index (left) plotted against SiO₂ for rocks of the Xixano Complex. The lines subdivide between calcic (**A**), calc-alkaline (**B**), alkali-calcic (**C**) and shoshonitic (**D**) rocks. Note the low contents of total alkalis for the mafic to intermediate rocks. Classification diagram (right) showing the subdivision of the rocks in magnesian (below) and ferroan (above). In the Xixano Complex, granitic rocks and some the evolved tonalites plot above the line and classify as ferroan. Diagrams from Frost et al. (2001).

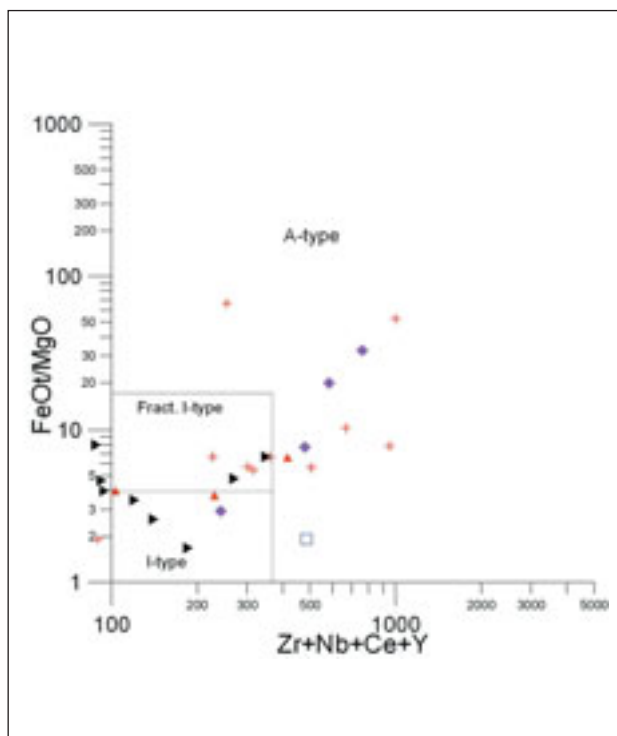


Figure 11. Total FeO/MgO vs $\text{Zr}+\text{Nb}+\text{Ce}+\text{Y}$ for rocks of the Xixano Complex. Legend as in Figure 10. The granitic and granodioritic rocks plot mainly in the field of fractionated I-type granite and into the A-type field. The same is the case for the volcanic rocks. Tonalites plot in the I-type field. Diagram from Whalen et al. (1987).

made up of Neoproterozoic lithologies formed between 820 and 740 Ma.

Geochemistry of the Xixano Complex

The Xixano Complex (Table 6) is mainly composed of mafic to felsic low-K magnesian rocks with very few samples of intermediate composition. Predominant

rocks types are calcic, mafic gabbro and diorite and low-K tonalite. The evolved rocks are mainly high-K calc-alkaline granite and granodiorite and plot in the ferroan field of Figure 10. Some samples of metavolcanic rocks are compositionally similar to the intrusive rocks. Apart from one sample of monzodiorite, monzonitic and syenitic rocks are notably absent in the Xixano Complex. The diagrams also show some samples of metavolcanic rocks. Apart from one shoshonitic sample, the volcanic rocks are compositionally very similar to the gneisses of intrusive origin.

The contents of LIL- and HFS-elements are low in the mafic rocks. This is particularly the case for Rb and Ba. Among the more evolved rocks there is a wide scatter in the contents of all trace elements. In the classification diagram of Whalen et al. (1987), the granitic rocks plot in the field of fractionated I-type granite and into the A-type field (Figure 11).

Muaquia Complex

The Muaquia Complex occurs southwest of Mavago, centered on 37°E 13°S (Figure 1). It structurally overlies the Marrupa Complex and is interpreted as a Pan-African nappe (Viola et al., 2008). In the western part of the complex, aeromagnetic data show conspicuously low relief, in contrast to most of the surrounding lithological units, which show contrasting high and low banded anomalies, parallel with the observed banding and lineaments on satellite images.

The Muaquia Complex (Table 7) mainly comprises part of a heterogeneous supracrustal sequence attributed to the Chiure Supergroup by Pinna et al. (1993). The term "Muaquia Group" was used by Costa et al. (1983) for the basal sequence of metasedimentary and ultramafic igneous rocks in the Mugeba klippe farther south. Exposure is sparse, but some general conclusions can be drawn:

- Compositions are mainly granitic and the textures are mainly mylonitic.

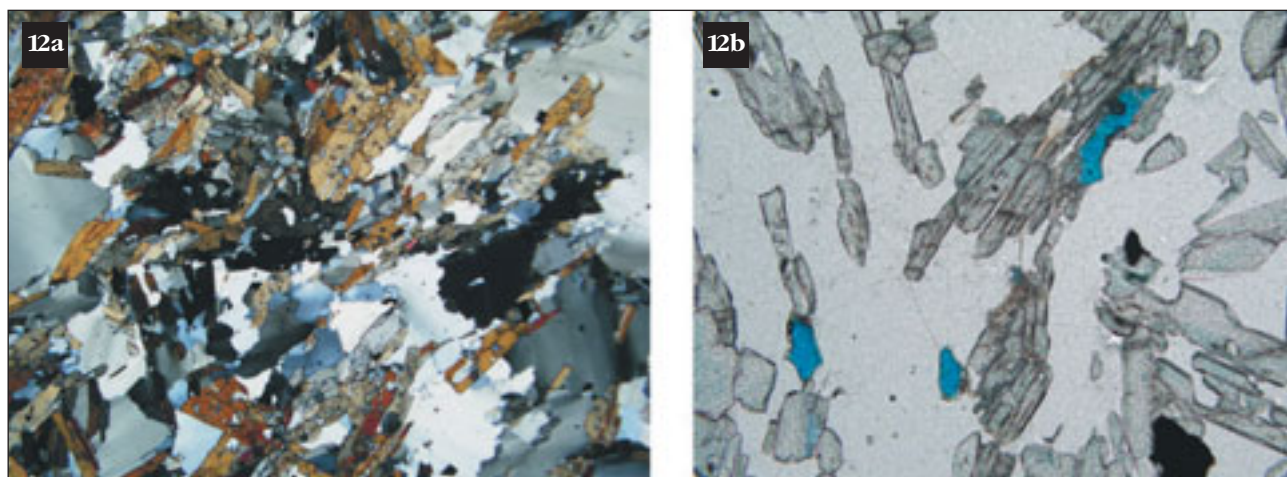


Figure 12. Muscovite-kyanite quartzite in the Muaquia Complex. (a) Randomly orientated kyanite in a groundmass of strained quartz (width of photo 6mm), (b) Kyanite and lazulite (vivid blue) in groundmass of quartz (width of photo 1.5 mm) (UTM 37S 228840, 8572186).

Table 7. Lithostratigraphy of the Muaquia and Msawize Complexes. Bold font indicates the dominant component in a compositional range.

MSAWIZE COMPLEX LITHOSTRATIGRAPHY			
INTRUSIVE ORTHOGNEISES			
Unit	Compositional range	Mineralogy	Notes
Tonalitic gneiss	Tonalite	Plagioclase-cpx-opx-hornblende±zircon±apatite±quartz	Variable gneissic foliation.
Gabbroic-granodioritic gneiss	Gabbro-tonalite-granodiorite-granite	Plagioclase-quartz-cpx-hornblende±garnet±titanite	High-P granulite facies mineralogy. Very heterogeneous lithologies on a local scale.
Metagabbro, amphibolite	Gabbro	Hornblende-cpx-plagioclase±garnet±scapolite±titanite±magnetite±quartz±rutile	Clear high-P granulite facies mineralogy
Banded migmatite	Pyroxenite-amphibolite-tonalite-granite	Hornblende-plagioclase-biotite-epidote-garnet	Charnockite, pyroxenite and amphibolite bands present locally. Variable deformation, locally mylonitic.

MUAQUIA COMPLEX LITHOSTRATIGRAPHY			
INTRUSIVE ORTHOGNEISES			
Unit	Compositional range	Mineralogy	Notes
Granitic-granodioritic gneiss	Tonalite-granodiorite-granite	Quartz-2 feldspars-biotite-hornblende±muscovite±epidote	Igneous textures commonly preserved. Locally, where mylonitic, contains possible quartz-feldspar paragneisses
Amphibolitic gneiss	Pyroxenite- gabbro-diorite	Plagioclase-amphibole-cpx-biotite-quartz±magnetic	Probably includes both volcanic and plutonic protoliths
Granitic-granodioritic gneiss, mylonitic	Tonalite-granodiorite-granite	Quartz-2 feldspars-biotite ± muscovite ± epidote	Mafic minerals in lenses < 1mm thick. Local augen texture.

SUPRACRUSTAL ROCKS			
Unit	Minor lithologies	Mineralogy	Notes
Quartzite		Quartz	Bands in mylonitic granitic-granodioritic gneiss
Muscovite-kyanite quartzite (Figure 12)		Quartz-kyanite-muscovite±plagioclase±titanite±rutile±lauzelite	Commonly homogeneous distribution of kyanite grains up to 1 cm long
Quartz-feldspar gneiss	Mafic bands occur locally.	Quartz-plagioclase±biotite±muscovite±epidote±fuchsite±malachite±azurite	Cu-minerals occur locally in blocks of a fine-grained siliciclastic rock
Muscovite-biotite gneiss	Schistose to mylonitic varieties	Quartz-biotite-muscovite±K-spar±garnet	Banded on scale of 1-100m; penetrative foliation.
Calc-silicate gneiss		Amphibole-plagioclase-quartz-epidote±garnet±opx	Local pseudomorphs after staurolite and sillimanite In situ blocks - no true outcrop

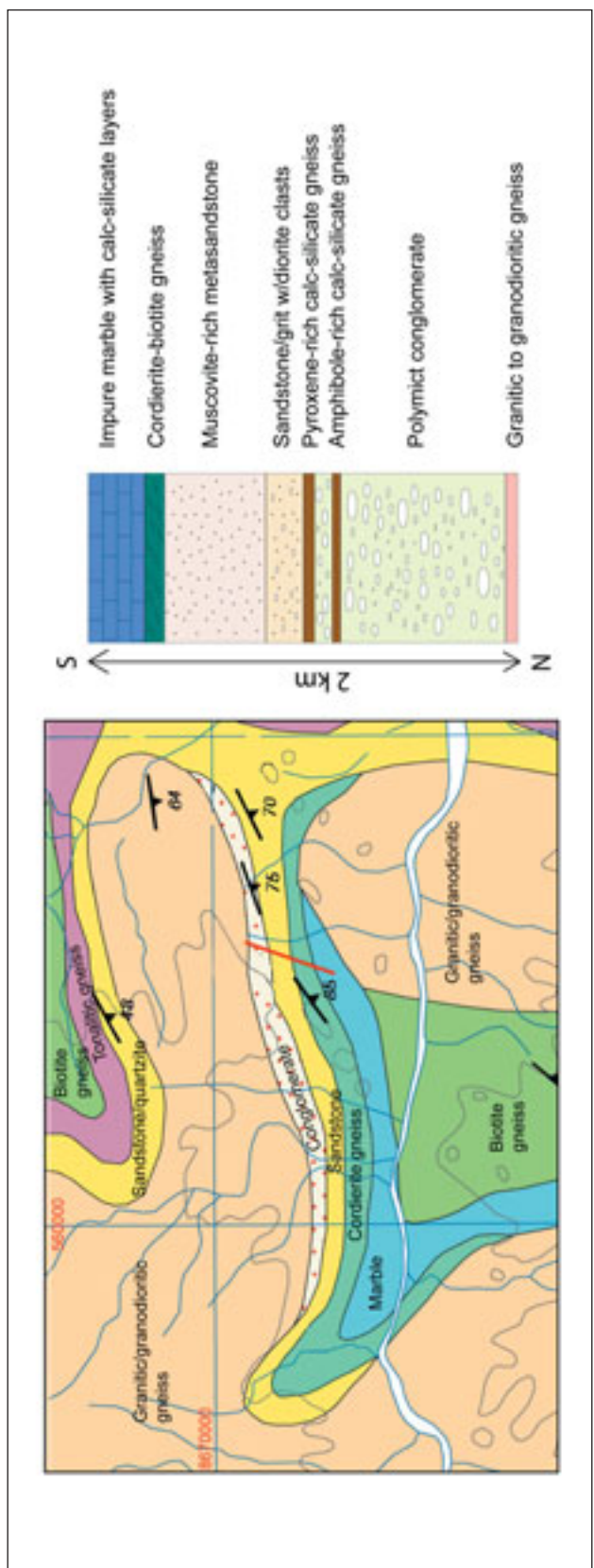


Figure 13. Part of sheet 1239 Meluco, showing the site of a well-exposed sedimentary sequence. The red line is 2 km long and shows the section sketched to the right. Chemostratigraphic dating (Melezhik et al., 2008) of marbles elsewhere in the Lalamo Complex suggests that the marble in this sequence has an age of 740 Ma.

- Small lenses of quartzite, kyanite quartzite (Figure 12) and quartz-rich two-mica schists are found, especially in the west. To the east the meta-supracrustal rocks are less fragmented and form larger units of quartz-feldspar paragneiss with infolded amphibolite and calc-silicate rocks.
- More weakly deformed mega-lenses (3 to 4 km across) of granite, tonalite and granodiorite are preserved within the main lithology near the contact with the Marrupa Complex in the eastern half of the Muaquia Complex.
- Late shear deformation has created shear surfaces and microshears in all lithologies, initiating growth of muscovite, chlorite and/or epidote. Deformation increases towards the contact with the Unango Complex to the west.
- There are a few, widely separated indications of an early high-pressure metamorphism.

M'Sawize Complex

The M'Sawize Complex, southwest of Mavago, overlies and is almost enclosed within the Muaquia Complex (Figure 1). The two complexes are characterized by strongly contrasting lithologies (Table 7) and textures, so it is necessary to define them as separate complexes. Both complexes have, however, experienced early high-grade metamorphism. The orthopyroxene-free garnet-clinopyroxene-plagioclase±quartz assemblage found in a foliated metagabbro in the M'Sawize Complex indicates an estimated P of 11.5 Kb and T of 800°C (Norconsult 2007a). Late epidote growth is present in both units, which may suggest that they were juxtaposed prior to final retrogression. An early phase of high-pressure granulite-facies metamorphism is recorded in the mafic gneisses of the M'Sawize Complex.

The M'Sawize Complex, as defined here, comprises part of the M'Sawize Group of Pinna et al. (1993), who included the unit in their Lurio Supergroup. The latter corresponds to the “eastern thrust granulite” preserved in synforms as nappe outliers (Pinna et al. 1993). The northern and western contacts of the M'Sawize Complex appear to be related to several shear zones that cross the region from the northeast and which are deflected sharply southwards southeast of Mavago, adjacent to the contact with the Unango Complex to the west. The M'Sawize Complex is interpreted as a nappe, thrust over the Muaquia Complex with an overall top-to-the-northwesterly transport direction (Viola et al., 2008). However, detailed kinematic analysis of shear zones associated with the M'Sawize Complex also shows top to the southeast kinematics (Norconsult 2007). These shear zones are folded about northeasterly to southwesterly upright kilometric-scale open folds, which suggests a pre-thrusting/folding phase of extension. In addition, a later regional northwest to southeast extensional phase was also documented by Viola et al. (2008) postdating thrusting and marking the collapse of the overthickened crust. Therefore these shear zones are likely to record



Figure 14. Polymict conglomerate, with flattened fragments mainly of various orthogneisses in a matrix of biotite gneiss (UTM 37S, 565363, 8668830).

evidence of a complex, long-lived structural history with several periods of reactivation.

The M'Sawize Complex is dominated by mafic to felsic, commonly granulite-facies metagneous rocks (Table 7). The intrusion of these orthogneisses and the “early” granulite-facies metamorphism are undated: they may be Irumide or Pan-African in age. However, U-Pb dating of a minor tonalite pluton in the complex yields an intrusion age of 622 ± 9 Ma (age reprocessed from 640 ± 4 Ma in Norconsult 2007a), showing that at least this intrusion is early Pan-African in age.

Lalamo Complex

The Lalamo Complex comprises part of the former Chiure Supergroup of Pinna et al. (1993). It is situated east and north of the Nairoto Complex. It is overlain by the Rovuma Basin to the east (Figure 1) and is interpreted as overlying the Nairoto and Meluco Complexes. The western contact against the Nairoto Complex is a steep dextral shear zone, along which various units of the Lalamo Complex are truncated. As described above, the contact between the Lalamo and Meluco Complexes is tectonised, probably a thrust (the Chiure Supergroup basal thrust of Pinna et al. 1993).

The Lalamo Complex is predominantly made up of various metasupracrustal rocks generally at amphibolite grade. It is made up mainly of biotite gneiss, meta-sandstone, quartzite, marble, amphibolite and conglomerate and minor meta-igneous rocks of granitic to ultramafic composition. The biotite gneiss includes graphite-bearing units which are exploited in the Ancuabe area. The timing of deposition of the supracrustal sequences has been estimated using chemostratigraphic methods on two thin marble layers which yielded deposition ages of around 740 Ma (Melezhik et al., 2008). An orthogneiss yielded a U-Pb zircon intrusion age of 696 ± 13 Ma (Norconsult, 2007a).

South of the village Homba, north of Meluco, a well-exposed section of metasediments illustrates the diversity of lithologies in the Lalamo Complex (Figure 13). The section includes (from north to south) horizons of conglomerate, meta-arenite and quartzite, alumina-rich, cordierite-bearing biotite gneiss and impure marble. The sequence is ~2 km thick and dips 70 to 80° south-southeast. The conglomerate is strongly

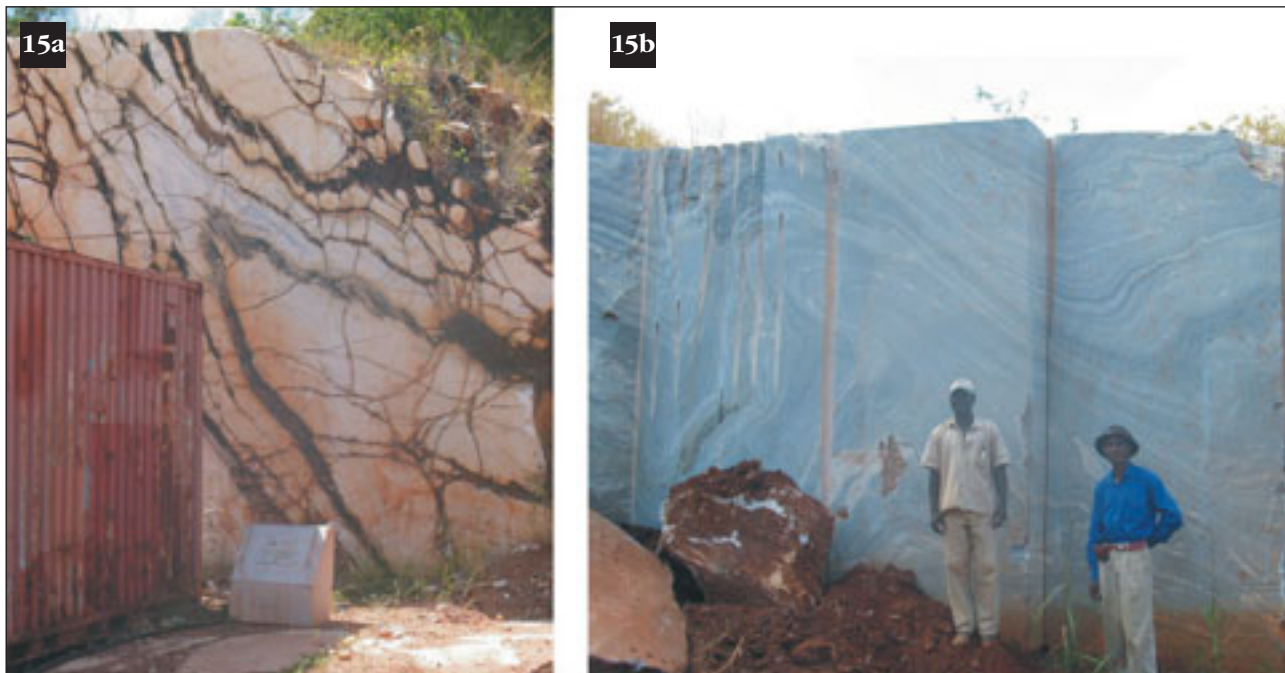


Figure 15. The Montepuez marble quarries, showing tight folding and foliation-parallel bedding in the marble.

Table 8. Lithostratigraphy of the Montepuez and Ocuá Complexes. Bold font indicates the dominant component in a compositional range. C-Sr ages are from Melezhi et al. (2007).

OCUA COMPLEX LITHOSTRATIGRAPHY				
INTRUSIVE ORTHOGNEISES				
Unit	Compositional range	Mineralogy		Notes
Syenitic gneiss	K-feldspar+cpx+biotite-hornblende±apatite±titanite±zircon	Quartz-2 feldspars-biotite-hornblende±garnet	Hornblende-plagioclase-biotite-epx±topx±garnet±titanite±pyrrhotite±chalcopyrite±chlorite	Banded on a cm scale due to variations in K-feldspar and biotite contents. Two clear rock types interbanded on a cm-m scale.
Granitic-tonalitic gneiss	Tonalite-granite			Locally contains sulphide veins
Dioritic-amphibolitic gneiss	Gabbro-diorite			
SUPRACRUSTAL ROCKS				
Unit	Minor lithologies	Mineralogy		Notes
Quartz-feldspar gneiss, mylonitic	Quartzite	Quartz-2 feldspars±biotite±muscovite±hornblende±opx±magnetite	Garnet-cpx-opx-plagioclase-Ca-amphibole-quartz-ilmenite±magnetite±biotite	Traces of mafic minerals suggest an earlier granulitic paragenesis Occurs interlayered with mafic granulite.
Felsic-intermediate granulitic gneiss	Pure marble		Garnet-cpx-plagioclase-quartz-ilmenite±magnetite±Ca-amphibole±biotite	Unclear whether this unit is para- or orthogneiss (or both)
Mafic granulite	Charnockite, biotite gneiss			
MONTEPUEZ COMPLEX LITHOSTRATIGRAPHY				
INTRUSIVE ORTHOGNEISES				
Unit	Compositional range	Mineralogy		Notes
Granitic gneiss	Tonalite-granodiorite-granite	Quartz-2 feldspars-biotite±amphibole±garnet		Contacts with the supracrustal rocks are concordant.
SUPRACRUSTAL ROCKS				
Unit	Minor lithologies	Mineralogy		Notes
Calcitic, dolomitic marble	Calcite-magnesite marble, amphibolitic gneiss	Calcite-tremolite-quartz-muscovite/dolomite-tremolite-graphite		Quarried as dimension stone. Montepuez tripartite unit dated at 1250-010 Ma by Sr-C chemostratigraphy. Montepuez W unit: 800-660 Ma.
Quartzitic gneiss	Quartzite, meta-arkose	Quartz-2 feldspars-biotite-muscovite±pyrite		
Quartz-feldspar gneiss		Quartz-2 feldspars-biotite-muscovite±garnet±amphibole		
Biotite gneiss, migmatitic		Quartz-plagioclase-hornblende±K-spar±graphite		Graphite-rich bands have possible economic potential.

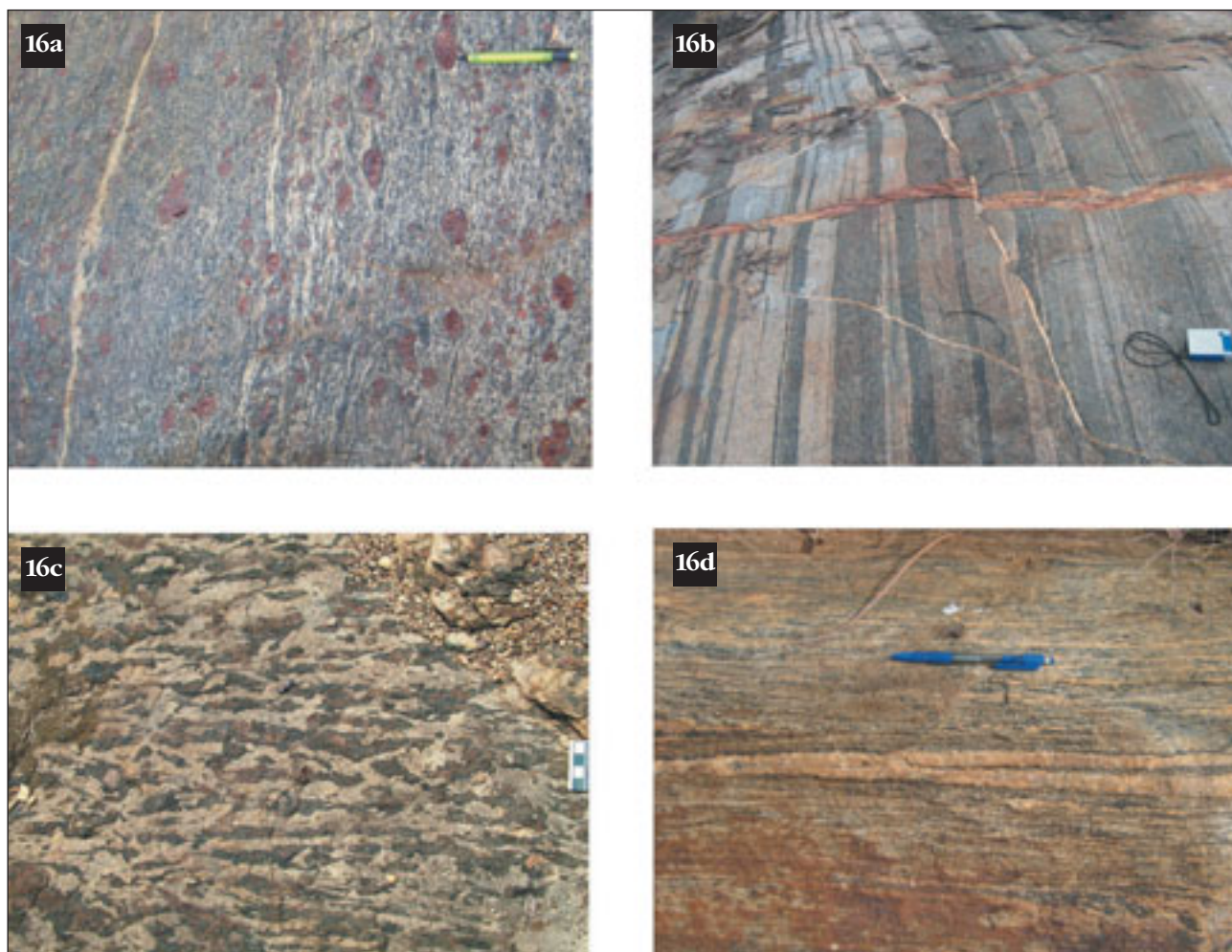


Figure 16. Ocua Complex lithologies: (a) Mafic granulite with cm scale garnet phenoblasts (UTM 37S, 608709, 8506268); (b) Well-defined compositional banding in felsic (light grey) to intermediate granulites (dark grey) in the Ocua Complex. Note the early set of leucocratic veins (left to right) occupying ductile shear zones in the granulites, while a younger set of veins occupies faults with late, brittle displacements (UTM 37S 260356, 8304548); (c) Coarse-grained charnockitic gneiss of the Ocua Complex. Note the strong foliation, mainly defined by coarse aggregates of elongate amphibole (black) and hypersthene (brown) with grey feldspar (UTM 37S 332641, 8391627); (d) Mylonitised granitic gneiss. The rock is pervasively injected by migmatitic leucosomes that are themselves sheared into the progressively developing foliation. (UTM 37S, 588132, 8492276).

foliated and sheared. It contains up to 20 to 30 cm large, sub-rounded clasts of fine-grained granite, diorite, quartz-feldspar gneiss, amphibolite and calc-silicate gneiss in a matrix of fine-grained biotite gneiss, which also seems to be clastic (Figure 14). To the south, across strike, there is fine-grained, strongly deformed amphibolitic gneiss, which probably represents metamorphosed calcareous sediment. This is structurally overlain by another layer of the conglomerate, followed by a fine-grained homogeneous layer of amphibole-pyroxene gneiss. Thin sections of this rock show it to be heteroblastic, with up to 5 mm strongly poikiloblastic grains of clinopyroxene (probably diopside) overgrowing a matrix of 0.1-1 mm grains, predominantly of quartz, clinoamphibole, K-feldspar and carbonate. This rock is also most likely a calcareous metasediment.

Structurally above the amphibole-pyroxene gneiss there is a thick unit of muscovite-biotite schist/gneiss,

which represents a meta-arenitic sandstone, quite strongly sheared with some mm-cm sized clasts of quartz clasts and of dioritic gneiss. This arenitic sandstone grades into a more fine-grained sandstone, now a biotite-muscovite schist/gneiss, which is muscovite-rich. It contains up to 2 to 3 mm quartz grains and is otherwise bedded to banded on a scale of a few dm. Above this metasandstone, about 1 km to the southwest, there is a dark argillaceous metasediment consisting of up to 25 to 30 cm long cordierite crystals in a “garben” texture with abundant cm-sized red garnet and biotite. The poikiloblastic grains of cordierite locally contain relict staurolite. Important accessories include chlorite, muscovite and gedrite.

This rock probably represents an aluminous meta sediment, and forms the top of a well-defined transgressive sequence that starts with the conglomerate at the structural base, grading into arenitic sandstone,

homogeneous finer-grained sandstone and then passes up to argillaceous metasediment at the structural top. This sequence is unusual in itself and in its level of exposure within the project area. Further up section (structurally), there is an impure, strongly sheared marble sequence about 100m thick, with interbedded calc-silicate gneiss. The marble contains fine-grained graphite and locally epidote and diopside. There are also individual calc-silicate layers up to 1 m thick. Between the cordierite gneiss and marble there are outcrops of pegmatite with abundant black tourmaline. The marble is probably coeval with other marble units in the Lalamo Complex and in the southern part of the Xixano Complex dated at ca. 740 Ma (Melezhik et al., 2008).

Montepuez Complex

The Montepuez Complex forms a wedge-shaped unit of strongly deformed para- and orthogneiss on the northern flank of the Lurio Belt (Figure 1). It includes part of the Montepuez and Chiure (s.s.) Groups of Pinna et al. (1993), defined as part of the their Chiure Supergroup. The Montepuez Complex is lithologically similar to the adjoining Lalamo and Xixano Complexes, though the Montepuez and Lalamo Complexes are everywhere separated by a felsic gneiss unit attributed to the Nairoto Complex. The Montepuez Complex comprises orthogneisses ranging from granitic to amphibolitic in composition, and paragneisses comprising mainly quartzite, meta-arkose, marble, quartz-feldspar gneiss and biotite gneiss (Table 8). The rocks are strongly folded into tight and isoclinal folds on all scales, and have later been cut by a number of mainly northeasterly to southwesterly trending shear zones. The strong deformation makes the lithological succession very complex, with large variations on all scales both within and between the lithologies. The mineral parageneses present (hornblende –plagioclase –quartz ±garnet) suggest that the complex has generally undergone amphibolite-grade metamorphism. Chemostratigraphic methods, using $^{87}\text{Sr}/^{86}\text{Sr}$ ratios (Melezhik et al., 2007), have yielded an age between 1.1 and 1.05 Ga for the “tripartite” marble unit which is exposed in the quarries near Montepuez (Figure 15), which produce blocks for export and for national consumption.

Ocua Complex

The term “Ocua Complex” was introduced by Norconsult (2007a) to clarify existing confusion around the term “Lurio”. The term Lurio has been used in a lithostratigraphic sense (e.g. Lurio “Group” and “Supergroup” of Pinna et al., 1993), and as a structural entity (e.g. the Lurio Belt of Pinna et al., 1993; Kröner et al., 1997; Sacchi et al., 2000). The newly defined Ocua Complex includes the lithologies in the core of the Lurio Belt, previously considered as the type lithologies of the Lurio Group, by Pinna et al. (1993). It is mainly made up of highly deformed gneisses, commonly mylonitic. Typically, the lithologies are granulites and include

orthogneisses, commonly mafic, and metasupracrustal rocks (Table 8, Figure 16).

The high-strain character of the eastern Lurio Belt fades progressively to the southwest, where it becomes infolded within the Marrupa Complex and, to a lesser extent, the Nampula Complex Viola et al., 2008). Consequently, in the east, the Ocua Complex forms a continuous, ca. 20 km wide unit, while to the west, closer to the border with Malawi, the complex comprises a series of belt-like bodies, layers and lenses on all scales, which are concentrated along the wide northeasterly to southwesterly trending tectonic zone that separates the Nampula and Unango Complexes.

Due to its structural complexity, therefore, the Ocua Complex is probably a composite unit, containing slices of diverse rock units, deformed, transposed and dismembered during Pan-African tectonic events, and not originally a single lithostratigraphic unit. The complex can thus be regarded as a tectonic mélange including granulites, sheared and transposed high-grade gneisses and metasediments. The traditional separation into paragneisses and orthogneisses cannot be confidently made for large parts of the complex. A detailed study of the metamorphic development of the Ocua Complex by Engvik et al. (2007) documented peak metamorphic conditions of up to 1.57 ± 0.14 GPa and $949 \pm 92^\circ\text{C}$, corresponding to crustal depths of c. 55 km, at 557 ± 16 Ma.

Neoproterozoic metasedimentary rocks

Overlying the Mesoproterozoic complexes, two sequences of low-grade Neoproterozoic metasedimentary rocks have been recognised in northeastern Mozambique, north of the Lurio Belt. These were termed the Cobué and Geci Groups by Pinna et al. (1993), but the former has been renamed the Txitonga Group after a prominent mountain peak centrally located in the group; the town of Cobué is located outside the group (Figure 1).

Txitonga Group

The Txitonga Group overlies and is bounded by the Palaeoproterozoic Ponta Messuli Complex in the west and is covered by Karoo Supergroup rocks of the Maniamba graben to the east. It is dominated by metasedimentary rocks, mainly metagreywacke, metasandstone and quartz-mica schist and chlorite-rich schist. In the northern part of the unit there are numerous bodies of metagabbroic rock, greenstone and greenschist and minor felsic metavolcanic rocks. One (meta) rhyolite yields a crystallization age of 714 ± 17 Ma (Bjerksgård et al., 2009), demonstrating a Neoproterozoic age for the group. There is no indication that the metamorphic grade ever exceeded greenschist facies in this area, though close to Cobué, garnet and staurolite are found, indicating higher (amphibolite) metamorphic grade in the east. Pinna et al. (1993) reported the same metamorphic distribution, with sillimanite in the Cobué area. A late retrogressive event has, however, affected

the Txitonga lithologies, leading to regional sericitisation and local carbonatisation, so that the pattern of the earlier metamorphic event is difficult to document.

Primary native gold occurs in quartz veins in low-grade metasedimentary rocks associated with mafic dykes and sills in the Txitonga Group. Artisanal gold mining has taken place in the Txitonga Group since 1990 (Bjerkgård et al., 2009), with both alluvial and primary gold in quartz veins exploited.

Geci Group

The Geci Group occurs as four northeasterly to southwesterly trending lenses tectonically emplaced within Unango Complex rocks, southeast of Metangula (Figure 1). The group includes low-grade metamorphosed volcanic rocks, clastic carbonates, mudstones, sandstones, conglomerates and rocks with possible glacial affinities. The two most closely studied lenses consist of low-grade metamorphosed carbonate rocks with subordinate chlorite-muscovite schist and conglomerate. Although contacts between the Geci rocks and the granulite complexes are not exposed, the sharp discordance in metamorphic grade indicates that the contacts are tectonic. In places, primary depositional features are well preserved (Melezhik et al., 2006). The dominant rocks are calcarenites, dolarenites, calcite matrix-supported and dolostone clast-supported carbonate breccias forming beds with erosional bases, normal and reverse graded bedding, and well-developed Bouma sequences. Dolomitic, microbial and oolitic dolostone clasts were apparently derived from the margin of a shallow-water carbonate platform and redeposited by turbidity currents on a continental slope with calcareous sedimentation. A chemostatigraphic study by Melezhik et al. (2006) showed that the least-altered $^{87}\text{Sr}/^{86}\text{Sr}$ and $\delta^{13}\text{C}$ ratios suggest an apparent depositional age of either 590 to 585 or 630 to 625 Ma. This provides a lower age limit for juxtaposition of the low-grade Geci Group rocks and granulite-facies rocks of the Unango Complex.

Pan-African (Cambrian) intrusive rocks

The Ocua Complexes and the southern parts of the Unango and Marrupa Complexes have been intruded extensively, but not uniformly, by late- to post-tectonic "Pan-African" granites, during and immediately after the Pan-African orogeny, between ca. 550 and 490 Ma (Jacobs et al., 2008; Bingen et al., 2009). In this region, two suites are known as the *Malema* and *Niassa Suites*. A further suite, the more voluminous *Murrupula Suite*, intrudes the Nampula Complex, south of the Lurio Belt. The *Malema* and *Niassa Suites* do not correspond to the alkaline/carbonatite intrusives, which were included in the overview by Woolley (2001) and which formed part of the basis for the proposal that such complexes indicate the location of Proterozoic sutures (Burke et al., 2003). Alkaline intrusives found in the Unango Complex (Lulin, 1984; Bingen et al., 2009) are Neoproterozoic in age.

Malema Suite

A number of sub-circular to ellipsoidal granitoid ring complexes occur along a north-northeasterly oriented line parallel to, and within the Lurio Belt, where they intrude rocks of the Marrupa and Ocua Complexes. They appear to be particularly associated with the western extension of the Lurio Belt, west of the zone of most intense flattening, in a tectonic regime where the flattening strain has given way to folding and splayed shear zones. A number of smaller plutons and irregularly shaped bodies of granite that have an identical geophysical signature and topographic expression similar to the ring complexes are included in the suite. Three of the plutons are compositionally zoned, the Serra Romulo, Serra Nampatua and Lalaua plutons. Others are sub-circular in plan form, but appear to be composed only of granite (e.g. Serra Mancuni, Monte Sirapi plutons), while others (e.g. Malema pluton) are composed of charnockite. Still others are irregular in shape, such as the Chihulo pluton.

About half of the larger Malema Suite plutons are zoned ring complexes consisting of various compositional phases arranged in a more or less concentric fashion. Some plutons have sub-parallel, curved, external satellite bodies which resemble ring dykes (e.g. the Lalaua pluton). Pluton cores are typically unfoliated, but a weak marginal fabric, parallel to the contacts is often observed. The compositional variations seen include granite (ss), monzogranite, monzonite, syenite and charnockite (the latter typically forming a small, sub-circular core) with rare gabbro. All compositions tend to be equigranular, but porphyritic phases also occur.

Niassa Suite

The Niassa Suite consists of several granitic to syenitic intrusions that form prominent mountains from Meponda in the N, and continue southeastwards along the border with Malawi along a northwest to southeast trend. The suite includes four major ring complexes (Mt. Metonia, Mt. Livigire, Mt. Nicucule and Mt. Chande). Except for the latter, which consists of alkali-syenite surrounding a core of alkali-granite, they are all mainly syenitic in composition. Minor phases of concordant medium-grained, leucocratic gneissic granite are also recognised.

The Mt. Metonia syenite, 40 km south-southwest of Lichinga, is the largest of the syenitic ring dykes. It is made up of medium- to coarse-grained, equigranular homogeneous, pink-weathering quartz-biotite-syenite. Towards the centre of the ring, the pink quartz syenite is coarse-grained with large pink microcline perthite, minor plagioclase and quartz, biotite clots with poikilitic hornblende and magnetite with accessory titanite, apatite and epidote/zoisite.

The Mt. Livigire alkali syenite forms a large horseshoe-shaped intrusive complex ca. 80 km south of Lichinga, comprised of texturally heterograngular, medium- to coarse-grained, locally slightly foliated

	Group/Complex	Major or distinctive lithologies	Metamorphism
	Geci Group	Limestone, mica schist, metaconglomerate	Greenschist/ Amphibolite
Neoproterozoic	Txitonga Group	Mica schist, chlorite schist, metagreywacke, metasandstone, iron formations, metagabbro, greenstone, quartz-feldspar porphyry	Greenschist/ Amphibolite
	Ocua Complex	Mafic to felsic granulite gneiss, mylonitic leucogneiss tonalitic, dioritic, syenitic & granitic gneiss quartz-feldspar gneiss	Amphibolite/ Granulite
	Montepuez Complex	Granitic to granodioritic gneiss, biotite gneiss, quartz-feldspar gneiss, marble, quartzite	Amphibolite
	Lalamo Complex	Various paragneisses, e.g. marble, biotite gneiss, mica schist & metasandstone, granitic to granodioritic gneiss	Amphibolite
	M'Sawize Complex	Mafic granulite, banded migmatitic gneiss metatonalite, metagabbro	Granulite
	Muaquia Complex	Granitic, tonalitic, gabbroic, amphibolitic gneiss mica gneiss, quartz-feldspar gneiss, calc-silicate gneiss	Amphibolite
	Xixano Complex	Mafic granulite, enderbite, amphibolitic-dioritic gneiss various paragneiss, e.g. marble, biotite gneiss, mica schist & metasandstone, metarhyolite, granitic gneiss	Amphibolite/ Granulite
Mesoproterozoic	Meluco Complex	Granitic to granodioritic gneiss	Amphibolite
	Nairoto Complex	Migmatitic granitic to granodioritic gneiss	Amphibolite
	Marrupa Complex	Granitic to granodioritic gneiss, amphibolitic gneiss, banded migmatitic gneiss, leucogneiss, quartz-feldspar gneiss	Amphibolite
	Unango Complex	Granitic to granodioritic gneiss, charnockitic gneiss, amphibolite, migmatitic biotite-hornblende-gneiss, muscovite-biotite gneiss, quartz-feldspar-gneiss, quartzite (+/-kyanite)	Amphibolite/ Granulite
	Nampula Complex	Granitic, granodioritic to tonalitic gneiss, banded migmatitic biotite gneiss, leucogneiss, augen gneiss sillimanite gneiss, quartz-feldspar gneiss, amphibolite	Amphibolite
Palaeo-	Ponta Messuli Complex	Migmatitic paragneiss, augen gneiss, talc schist, amphibolite	Amphibolite/ Granulite

Figure 17. Overview of the main Proterozoic tectonostratigraphic units in northeast Mozambique north of the Lurio Belt. The Nampula complex, south of the Lurio Belt is also shown. The main tectonic boundaries are shown by the saw-tooth lines.

biotite-bearing alkali-granite to alkali syenite. The Mt. Nicucule intrusion forms a syenitic ring dyke with a diameter of 6.5 km, while the undeformed Mt. Chande alkali-syenite forms a ring structure around the central peak of alkali-granite.

Some members of the suite are granitic. For example the Mt. Lissiete granite is a distinctive intrusion forming the prominent mountain of Lissiete together with a number of large koppies to the east and north. The coarse-grained granite is homogeneous, unfoliated and composed of white to pale-pink feldspar, quartz, amphibole and abundant books of biotite reaching more than a centimetre in size. Some K-feldspar is evident.

Discussion

Lithostratigraphy and tectonostratigraphy

The ambition of this publication is to establish the lithostratigraphic/tectonostratigraphic framework adopted in the new map of northeastern Mozambique (Norconsult, 2007a; b). Hereafter, this framework, as summarized in Figure 17, is compared with the one of Pinna et al. (1993). The seminal work of Pinna et al. (1993) followed the first 1:1 000 000 scale geological map of the country (Pinna and Marteau, 1987), in which the major tectonostratigraphic units then recognized, were defined and delimited.

According to Pinna and Marteau (1987) the same fundamental Mesoproterozoic ("Mozambiquan") crustal blocks were continuous north and south of the Lurio Belt. With a revised and complex nomenclature, Pinna et al. (1993) subdivided the area into six broad tectonostratigraphic units (in bold), listed here with our approximate equivalent units (in italics). The Lurio Belt is considered to be a major terrane boundary separating the Nampula Complex to the south, with its distinctive and different lithostratigraphic package, from those to the north (e.g. Viola et al., 2008). High-convergence in the Lurio Belt resulted in formation of a tectonic mélange and in high-pressure granulite-facies metamorphism at 557 ± 16 Ma (Engvik et al. 2007; Viola et al., 2008). Hence, no pre-Lurio Belt units cross the belt.

- In the northwest, "**Unango Group**" granulites, corresponding to our (Palaeoproterozoic) *Ponta Messuli Complex*. However, Pinna et al (1993, p. 38) also point out that alternative interpretations have also been made for this unit, including "an extension of the Ubendian terrane of northern Malawi";
- Southeast of the above, a narrow belt of Neoproterozoic metasedimentary "Katangan" rocks of the **Geci** and **Cobué Groups** which we also recognize, as the *Geci* and *Txitonga Groups* respectively;
- To the southeast and along most of the border with Malawi, a series of granulite nappes referred to as the "**Unango Group**" of the "**Axial Granulite Complex**", including the **Lichinga Unit**, **Cuamba Unit** and **Meponda Unit**" (Pinna et al., 1993, Figure 3 and Table 1), which together roughly correspond to our *Unango Complex*.

These rocks were translated eastwards over the central and eastern parts of the region comprised of a broadly antiformal structure which contained a deformed sequence of Mesoproterozoic rocks comprising, in the model of Pinna et al. (1993), from bottom to top:

- Autochthonous migmatites of the "**Nampula Supergroup**" (Partly our *Nampula Complex*, south of the Lurio Belt and not the subject of this paper) in which the **Marrupa Group** approximately corresponds to our *Marrupa Complex*, the Nairoto Group to part of our Nairoto Complex and the Meluco Group, which includes our Meluco Complex, but is much more extensive (Pinna et al, 1993, Figure 12 and Table 11). We do not recognize Nampula Complex rocks north of the Lurio Belt;
- **Autochthonous supracrustal** rocks, including mylonites. We do not recognize this unit as such – it corresponds to various autochthonous units in the Mesoproterozoic *Marrupa Complex* and allochthonous Neoproterozoic rocks of the *Lalamo, Xixano, M'Sawize and Montepuez Complexes*;
- Rocks of the **Chiure** and **Metangula Supergroups**. Again these rocks do not correspond to any single units in our model, and occupy areas we interpret as forming units of the Neoproterozoic nappe complexes.

From the above it is clear that the differences in regional distribution and tectonostratigraphic classification between Pinna et al. (1993) and our work are considerable: the contrast is further complicated by differences in application of lithostratigraphic terms (see above).

Geochanical signatures and geological evolution

Using Rb-Sr isotope data in conjunction with their tectonostratigraphic model, Pinna et al. (1993) proposed a regional geological model involving the following sequence of events:

- 1100 to 850 Ma: Massive plutonic activity, limited deposition of supracrustal successions, granulite-facies metamorphism, orthogneiss emplacement and nappe tectonics during the "Mozambican orogeny". The Mesoproterozoic crustal blocks were considered to be continuous across the Lurio Belt;
- 900 to 538 Ma: Deposition of sediments (some units with a possible glacial affinity), correlated with the Katangan Supergroup of Zambia;
- ca. 550 Ma: Pan-African retrograde metamorphism and tectonics (including some thrusting) in an intra-continental environment.

The new mapping (Norconsult, 2007a, b), supported by geochemical data (Appendix), chemostratigraphic data (Melezhik et al., 2006; 2008) and some 60 U-Pb zircon or monazite age determinations (Kröner et al., 1997; Engvik et al., 2007; Jacobs et al., 2008; Viola et al., 2008; Bjerksgård et al., 2009; Bingen et al., 2009) leads to an improved, and quite different regional interpretation.

Palaeoproterozoic high grade felsic rocks, exposed in the northwestern corner of the country in the Ponta Messuli Complex, show a Archaean Sm/Nd depleted mantle model age and record a granulite-facies event dated at 1950 ± 15 Ma (Bingen et al., 2009). They are interpreted as forming a part of the northwestern foreland to the East African Orogen. This cratonic foreland extends westwards into Malawi and northwards into Tanzania and can be considered as the southeastern termination of the Ubendian and Usagaran Belts attached to the Congo-Tanzania Craton.

Four late-Mesoproterozoic to early-Neoproterozoic crustal blocks, the Unango, Marrupa, Nairobi and Meluco Complexes, form the greater part of the lower tectonostratigraphic level (Mesoproterozoic "basement") of the Mozambique Belt north of the Lurio Belt (Figures 1, 17; Viola et al., 2008). These complexes comprise mainly orthogneisses but also with significant sequences of supracrustal gneisses. The orthogneisses are largely intermediate to felsic in composition, metaluminous, medium- to high-K, alkali-calcic to shoshonitic. They intruded during a comparatively short time span, extending from ca. 1.06 to 0.95 Ga in the Unango Complex, ca. 1.03 to 0.95 Ga in the Marrupa Complex and ca. 0.95 Ga in the Meluco Complex. The most probable geotectonic setting for such extremely voluminous magmatism with the compositions seen is in a volcanic arc. Most of the high-K granitic to charnockitic rocks probably represents a significant degree of recycling of previously formed crust. Plutonic rocks of this type are commonly emplaced in relatively mature continental volcanic arcs and as large, post-collisional batholiths following terrane accretion. The presence of Palaeoproterozoic to Archaean detrital zircons in supracrustal rocks and (uncommon) inherited Archean zircons in some weakly peraluminous granitic gneisses is consistent with this interpretation (Bingen et al., 2009). The Unango Complex was affected by a first granulite-facies metamorphic event at 955 ± 9 Ma. This event can be broadly related to the Irumide orogeny in the Irumide Belt of Zambia (De Waele et al., 2006; Bingen et al., 2009), during which volcanic arcs probably accreted at the margin of the Congo-Tanzania Craton. Nevertheless, we find no clear evidence for major nappe tectonics and orogenesis during this stage (Viola et al., 2008). Consequently, the exact nature of this event is a matter of speculation, and could represent the products of a thermal pulse in the crust following voluminous magmatism or orogeny.

Deposition of the Txitonga and Geci Groups took place in the Neoproterozoic on the crystalline basement. The former overlies the Ponta Messuli Complex foreland and is unaffected by Pan-African high-grade metamorphism. The latter was deposited on the Unango Complex close to the foreland and also escaped high-grade metamorphism. The Geci group reflects platform to continental-slope sedimentation between ca. 630 and 585 Ma (Melezhik et al., 2006).

The Xixano, Muaquia, M'Sawize, Lalamo and Montepuez Complexes overlie the Mesoproterozoic basement with tectonic contacts and are interpreted as Pan-African nappes (Figures 1, 17; Viola et al. 2008). The coverage of geochemical data is not very dense for these complexes. Nevertheless, the Xixano Complex displays a very specific geochemical signature and can be used to extrapolate to the other Neoproterozoic nappe complexes. The large bodies of mafic to intermediate calcic, low-K orthogneisses in the Xixano Complex, dated at around 740 Ma (Bingen et al., 2009), and characterized by a weak radiometric signature on airborne geophysical surveys (Viola et al., 2008), are characteristic of primitive volcanic arcs. The evolved rocks appear to have a bimodal distribution including low-K tonalite and high-K granite. The mafic to intermediate rocks display granulite-facies assemblages and are interpreted as the lower part of a volcanic arc, either oceanic or pericontinental. The bulk of the magmatic activity in the Xixano, Lalamo and Montepuez Complexes is bracketed between ca. 820 and 700 Ma and consequently these complexes are interpreted as part of one arc or an assembly of arcs developed "outboard" of the Mesoproterozoic continent (Viola et al. 2008). In this context, the metasedimentary sequences they contain can be interpreted as having formed in fore-arc and/or back-arc basins. The occurrence of a continental "basement" older than ca. 820 Ma in the Xixano, Muaquia, M'Sawize, Lalamo and Montepuez Complexes is controversial. Possible evidence includes the ca. 1.1 to 1.05 Ga Montepuez marbles (Melezhik et al., 2008). Establishing the presence of a "basement" in these complexes is nevertheless a key element to reconstruct their paleogeography (oceanic vs. pericontinental arc complexes), and is a task for future research. The evolutionary reconstruction of ancient polyphase orogenic belts is a common problem. In the northernmost part of the East African Orogeny, for example, Şengör and Natal'in (1996) regarded the Arabian-Nubian shield as an example of Neoproterozoic "Turkic-type" orogeny, the key features of which are the formation of very large subduction-accretion complexes (fore-arc basins) into which magmatic arcs migrate, and produce net crustal growth. The assembly of the Xixano, Muaquia, M'Sawize, Lalamo and Montepuez Complexes has the characteristics of such an orogeny. The late-Neoproterozoic (Pan-African) compressional tectonic event was responsible for the final juxtaposition of all the crustal blocks including a major phase of nappe tectonics, leading to crustal stacking, deep burial and granulite-facies metamorphism at about 550 Ma (Engvik et al., 2007; Viola et al., 2008). The Neoproterozoic microcontinents formed "outboard" of the Mesoproterozoic continent were transported as nappes northwestwards onto the Mesoproterozoic crust (Viola et al. 2008). High-convergence in the Lurio Belt resulted in formation of a tectonic mélange under high-pressure granulite-facies metamorphic conditions at 557 ± 16 Ma (Engvik et al., 2007; Viola et al., 2008).

Limited Pan African granites and syenites were emplaced in the period between 550 and 490 Ma, mainly as late- to post-tectonic ring complexes, with plutons following regional tectonic lineaments (e.g. the Malema Suite plutons parallel the Lurio Belt).

Conclusion

New geological mapping and geochemical characterization of the main rock units in northeast Mozambique, north of the Lurio Belt, (Norconsult, 2007a; b) lead to a division of the crust into three fundamental tectonostratigraphic levels.

1. The Palaeoproterozoic Ponta Messuli Complex is regarded as part of the Ubendian-Usagaran foreland of the East African Orogen.
2. The Mesoproterozoic Unango, Marrupa, Nairoto and Meluco Complexes represent juvenile alkali-calcic to shoshonitic felsic crust that evolved between ca. 1.06 and 0.95 Ga. This crust probably formed in a continental-arc setting and was assembled at the southeastern margin of the Congo-Tanzania craton during the Irumidian orogeny.
3. The Xixano, Muaquia, M'Sawize, Lalamo and Montepuez Complexes are juvenile Neoproterozoic complexes, which overlie the Mesoproterozoic crust, which acted as their basement. Mafic to intermediate calcic, low-K, magmatic rocks in these complexes are characteristic of a primitive volcanic arc setting and suggest they developed as volcanic arcs “outboard” of the Mesoproterozoic continent. It is unclear if the four Mesoproterozoic complexes were juxtaposed before this and acted as a single crustal entity. These three tectonostratigraphic levels were juxtaposed into their present-day relative position during the Pan-African orogeny, peaking at around 550 Ma.

Acknowledgements

This work has been carried out as part of the Mineral Resources Management Capacity Building Project, Ministry of Mineral Resources of Mozambique, funded by the Nordic Development Fund and the World Bank, and implemented by a team mainly from the Geological Survey of Norway, the British Geological Survey and the National Directorate of Geology of Mozambique. The authors would like to dedicate the paper to the memory of the late Dr. Eric Hammerbeck, whose ever courteous encouragement played a major role in this project. We would also like to acknowledge the assistance of numerous individuals working at the offices of the Provincial Governors in Niassa, Cabo Delgado, Nampula and Zambesia Provinces. Finally, we thank Kevin Burke, Alex Kisters, Guido Schreurs and the editors for their helpful comments. The paper is being published with the permission of the National Directorate for Geology, Maputo and the Executive Director, BGS.

References

- Andreoli, M.A.G., 1984. Petrochemistry, tectonic evolution and metasomatic mineralisation of Mozambique Belt granulites from S. Malawi and Tete, Mozambique. *Precambrian Research*, 25, 161–186.
- Aquater, 1983a. Notícia explicativa Fohla Munhamade 16736 D2 (644), Maputo, 99pp.
- Aquater, 1983b. Carta dos Indícios não conhecidos pesquisas e minas (na escala 1: 50 000). Notícia explicativa Fohla Munhamade 1636 D 2 (644), Maputo, 73pp.
- Aquater, 1983c. Notícia explicativa Fohla Mocuba 1636 D4 (672), Maputo, 124pp.
- Aquater, 1983d. Quadrado 1636 (Munhamade) Blocos 52, Geological Map, scale 1: 50 000. Unpublished map, Maputo.
- Aquater, 1983e. Quadrado 1636 (Mocuba) Blocos 52, Geological Map, scale 1: 50 000. Unpublished geological map, Maputo.
- Aquater, 1983f. Carta dos Indícios não conhecidos pesquisas e minas (na escala 1: 50 000). Notícia explicativa Fohla Mocuba 1636 D4 (672), Maputo, 72pp.
- Barbarin, B., 1990. Granitoids: main petrogenetic classifications in relation to origin and tectonic setting. *Geological Journal* 25, 227–238.
- Bingen, B., Jacobs, J., Viola, G., Henderson, I.H.C., Skár, O., Boyd, R., Thomas, R.J., Solli, A., Key, R.M. and Daudi, E.X.F., 2009. Geochronology of the Precambrian crust in the Mozambique Belt of NE Mozambique, and implications for Gondwana assembly. *Precambrian Research*, 170, 231–255.
- Bjerkård, T., Stein, H. J., Bingen, B., Henderson, I. H. C., Sandstad, J. S. and Moniz, A., 2009. The Niassa Gold Belt, northern Mozambique – a segment of a continental-scale Pan-African gold-bearing structure. *Journal of African Earth Sciences*, 53, 45–58.
- Bloomfield, K., 1968. The pre-Karoo geology of Malawi, 5. Geological Survey of Malawi, Memoir, 166pp.
- Burke, K., Ashwal, L.F. and Webb, S.J., 2003. New way to map old sutures using deformed alkaline rocks and carbonatites. *Geology*, 31, 391–394.
- Costa, M., Casati, C. and di Bartolomeo, G., 1983. Cartografia geológica e prospecção mineira e geoquímica nas províncias de Nampula e da Zambésia (área de Alto Ligonha). Rel. AQUATER SPA, ING, Maputo.
- Costa, M., Ferrara, G., Sacchi, R. and Tonarini, S., 1992. Rb/Sr dating of the Upper Proterozoic basement of Zambesia, Mozambique. *Geologische Rundschau*, 81, 487–500.
- De Waele, B., Liégeois, J.P., Nemchin, A.A. and Tembo, F., 2006. Isotopic and geochemical evidence of Proterozoic episodic crustal reworking within the Irumide Belt of South-Central Africa, the southern metacratonic boundary of an Archaean Bangweulu Craton. *Precambrian Research*, 148, 225–256.
- Direcção Nacional de Geologia, 2001. Mozambique code of stratigraphic terminology and nomenclature, First edition (preliminary)
- Engvik, A.K., Tveten, E., Bingen, B., Viola, G., Erambert, M., Feito, P. and de Azavedo, S., 2007. P-T-t evolution and decompression textures of Pan-African high-pressure granulites, Lurio Belt, northeastern Mozambique. *Journal of Metamorphic Geology*, 25, 935–952.
- Frost, B.R., Barnes, C.G., Collins, W.J., Arculus, R.J., Ellis, W.J. and Frost, D.J., 2001. A geochemical classification for granitic rocks. *Journal of Petrology*, 42, 2033–2048.
- Grantham, G.H., Macey, P.H., Ingram, B.A., Roberts, M.P., Armstrong, R.A., Hokada, T., Shiraishi, K., Jackson, C., Bisnath, A., and Manhica, V., 2008. Terrane correlation between Antarctica, Mozambique and Sri Lanka; comparison of geochronology, lithology, structure and metamorphism and possible implications for the geology of southern Africa and Antarctica. In: M. Satish-Kumar, Y. Motoyoshi, Y. Osanai, Y. Hiroi and K. Shiraishi, (Editors), *Geodynamic evolution of East Antarctica: a key to the East-West Gondwana connection*. Geological Society, London, Special Publications 308, 91–119.
- Holmes, A., 1951. The sequence of Pre-Cambrian orogenic belts in South and Central Africa. In: K.S. Sandford and F. Blondel (Editors), *Proceedings of the 18th International Geological Congress. Association des Services Géologiques Africains*, London, pp. 254–269.
- Huntings Geology and Geophysics Ltd., 1984. Mineral Inventory Project. Final Report. ING, Maputo.
- Jacobs, J., Bingen, B., Thomas, R.J., Bauer, W., Wingate, M. and Feito, P., 2008. Early Palaeozoic orogenic collapse and voluminous late-tectonic magmatism in Dronning Maud Land and Mozambique: insights into the

- partially delaminated orogenic root of the East African–Antarctic Orogen? In: M. Satish-Kumar, Y. Motoyoshi, Y. Osanai, Y. Hiroi and K. Shiraishi (Editors) *Geodynamic evolution of East Antarctica: a key to the East-West Gondwana connection*. Geological Society, London, Special Publications, 308, 69–90.
- Jamal, D., 2005. Crustal evolution in NE Mozambique – implications for Gondwana reconstruction. PhD thesis. University of Cape Town, Cape Town.
- Jourde, G. and Wolff, J.P., 1974. Contribuição para o conhecimento da geologia da área de Montepuez (Grau quadrado 1339). BRGM, Orléans, DNG Rel., Maputo, 66pp.
- Jourde, G. and Vialette, Y., 1980. La chaîne du Lurio (Nord Mozambique). Un témoin de l'existence de chaînes Kibariennes (800–1350 Ma) en Afrique Orientale, Open File report, BRGM, Orléans, 75pp.
- Kröner, A., 2001. The Mozambique belt of East Africa and Madagascar: significance of zircon and Nd model ages for Rodinia and Gondwana supercontinent formation and dispersal. *South African Journal of Geology*, 104, 151–166.
- Kröner, A., Sacchi, R., Jaeckel, P. and Costa, M., 1997. Kibaran magmatism and Pan-African granulite metamorphism in northern Mozambique: single zircon ages and regional implications. *Journal of African Earth Sciences*, 25, 467–484.
- Kröner, A., Willner, A.P., Hegner, E., Jaeckel, P. and Nemchin, A.A., 2001. Single zircon ages, PT evolution and Nd isotopic systematics of high-grade gneisses in southern Malawi and their bearing on the evolution of the Mozambique belt in southeastern Africa. *Precambrian Research*, 109, 257–291.
- Lächelt, S., 1993. Carta Metalógénica de Moçambique. 1:1.000.000. ING, Maputo.
- Lächelt, S., 2004. Geology and mineral resources of Mozambique. Direcção Nacional de Geologia Moçambique, 515pp.
- Lächelt, S. and Daudi, E.X.F., 1999. Metallogenic epochs and phases in the Mozambican territory. *Journal of African Earth Sciences*, 28, 40–41.
- Lulin, J.M., 1984. Un nouveau gîte à Nb, Ta, U, REE d'origine magmatique en Afrique orientale: le complexe alcalin tectonisé de Meponda, Précambrien, province de Niassa, Mocambique, PhD thesis, Université d'Orléans, Doc. Bureau de Recherche Géologique et Minère, BRGM 87, Orléans.
- Marques, J.M., 2002. Mineral resources potential of Mozambique. unpublished manuscript, Maputo, 34pp.
- Marques, J.M., Lächelt, S. and Ferrara, M., 2000. Carta de jazigos e ocorrências minerais, escala 1:1.000.000. DNG, Maputo.
- McGregor, V. R. and Friend, C. R. L., 1997. Field recognition of rocks totally retrogressed from granulite facies; an example from Archaean rocks in the Paamiut region, South-West Greenland. *Precambrian Research*, 86, 59–70.
- Meert, J.G., 2003. A synopsis of events related to the assembly of eastern Gondwana. *Tectonophysics*, 362, 1–40.
- Melezhik, V.A., Kuznetsov, A.B., Fallick, A.F., Smith, R.A., Gorokhov, I.M., Jamal, D. and Catuane, F., 2006. Depositional environments and an apparent age of the Geci meta-limestones: constraints on geological history of northern Mozambique. *Precambrian Research* 148, 19–31.
- Melezhik, V.A., Bingen, B., Fallick, A.F., Gorokhov, I.M., Kuznetsov, A.B., Sandstad, J.S., Solli, A., Bjerkård, T., Henderson, I., Boyd, R., Jamal, D. and Moniz, A., 2008. Isotope chemostratigraphy of marbles in northeastern Mozambique. apparent depositional ages and regional implications. *Precambrian Research* 162, 540–558.
- Norconsult Consortium, 2007a. Mineral resources management capacity building project, Republic of Mozambique; Component 2: Geological infrastructure development project, Geological Mapping Lot 1; Sheet explanation: 32 sheets; scale: 1:250000, 778pp. + annexes. Credit No. NDF335, Report No. B6.f., National Directorate of Geology, Republic of Mozambique.
- Norconsult Consortium, 2007b. Mineral resources management capacity building project, Republic of Mozambique; Component 2: Geological Infrastructure Development Programme, Geophysical Interpretation (Lot1), 146pp., Credit No. NDF335, Report No. B4, National Directorate of Geology, Republic of Mozambique.
- Pinna, P., Jourde, G., Calvez, J.Y., Mroz, J.P. and Marques, J.M., 1993. The Mozambique Belt in northern Mozambique; Neoproterozoic (1100–850 Ma) crustal growth and tectogenesis, and superimposed Pan-African (800–550 Ma) tectonism. *Precambrian Research*, 62, 1–59.
- Pinna, P. and Marteau, P., 1987. Carta geológica de Moçambique, 1:1 000 000 scale, with explanatory notes. Instituto Nacional de Geología, Maputo, Maputo.
- Sacchi, R., Cadoppi, P. and Costa, M., 2000. Pan-African reactivation of the Lurio segment of the Kibaran Belt system: a reappraisal from recent age determinations in northern Mozambique. *Journal of African Earth Sciences*, 30, 629–639.
- Sacchi, R., Marques, J.M., Costa, M. and Casati, C., 1984. Kibaran events in the southernmost Mozambique belt. *Precambrian Research*, 25, 141–159.
- Saranga de Sousa, I., unpublished manuscripts. Niassa: Notícia Explicativa – 1999, 2000, 2001. DNG, Maputo.
- Sengör, A.M.C. and Natal'in, B.A., 1996. Turkic-type orogeny and its role in the making of the continental crust. *Annual Review of Earth and Planetary Science*, 24, 263–337.
- Thomas, R.J., Bauer, W., Bingen, B., de Azevedo, S., de Sousa Soares, H., Hollick, L., Feitio, P., Fumo, C., Gonzalez, E., Jacobs, J., Manhica, V., Manuel, S., Motuza, G., Tembe, D., Uachave, B. and Viola, G., 2006. Mozambique belt in the Milange-Mocuba-Malembo area, Moçambique. Abstract, 21st Colloquium of African Geology (CAG 21), Maputo, 161–163.
- Viola, G., Henderson, I.H.C., Bingen, B., Thomas, R.J., Smethurst, M.A. and De Azavedo, S., 2008. Growth and collapse of a deeply eroded orogen: Insights from structural and geochronological constraints on the Pan-African evolution of NE Mozambique. *Tectonics*, 27, TC5009, doi:10.1029/2008TC002284.
- Whalen, J.B., Currie, K.L. and Chappell, B.W., 1987. A-type granites: geochemical characteristics, discrimination and petrogenesis. *Contributions to Mineralogy and Petrology*, 95, 407–419.
- Woolley, A.R., 2001. Alkaline rocks and carbonatites of the world. Part 3: Africa. Geological Society of London, London. 372pp.

Editorial handling: L. D. Ashwal

Appendix. Whole-rock geochemical data, collected by XRF. Major elements in wt%, trace elements in ppm

Sample	UTM, E	UTM, N	Zone	Field name	Tectonic Unit	SiO ₂	TiO ₂	Al ₂ O ₃	Fe ₂ O ₃	FeOt	MgO	CaO	Na ₂ O	K ₂ O	MnO	P ₂ O ₅	Gltrap	SUM
31965	690892	8573736	36	Biotite-granite	Unango Complex	71.20	0.09	16.01	1.44	1.30	0.17	0.94	4.35	4.75	0.01	0.05	0.71	99.72
31341	697297	8538630	36	enderbite	Unango Complex	44.67	2.58	11.70	20.59	18.53	8.46	6.85	2.34	0.83	0.29	0.32	-0.28	98.35
31863	698895	8594032	36	Granitic gneiss	Unango Complex	78.34	0.10	11.54	1.14	1.03	0.10	0.58	3.29	3.94	<0.01	0.03	0.33	99.40
31319	699145	8534780	36	granitic gneiss	Unango Complex	60.34	0.97	17.57	6.35	5.72	0.40	2.92	4.82	5.20	0.21	0.28	0.07	99.14
31862	699167	8573686	36	Iron ore	Unango Complex	0.01	16.40	4.60	68.98	62.08	1.87	0.15	<0.1	0.02	0.26	0.02	-1.13	89.09
31861	701475	8572098	36	Chlorite amphibole rock	Unango Complex	45.50	3.37	14.11	14.45	13.01	6.25	8.52	2.82	0.79	0.18	0.52	1.89	98.41
31335	702235	8518106	36	porphyritic diorite	Unango Complex	52.91	2.16	15.68	9.25	8.33	2.79	5.20	4.15	3.07	0.11	1.25	0.87	97.45
31336	702235	8518106	36	granitic gneiss	Unango Complex	73.16	0.15	14.08	1.15	1.04	0.20	1.06	3.69	5.14	0.03	0.04	0.23	98.92
31334	702235	8518106	36	amphibolite	Unango Complex	48.40	2.42	14.36	12.15	10.94	6.63	10.18	3.02	0.76	0.17	0.37	0.55	99.02
31860	703050	8572330	36	Granulitic pyroxene gneiss	Unango Complex	56.00	1.68	16.14	9.89	8.90	1.28	4.01	4.48	4.49	0.24	0.42	0.20	98.82
31310	703060	8517170	36	metagabbroic gneiss	Unango Complex	47.67	1.66	13.27	15.00	13.50	6.80	11.05	2.18	0.20	0.22	0.12	0.64	98.81
31309	703060	8517170	36	andesitic dike	Unango Complex	55.71	1.62	14.33	6.48	5.83	2.46	1.80	3.91	3.37	0.06	0.94	6.99	97.66
31317	704410	8531985	36	granitic gneiss	Unango Complex	63.18	0.76	15.31	6.13	5.52	2.12	4.56	3.78	2.22	0.11	0.25	0.51	98.92
31311	704700	8529390	36	granitic gneiss	Unango Complex	70.28	0.56	13.80	3.36	3.02	0.55	1.60	4.46	3.81	0.08	0.13	0.16	98.78
31322	707600	8517530	36	quartz dioritic gneiss	Unango Complex	63.99	0.85	15.43	5.02	4.52	2.17	4.15	3.97	2.73	0.09	0.26	0.36	99.01
31823	707690	8586282	36	Metagabbro	Unango Complex	46.00	3.51	13.91	15.26	13.73	5.37	8.93	2.82	1.13	0.22	0.63	0.71	98.49
31321	708070	8517915	36	Gneiss granite	Unango Complex	74.91	0.25	11.13	4.61	4.15	0.02	0.57	2.16	5.39	0.04	0.04	0.18	99.29
31951	709534	8588644	36	Mafic granulite, gabbroic	Unango Complex	49.16	0.28	24.32	5.53	4.98	5.16	10.15	3.31	0.22	0.07	0.03	1.41	99.63
31327	711010	8521060	36	Mafic dike	Unango Complex	49.06	3.24	13.85	12.27	11.04	4.75	7.17	3.10	2.17	0.14	1.66	0.50	97.91
31326	711010	8521060	36	quartz dioritic gneiss	Unango Complex	48.49	3.22	13.49	12.16	10.94	4.74	7.09	2.92	2.47	0.16	1.76	1.45	97.94
31312	712835	8557540	36	biotite gneiss	Unango Complex	58.87	0.65	16.14	6.62	5.96	3.38	6.40	4.14	2.27	0.11	0.21	0.59	99.38
31328	713600	8530730	36	biotite-hbl gneiss	Unango Complex	62.47	0.91	15.48	5.32	4.79	2.34	4.42	3.99	2.50	0.09	0.29	0.40	98.21
31950	720830	8576368	36	Granitic/monzonitic gneiss	Unango Complex	64.39	0.82	15.90	5.41	4.87	0.46	0.93	4.34	6.02	0.16	0.11	0.92	99.45
31339	726277	8534962	36	qtz-diorite, dark	Unango Complex	56.01	0.97	18.56	6.89	6.20	3.45	6.43	4.88	1.47	0.12	0.31	0.04	99.14
31814	731245	8605294	36	felsic intermediate dyke	Unango Complex	63.39	0.50	13.59	7.24	6.52	0.07	1.60	4.96	3.85	0.25	0.07	4.37	99.87
31315	733640	8541300	36	metagabbroic gneiss	Unango Complex	51.47	0.73	16.79	9.05	8.15	8.00	9.64	2.59	0.76	0.15	0.14	0.19	99.52
31330	735675	8509020	36	biotite-gneiss	Unango Complex	60.37	0.74	15.94	6.68	6.01	3.25	5.25	3.26	2.85	0.11	0.24	0.40	99.09
31313	736675	8539785	36	quartz porphyry	Unango Complex	74.99	0.33	12.54	1.66	1.49	0.11	0.27	4.06	4.90	0.08	0.07	0.17	99.16
31244	745306	8492000	36	Pale grey granodioritic gneiss	Unango Complex	66.13	0.54	15.20	4.58	4.12	1.80	3.90	3.36	2.57	0.10	0.11	0.57	98.87
33598	748853	8187242	36	Amphibolite/metagabbro	Unango Complex	47.69	1.97	13.83	16.71	15.04	5.51	7.41	2.90	1.39	0.29	0.30	0.16	98.17
33579	750065	8174161	36	Metagabbro/ultramafics	Unango Complex	50.80	0.80	13.88	11.97	10.77	8.85	10.86	2.25	0.47	0.20	0.09	0.29	100.44
31262	750417	8559106	36	Granite	Unango Complex	77.15	0.14	12.05	0.65	0.59	0.07	0.43	3.46	4.60	<0.01	0.02	0.27	98.85
31215	750565	8471495	36	Amphibolite?, plagioclase rich,	Unango Complex	51.96	1.53	15.47	14.82	13.34	1.71	4.79	4.25	2.75	0.30	0.76	-0.07	98.26
33578	752917	8180764	36	Metagabbro/ultramafics	Unango Complex	41.50	1.86	14.79	19.14	17.23	7.82	14.95	0.70	0.22	0.32	0.16	-0.18	101.28
31898	755753	8642594	36	Granite	Unango Complex	78.41	0.05	11.77	0.56	0.50	0.12	0.82	3.41	4.09	0.02	0.02	0.29	99.56
31833	758179	8608226	36	Pyroxene-gabbro	Unango Complex	50.07	0.78	4.92	11.38	10.24	16.05	15.27	0.54	0.10	0.22	0.05	0.38	99.78
31828	759233	8597152	36	Quartz-feldsp argneiss	Unango Complex	75.21	0.17	13.05	1.46	1.31	0.16	0.87	3.42	4.96	0.05	0.04	0.26	99.65
33562	759561	8196993	36	Precambrian syenite	Unango Complex	59.95	1.14	16.47	5.41	4.87	1.11	2.26	4.51	6.01	0.18	0.40	0.91	98.35
31277	759649	8509634	36	Migmatitic granitic orthogneiss	Unango Complex	71.97	0.32	13.75	1.90	1.71	0.41	1.31	3.51	4.86	0.05	0.07	0.24	98.39
31220	759926	8477771	36	Grey, charnockitic gneiss with q-pl-granofels	Unango Complex	55.96	1.45	17.86	6.23	5.61	1.82	3.82	5.17	4.58	0.11	0.56	0.24	97.81
31790	760473	8620032	36	Metagabbro/ultramafics	Unango Complex	74.91	0.30	12.95	1.47	1.32	0.17	0.44	3.62	5.27	0.06	0.03	0.14	99.36
33581	761480	8188906	36	Metagabbro/ultramafics	Unango Complex	51.93	0.29	3.55	8.84	7.96	18.61	14.77	0.83	0.20	0.20	0.03	0.37	99.62
33582	761480	8188906	36	Metagabbro/ultramafics	Unango Complex	35.91	0.06	0.93	14.84	13.36	34.95	0.10	<0.1	0.02	0.13	0.03	11.86	98.84
31826	762328	8600342	36	Quartz-feldspar gneiss	Unango Complex	76.58	0.17	12.13	1.23	1.11	0.12	0.57	3.13	4.86	<0.01	0.04	0.99	99.82
33591	763318	8202216	36	Grey feldspar augen gneiss	Unango Complex	59.33	0.89	19.17	3.54	3.19	0.93	2.79	4.39	6.52	0.05	0.24	0.30	98.16
31943	763450	8642296	36	Microgranite/leptite	Unango Complex	76.95	0.11	11.90	0.26	0.23	0.09	0.18	2.20	6.87	<0.01	0.03	0.34	98.94
31827	763963	8592848	36	Granitic gneiss	Unango Complex	77.67	0.16	11.62	1.14	1.03	0.14	0.59	3.07	4.37	0.05	0.01	0.23	99.05
33590	764775	8202277	36	Grey feldspar augen gneiss	Unango Complex	66.30	0.62	15.51	3.24	2.92	1.02	2.26	3.84	5.63	0.05	0.25	0.26	98.97
33589	765330	8202319	36	Grey feldspar augen gneiss	Unango Complex	61.62	1.04	16.92	4.47	4.02	1.21	2.89	4.10	5.92	0.05	0.33	0.20	98.74
22780	765588	8469748	36	Metasupracrustal	Unango Complex	73.41	0.98	12.67	6.07	5.46	1.49	0.69	0.69	2.00	0.10	0.04	0.43	98.57
31247	766306	8499462	36	Felsic band in migm granulitic rock	Unango Complex	65.36	0.46	16.63	3.70	3.33	1.08	3.23	5.47	1.57	0.08	0.19	0.24	98.01
31784	767612	8617840	36	px-q-pl-granofels	Unango Complex	65.18	0.52	16.74	3.90	3.51	1.03	2.96	4.70	3.39	0.09	0.19	0.28	98.99
31756	767799	8562646	36	enderbite?, retrogr	Unango Complex	61.63	0.71	15.33	6.58	5.92	1.38	3.09	5.58	3.76	0.20	0.25	0.13	98.62
31259	771129	8481688	36	Basalt dyke in migmatite	Unango Complex	52.84	2.41	14.71	9.61	8.65	4.11	5.89	3.38	2.99	0.12	1.33	0.51	97.91
31971	771225	8645666	36	Granite	Unango Complex	78.44	0.09	11.77	0.86	0.77	0.20	0.86	3.03	4.33	0.02	0.06	0.50	100.16
31261	774403	8486350	36	Migmatitic biotite-gneiss	Unango Complex</													

S	Cl	F	Mo	Nb	Zr	Y	Sr	Rb	U	Th	Pb	Cr	V	As	Sc	Hf	Ba	Sb	Sn	Ga	Zn	Cu	Ni	Yb	Co	Ce	La	Nd	W	Cs	Ta	Pr
<0.1	<0.1	<5	5	114	5	567	141	<10	27	60	11	23	<5	<10	<10	1725	<10	<10	17	16	10	<5	<15	6	18	13	<10	23	<10	<10	<10	
<0.1	<0.1	0.4	<5	14	116	28	386	16	<10	8	<10	64	339	<5	28	<10	367	<10	<10	14	178	110	73	<15	108	65	17	32	<10	<10	16	12
<0.1	<0.1	<0.1	<5	6	153	34	126	151	<10	31	34	<10	10	<5	<10	<10	231	<10	<10	15	19	<10	<5	<15	5	51	27	27	30	<10	<10	<10
<0.1	<0.1	<0.1	<5	5	39	22	172	20	<10	6	<10	21	10	<5	20	<10	1872	<10	<10	23	73	13	<5	<15	7	20	<10	19	16	<10	<10	<10
<0.1	<0.1	1.48	<5	5	28	5	8	11	<10	13	<10	1089	5719	<5	<10	29	<10	18	<10	54	717	<10	187	32	600	<10	44	<10	<10	<10	120	<10
0.10	<0.1	0.52	<5	21	192	29	531	12	<10	5	<10	109	284	5	37	<10	359	<10	<10	14	128	44	79	<15	61	66	35	35	<10	<10	14	11
<0.1	<0.1	0.37	<5	27	351	29	2262	71	<10	12	47	13	140	<5	21	42	3592	<10	<10	20	133	22	8	<15	18	350	146	143	<10	<10	<10	32
<0.1	<0.1	<0.1	<5	8	134	5	296	272	<10	28	77	18	13	<5	<10	<10	947	<10	<10	22	31	11	<5	<15	<5	30	22	19	33	14	<10	<10
<0.1	<0.1	0.32	<5	17	170	27	418	14	<10	5	<10	217	246	<5	37	12	290	<10	<10	21	96	70	70	<15	51	45	27	33	<10	<10	<10	
<0.1	0.10	0.16	<5	7	22	50	247	22	<10	5	<10	16	43	<5	24	<10	1875	<10	<10	25	211	21	<5	<15	17	61	26	59	16	<10	<10	<10
<0.1	<0.1	0.28	<5	5	91	37	137	8	<10	5	<10	161	470	<5	54	<10	980	<10	<10	17	83	222	62	<15	60	<10	14	<10	<10	<10		
<0.1	<0.1	0.5	<5	30	538	35	888	144	<10	31	17	46	123	<5	13	25	4434	<10	<10	15	94	23	14	<15	17	326	166	135	<10	<10	22	
<0.1	<0.1	<0.1	<5	5	107	15	541	36	<10	8	<10	59	130	<5	20	<10	814	<10	<10	15	77	29	8	<15	18	24	19	21	22	<10	<10	<10
<0.1	<0.1	<0.1	<5	9	234	31	278	67	<10	13	<10	13	25	<5	<10	<10	752	<10	<10	14	93	16	<5	<15	8	46	19	32	24	<10	<10	<10
<0.1	<0.1	<0.1	<5	7	211	24	535	85	<10	10	12	52	86	<5	22	<10	715	<10	<10	16	62	33	19	<15	15	44	26	22	18	<10	<10	<10
0.10	<0.1	0.55	<5	32	246	39	450	21	<10	5	<10	56	338	<5	33	12	561	<10	<10	16	148	37	24	<15	59	133	35	54	<10	<10	17	12
<0.1	<0.1	<0.1	<5	43	1104	89	175	102	<10	28	<10	12	<10	<5	<10	27	501	<10	<10	16	48	13	<5	<15	<5	262	136	119	12	<10	<10	31
<0.1	<0.1	<0.1	<5	5	<5	829	<5	<10	5	<10	275	43	<5	22	<10	176	<10	<10	13	36	25	100	<15	31	<10	<10	<10	<10	<10	<10	<10	
<0.1	<0.1	0.42	<5	26	344	44	1288	45	<10	5	16	106	191	<5	29	22	1768	<10	<10	22	132	34	57	<15	37	198	82	105	<10	12	10	24
<0.1	<0.1	0.29	<5	28	353	42	1141	57	<10	5	11	101	196	7	24	16	1736	<10	<10	16	158	32	51	<15	37	205	70	103	<10	<10	<10	12
<0.1	<0.1	<0.1	<5	5	67	24	546	57	<10	6	17	108	118	<5	22	<10	777	<10	<10	14	74	38	26	<15	21	19	17	12	24	<10	<10	<10
<0.1	<0.1	0.1	<5	7	196	23	549	77	<10	8	11	126	94	<5	15	<10	681	<10	<10	12	68	23	22	<15	19	52	24	31	20	<10	<10	<10
<0.1	<0.1	<0.1	<5	22	1070	67	133	77	<10	6	30	11	<10	<5	15	25	1138	<10	<10	20	159	<10	<5	<15	8	111	63	84	10	<10	<10	13
<0.1	<0.1	<0.1	<5	7	106	17	1050	11	<10	5	<10	41	122	<5	21	18	706	<10	<10	15	76	39	20	<15	21	30	29	19	11	<10	<10	<10
<0.1	<0.1	0.2	<5	125	566	113	154	48	<10	21	<10	10	<10	<5	15	16	239	<10	<10	23	331	<10	<5	<15	7	220	113	107	15	<10	10	24
<0.1	<0.1	<0.1	<5	5	94	19	355	18	<10	7	<10	302	163	<5	30	<10	298	<10	<10	10	67	84	128	<15	42	25	17	18	19	<10	<10	<10
<0.1	<0.1	<0.1	<5	10	151	25	526	100	<10	26	<10	53	144	<5	23	<10	850	<10	<10	17	75	41	18	<15	20	102	58	46	16	<10	<10	14
<0.1	<0.1	<0.1	<5	10	192	91	60	75	<10	6	<10	11	17	<5	10	<10	346	<10	<10	17	53	<10	<5	<15	6	51	26	39	31	<10	<10	<10
<0.1	<0.1	<0.1	<5	6	120	16	358	67	<10	10	<10	42	61	<5	31	<10	1042	<10	<10	12	67	<10	<5	<15	14	27	12	23	26	<10	<10	<10
<0.1	<0.1	<0.1	<5	6	67	41	217	22	<10	5	<10	45	382	<5	49	<10	306	11	<10	<10	125	22	<5	<15	55	21	20	17	<10	<10	28	12
0.11	<0.1	<0.1	<5	37	17	487	9	<10	5	<10	353	270	<5	34	<10	166	11	<10	<10	103	83	85	<15	54	16	12	17	<10	17	<10		
<0.1	<0.1	<0.1	<5	5	108	5	43	73	<10	10	11	13	10	<5	<10	<10	457	<10	<10	10	18	12	<5	<15	<5	<10	<10	12	33	<10	<10	<10
<0.1	<0.1	0.25	6	77	531	95	473	49	<10	9	<10	10	21	<5	24	26	1379	<10	<10	26	211	21	<5	<15	31	224	98	131	<10	14	13	38
<0.1	<0.1	<0.1	<5	5	83	39	88	5	<10	10	<10	135	499	<5	53	<10	48	<10	<10	<10	98	75	50	<15	79	30	<10	31	<10	18	<10	
<0.1	<0.1	<0.1	<5	5	102	5	195	57	<10	19	<10	10	10	<5	<10	<10	1031	<10	<10	10	11	<10	<5	<15	5	<10	<10	23	<10	<10	<10	
<0.1	<0.1	0.16	<5	5	39	17	97	<5	<10	7	<10	468	266	5	70	<10	144	<10	<10	10	75	178	302	<15	72	<10	<10	12	<10	<10	<10	
<0.1	<0.1	<0.1	<5	5	148	13	67	98	<10	7	<10	16	10	<5	18	<10	478	<10	<10	10	32	12	<5	<15	5	17	17	19	31	<10	<10	<10
<0.1	<0.1	0.11	<5	34	587	51	240	145	<10	11	44	<10	22	<5	11	42	2003	<10	<10	10	154	15	<5	<15	7	200	94	77	10	<10	<10	25
<0.1	<0.1	<0.1	<5	6	241	18	263	137	<10																							

Sample	UTM, E	UTM, N	Zone	Field name	Tectonic Unit	SiO ₂	TiO ₂	Al ₂ O ₃	Fe ₂ O ₃	FeO	MgO	CaO	Na ₂ O	K ₂ O	MnO	P ₂ O ₅	Gt _{lap}	SUM
33510	787095	8435113	36	Charnockitic gneiss	Unango Complex	73.66	0.29	12.29	2.34	2.11	0.07	0.69	3.29	5.41	0.04	0.02	0.10	98.21
31897	787955	8654778	36	Charnokite	Unango Complex	75.23	0.17	13.30	1.09	0.98	0.32	1.98	4.00	2.96	0.02	0.05	0.52	99.65
31212	788690	8558874	36	Brownish granulitic gneiss, fine grained	Unango Complex	69.57	0.43	14.36	3.01	2.71	0.59	1.46	3.58	5.19	0.06	0.12	0.75	99.12
31211	788959	8557434	36	Fine grained granitic gneiss,	Unango Complex	75.27	0.13	12.82	1.54	1.39	0.13	0.71	4.50	3.80	0.05	0.03	0.16	99.14
31217	790176	8461102	36	Granitic gneiss, K-feldspar phryic	Unango Complex	68.77	0.50	14.63	3.38	3.04	0.90	2.46	3.08	4.31	0.08	0.17	0.35	98.63
31229	793775	8526498	36	Migmatitic biotite-granodioritic gneiss	Unango Complex	72.14	0.45	12.80	3.17	2.85	0.22	0.95	3.92	5.30	0.10	0.06	0.26	99.36
31202	793813	8557092	36	Hornblende diorite, med-grained	Unango Complex	58.78	0.73	16.82	5.59	5.03	2.75	4.43	3.52	3.50	0.11	0.22	1.80	98.25
31238	795362	8527310	36	Grey fine-gr quartz-feldspathic gneiss	Unango Complex	68.80	0.56	14.00	3.48	3.13	0.27	1.29	4.39	4.90	0.12	0.10	1.02	98.92
31870	798031	8573358	36	Granodiorite	Unango Complex	66.49	0.48	16.67	2.85	2.57	0.74	2.07	5.09	3.81	0.06	0.16	0.60	99.02
31842	798317	8707936	36	Pyroxene-plagioclase gneiss	Unango Complex	60.94	0.89	16.47	5.86	5.27	2.46	4.76	3.11	3.65	0.10	0.30	0.71	99.26
31753	799467	8573177	36	Med-grained quartzofeldspathic gneiss	Unango Complex	74.10	0.28	13.25	2.08	1.87	0.29	0.76	3.90	4.50	0.08	0.07	0.38	99.69
31843	799489	8711446	36	Gneissic granite	Unango Complex	72.63	0.12	12.79	2.02	1.82	0.06	1.36	3.53	4.59	0.03	0.02	0.93	98.07
31776	799836	8634248	36	foliated granite / quartzofeldspathic gneiss	Unango Complex	66.17	0.41	16.68	3.19	2.87	0.93	2.47	4.87	3.95	0.08	0.17	0.82	99.75
31221	801478	8480199	36	K-feldspar phryic, granitic gneiss	Unango Complex	72.70	0.27	12.98	1.79	1.61	0.29	1.51	3.07	5.25	0.03	0.06	0.45	98.39
31772	802248	8588401	36	tonalite, porphyric	Unango Complex	65.89	0.44	15.98	3.52	3.17	1.25	3.00	4.59	3.13	0.08	0.16	0.84	98.90
31773	802387	8588307	36	granodiorite, porphyric, foliated	Unango Complex	66.50	0.47	15.61	3.56	3.20	1.24	2.67	4.07	3.76	0.07	0.17	0.98	99.10
31754	803492	8582917	36	foliated tonalite	Unango Complex	68.45	0.39	15.57	2.51	2.26	1.03	2.45	4.22	3.84	0.06	0.11	0.54	99.16
31251	808494	8526410	36	Kfeldspar-phryic monzo-granite	Unango Complex	63.42	0.84	14.50	5.10	4.59	2.58	3.43	3.72	4.29	0.09	0.33	0.20	98.49
31752	813454	8584335	36	foliated tonalite	Unango Complex	67.21	0.46	15.13	3.30	2.97	1.65	2.96	3.70	3.77	0.06	0.11	0.97	99.32
31223	814130	8481778	36	Granulitic gneiss	Unango Complex	66.56	0.73	15.02	4.62	4.16	0.62	3.11	3.85	3.75	0.13	0.25	0.38	99.03
33573	814470	8243889	36	Metarhyolite	Unango Complex	63.04	0.50	18.14	3.06	2.75	0.26	1.01	5.63	6.73	0.11	0.07	0.23	98.79
31803	818090	8699075	36	px-pl gneiss	Unango Complex	61.59	1.51	13.99	8.00	7.20	1.54	3.65	3.35	4.33	0.14	0.56	0.25	98.93
31237	822419	8517280	36	Grey fine grained bi-rich gneiss	Unango Complex	62.73	1.00	16.46	6.82	6.14	2.97	3.88	2.79	2.58	0.08	0.06	0.37	99.74
31224	822967	8489034	36	Granulitic orthogneiss, K-feldspar phryic	Unango Complex	74.51	0.30	12.47	2.10	1.89	0.35	1.35	2.55	5.04	0.03	0.08	0.32	99.12
35230	727598	8595436	36	GREENSTONE	Unango Complex	43.08	3.15	14.89	16.75	15.08	5.71	8.16	2.70	0.88	0.23	0.92	2.19	98.65
35231	731530	8599388	36	PHYRIC GREENSTONE.	Unango Complex	46.29	1.68	16.50	12.32	11.09	6.56	9.11	2.18	1.03	0.22	0.19	2.51	98.59
33472	177075	8420431	37	Syenite, Na-rich	Unango Complex	56.69	0.11	23.46	2.68	2.41	0.09	0.25	10.02	4.43	0.06	<0.01	0.26	98.05
37219	179929	8531824	37	HORNBLENDE GNEISS	Unango Complex	61.06	0.85	16.00	7.95	7.16	0.68	3.60	3.48	4.10	0.21	0.25	0.06	98.24
31891	180554	8710022	37	Granite gneiss	Unango Complex	73.83	0.21	13.25	1.87	1.68	0.24	1.09	3.23	5.22	0.03	0.05	0.21	99.24
31890	181567	8709812	37	Granite	Unango Complex	75.39	0.11	13.19	1.07	0.96	0.01	0.49	3.07	6.24	<0.01	0.02	0.17	99.77
31889	182163	8709595	37	Granite	Unango Complex	71.04	0.25	14.04	1.81	1.63	0.19	0.80	3.44	6.19	0.03	0.04	0.19	98.01
31888	183147	8709600	37	Augen gneiss	Unango Complex	61.68	0.77	17.93	4.86	4.37	1.06	2.80	4.27	5.40	0.10	0.25	0.27	99.39
31960	183240	8702869	37	Feldspar-phryic rock	Unango Complex	65.19	0.69	16.04	3.94	3.55	1.82	3.54	4.28	3.25	0.08	0.17	0.34	99.35
31887	184074	8709709	37	Plagioclase-pyroxene-biotite-garnet (quartz) rock (mongerite ?)	Unango Complex	57.67	1.10	16.63	7.73	6.96	3.72	6.86	3.59	1.32	0.15	0.38	0.17	99.31
31885	184786	8709707	37	Garnet-rich quartz-feldspar rock	Unango Complex	62.02	0.75	14.70	10.37	9.33	0.29	3.34	1.75	5.50	0.38	0.22	0.05	99.37
31886	184786	8709707	37	Plagioclase-biotite-amphibole-quartz garnet-rich rock	Unango Complex	42.21	3.33	13.36	20.64	18.58	6.25	10.87	1.89	0.21	0.25	0.02	0.06	99.08
22776	185894	8548072	37	Mangeritic gneiss	Unango Complex	57.47	1.73	15.43	8.81	7.93	2.60	4.95	3.69	2.76	0.17	0.49	0.11	98.21
31884	185957	8709911	37	Quartz-rich biotite gneiss	Unango Complex	77.32	0.17	11.07	1.53	1.38	0.06	0.50	2.64	5.15	0.03	0.02	0.13	98.63
31883	186587	8709796	37	Biotite granite gneiss	Unango Complex	62.97	0.17	19.51	3.34	3.01	0.09	0.37	7.83	4.07	0.10	0.01	0.29	98.74
31946	189485	8596462	37	Plagioclase porphyry	Unango Complex	69.53	0.64	13.95	3.64	3.28	0.77	1.90	3.88	4.32	0.10	0.17	0.15	99.06
34291	189718	8540600	37	Granitic gneiss	Unango Complex	69.37	0.44	14.40	2.76	2.48	0.52	1.52	3.79	5.13	0.07	0.14	0.17	98.29
22782	190728	8508496	37	Charnockite	Unango Complex	70.22	0.35	14.54	2.08	1.87	0.29	1.68	3.45	5.20	0.04	0.09	0.32	98.27
34295	191900	8553800	37	Quartz monzonite	Unango Complex	64.77	1.06	14.72	5.36	4.82	1.15	2.94	3.85	4.14	0.11	0.29	0.14	98.54
31955	193760	8602002	37	Hornblende-plag-qtz-garnet gneiss	Unango Complex	59.78	0.98	16.38	8.42	7.58	0.76	2.85	5.81	2.89	0.24	0.32	0.11	98.52
34273	196247	8513422	37	Mangeritic gneiss	Unango Complex	57.88	0.98	17.08	8.46	7.61	0.82	4.36	4.86	3.31	0.28	0.37	-0.10	98.30
22790	196949	8506256	37	Quartz monzonite	Unango Complex	65.02	0.68	16.09	3.93	3.54	0.72	2.60	4.02	4.45	0.10	0.21	0.26	98.08
22788	199332	8501376	37	Quartz monzonite	Unango Complex	72.53	0.31	13.65	1.92	1.73	0.34	1.38	3.17	5.22	0.03	0.07	0.56	99.18
34275	199454	8509226	37	Augengneiss	Unango Complex	66.11	0.62	15.45	3.70	3.33	0.64	2.67	3.80	4.58	0.08	0.18	0.38	98.22
31801	201521	8655856	37	bio(px)-pl gneiss	Unango Complex	59.32	0.96	18.19	5.84	5.26	0.76	3.61	5.22	3.91	0.19	0.37	0.09	98.46
31957	204074	8575166	37	Quartzitic rock	Unango Complex	96.52	0.05	1.06	1.27	1.14	0.05	0.02	<0.1	0.08	<0.01	0.02	0.29	99.31
31956	204255	8576572	37	Granitic Gneiss	Unango Complex	62.58	0.20	21.22	1.43	1.29	0.48	2.83	6.63	3.30	0.04	0.03	0.86	99.60
33507	206404	8370252	37	Mangerite	Unango Complex	62.40	0.75	17.95	2.67	2.40	0.53	1.43	4.01	8.17	0.06	0.13	0.18	98.27
31805	206967	8583214	37	syenite	Unango Complex	59.28	0.50	13.97	8.15	7.34	1.78	0.69	7.44	4.72	0.09	0.53	1.79	98.93
31806	207210	8583830	37	pyroxenite	Unango Complex	52.54	0.27	11.65	10.49	9.44	1.83	4.85	4.46	7.72	0.31	1.06	3.03	98.21
31807	207210	8583830	37	pyroxenite	Unango Complex	55.64	0.21	9.44	16.86	15.17	0.67	1.62	8.75	3.70	0.30	0.20	1.10	98.50
31808	207210	8583830	37	pyroxenite	Unango Complex	14.94	0.06	4.04	8.40	7.56	3.89</td							

S	Cl	F	Mo	Nb	Zr	Y	Sr	Rb	U	Th	Pb	Cr	V	As	Sc	Hf	Ba	Sb	Sn	Ga	Zn	Cs	Ni	Yb	Co	Ce	La	Nd	W	Cs	Ta	Pr	
<0.1	<0.1	<0.1	<5	24	486	110	37	141	<10	17	16	20	<10	<5	<10	<10	338	<10	<10	16	58	<10	7	<15	<5	124	73	57	37	<10	<10	12	
<0.1	<0.1	<0.1	<5	5	61	5	214	81	<10	12	<10	23	16	<5	<10	<10	357	<10	<10	11	25	10	<5	<15	6	<10	11	<10	22	<10	<10	<10	
<0.1	<0.1	0.1	<5	13	441	47	217	212	<10	14	20	19	38	<5	12	11	1093	<10	<10	16	57	13	<5	<15	7	131	42	47	17	12	<10	<10	
<0.1	<0.1	<0.1	<5	5	135	25	74	72	<10	9	<10	27	<10	<5	<10	<10	984	<10	<10	14	42	14	<5	<15	7	15	19	11	30	<10	<10	<10	
<0.1	<0.1	<0.1	<5	18	154	47	304	163	<10	18	15	50	51	<5	19	<10	1231	<10	<10	13	53	12	<5	<15	8	51	28	26	27	<10	<10	<10	
<0.1	<0.1	<0.1	<5	19	558	61	49	126	<10	11	12	26	<10	<5	15	<10	440	<10	<10	20	82	19	<5	<15	<5	103	62	53	19	<10	<10	<10	
<0.1	<0.1	0.17	<5	7	132	43	564	96	<10	9	<10	39	104	<5	14	<10	1187	<10	<10	13	73	19	18	<15	17	45	24	23	19	<10	<10	<10	
<0.1	<0.1	<0.1	<5	21	560	80	87	127	<10	18	18	16	11	<5	17	14	717	<10	<10	19	91	17	<5	<15	5	128	52	67	15	<10	<10	<10	
<0.1	<0.1	<0.1	<5	8	197	24	424	104	<10	10	12	<10	39	<5	11	<10	1281	<10	<10	17	55	17	<5	<15	6	58	34	33	25	<10	<10	<10	
<0.1	<0.1	0.16	<5	9	174	20	553	102	<10	6	19	67	116	<5	20	<10	1342	<10	<10	19	83	23	7	<15	17	50	28	23	18	<10	<10	<10	
<0.1	<0.1	<0.1	<5	5	181	7	105	118	<10	17	28	31	10	<5	<10	<10	726	<10	<10	11	49	<10	<5	<15	7	138	105	46	31	13	<10	<10	
<0.1	<0.1	0.41	<5	117	180	129	55	292	19	62	30	12	<10	<5	<10	<10	97	<10	<10	25	75	<10	<5	<15	6	85	58	49	39	<10	<10	<10	
<0.1	<0.1	<0.1	<5	7	151	33	385	111	<10	10	22	24	45	<5	<10	<10	1528	<10	<10	17	75	10	<5	<15	8	10	28	14	23	<10	<10	<10	
<0.1	<0.1	<0.1	<5	8	167	17	175	121	<10	20	15	25	14	<5	14	<10	1045	<10	<10	10	34	13	<5	<15	6	148	92	63	29	<10	<10	<10	
<0.1	<0.1	<0.1	<5	11	129	21	452	216	<10	15	18	41	61	<5	10	<10	920	<10	<10	15	54	15	<5	<15	10	25	52	31	24	<10	<10	<10	
<0.1	<0.1	<0.1	<5	7	142	28	433	149	<10	11	<10	39	52	<5	11	<10	912	<10	<10	15	58	<10	6	<15	11	37	36	37	29	<10	<10	<10	
<0.1	<0.1	<0.1	<5	6	114	14	387	108	<10	9	15	21	42	<5	<10	<10	848	<10	<10	12	46	14	<5	<15	9	22	17	13	29	<10	<10	<10	
<0.1	<0.1	<0.1	<5	10	192	25	430	140	<10	11	16	136	120	<5	16	<10	1017	<10	<10	15	67	54	32	<15	18	59	34	33	18	<10	<10	<10	
<0.1	<0.1	<0.1	<5	5	90	17	516	78	<10	11	<10	48	62	<5	13	<10	1363	<10	<10	10	43	10	12	<15	12	13	14	16	28	<10	<10	<10	
<0.1	<0.1	<0.1	<5	16	579	38	318	48	<10	7	14	15	29	<5	14	14	1757	<10	<10	15	85	13	<5	<15	8	65	35	45	18	<10	<10	<10	
<0.1	<0.1	<0.1	<5	51	751	25	29	125	<10	55	37	<10	<10	<5	<10	56	123	<10	<10	15	69	<10	<5	<15	7	389	257	133	18	<10	<10	41	
<0.1	<0.1	0.17	5	23	551	82	267	117	<10	10	19	38	88	<5	14	18	1094	<10	<10	22	116	18	<5	<15	19	124	59	72	<10	<10	15		
<0.1	<0.1	<0.1	<5	13	131	5	488	93	<10	25	12	149	115	<5	17	<10	1168	<10	<10	17	80	22	26	<15	23	107	59	39	10	<10	<10	13	
<0.1	<0.1	<0.1	<5	6	194	18	157	119	<10	12	15	<10	19	<5	19	<10	778	<10	<10	10	44	13	<5	<15	5	102	65	42	27	<10	<10	<10	
<0.1	<0.1	0.26	<5	19	95	32	513	25	<10	<5	<10	44	262	<5	28	<10	490	<10	<10	10	126	21	51	<15	72	59	43	27	<10	<10	<10		
<0.1	<0.1	0.23	<5	6	58	18	449	31	<10	6	<10	76	168	<5	33	<10	438	<10	<10	13	103	35	54	<15	54	<10	<10	10	<10	14	10		
<0.1	<0.1	<0.1	<5	17	1188	45	381	65	<10	5	11	<10	39	<5	22	44	2822	<10	<10	14	112	<10	5	<15	8	84	34	48	14	18	<10	<10	12
<0.1	<0.1	<0.1	<5	5	208	5	319	75	<10	6	<10	25	22	<5	13	<10	969	<10	<10	11	36	<10	<5	<15	7	29	23	15	23	<10	<10	<10	
<0.1	<0.1	<0.1	<5	5	204	5	28	140	<10	12	16	11	<10	<5	<10	<10	120	<10	<10	11	22	11	<5	<15	6	69	36	24	26	<10	<10	<10	
<0.1	<0.1	<0.1	<5	8	294	24	81	102	<10	10	13	14	<10	<5	17	<10	437	<10	<10	10	47	<10	<5	<15	5	94	54	45	21	<10	<10	<10	
<0.1	<0.1	<0.1	<5	13	457	30	287	79	<10	<5	12	<10	42	<5	16	12	1621	<10	<10	18	62	12	<5	<15	9	25	18	19	11	<10	<10	<10	
<0.1	<0.1	<0.1	<5	8	164	22	511	72	<10	7	13	42	76	<5	18	<10	1289	<10	<10	13	62	13	8	<15	12	53	22	23	20	<10	<10	<10	
<0.1	<0.1	<0.1	<5	10	120	43	607	19	<10	<5	<10	25	163	<5	31	<10	361	<10	<10	16	86	15	<5	<15	21	58	30	46	22	<10	<10	<10	
<0.1	<0.1	<0.1	<5	14	52	43	101	82	<10	10	11	10	10	<10	<5	37	10	662	<10	<10	14	70	<10	<5	<15	10	42	10	28	13	<10	<10	<10
0.28	<0.1	0.27	<5	5	21	14	329	<5	<10	<5	<10	15	749	<5	43	<10	110	<10	<10	15	141	22	<5	<15	81	<10	<10	<10	<10	<10	11	<10	
<0.1	<0.1	<0.1	<5	14	249	51	416	55	<10	<5	<10	45	141	<5	17	<10	1237	<10	<10	18	108	16	6	<15	20	106	44	54	26	<10	<10	15	
<0.1	<0.1	<0.1	<5	5	437	13	35	94	<10	17	18	12	<10	<5	<10	<10	255	<10	<10	11	31	<10	<5	<15	5	144	94	68	23	<10	<10	17	
<0.1	<0.1	<0.1	<5	73	1549	5	221	107	<10	10	<10	10	<10	<5	<10	<10	27	<10	<10	13	51	<10	<5	<15	7	32	<10	13	<10	<10	<10		
<																																	

Sample	UTM, E	UTM, N	Zone	Field name	Tectonic Unit	SiO ₂	TiO ₂	Al ₂ O ₃	Fe ₂ O ₃	FeO	MgO	CaO	Na ₂ O	K ₂ O	MnO	P ₂ O ₅	Gt _{tp}	SUM
33593	241969	8305992	37	Granitic orthogneiss	Unango Complex	74.19	0.25	12.88	1.25	1.13	0.23	1.02	3.05	5.31	0.02	0.05	0.21	98.47
33592	248021	8309992	37	Granitic orthogneiss	Unango Complex	65.86	0.97	13.68	6.23	5.61	0.83	2.35	3.27	4.90	0.08	0.26	0.57	98.99
33586	250368	8303631	37	Felsic/intermediate granulites/charnockites	Unango Complex	75.01	0.28	11.99	2.84	2.56	0.08	0.85	2.33	5.97	0.03	0.05	0.13	99.55
33556	262351	8317840	37	Pan-African granites	Unango Complex	69.30	0.50	14.11	3.26	2.93	0.48	1.81	2.70	5.78	0.02	0.11	0.81	98.89
34288	742064	8527300	37	Quartz monzonite	Unango Complex	64.50	0.94	15.60	4.60	4.14	1.28	3.18	4.26	3.51	0.08	0.27	0.22	98.45
22792	218416	8494372	37	Granitic gneiss	Marrupa Complex	74.38	0.19	12.66	1.57	1.41	0.26	1.13	3.61	4.01	0.06	0.06	0.15	98.08
22773	231051	8512990	37	Tonalitic gneiss	Marrupa Complex	75.17	0.17	13.64	1.41	1.27	0.26	1.03	4.31	3.45	0.05	0.09	0.28	99.88
37241	231954	8684996	37	Dioritic gneiss	Marrupa Complex	61.60	1.28	15.56	6.42	5.78	1.65	2.96	4.48	3.77	0.15	0.51	0.30	98.69
37242	231954	8684996	37	Granitic orthogneiss	Marrupa Complex	69.83	0.49	14.58	3.20	2.88	0.62	1.57	4.14	3.93	0.04	0.16	0.47	99.03
34292	244835	8480275	37	Granitic gneiss	Marrupa Complex	69.13	0.31	15.70	2.35	2.12	0.94	1.79	4.57	3.57	0.07	0.10	0.34	98.86
34293	246159	8479490	37	Granitic gneiss	Marrupa Complex	70.92	0.23	15.01	1.88	1.69	0.63	2.09	4.94	1.97	0.06	0.10	0.22	98.04
34287	247880	8469118	37	Granitic gneiss	Marrupa Complex	75.42	0.26	12.66	1.37	1.23	0.28	0.95	3.36	4.70	0.06	0.07	0.12	99.26
33503	250690	8404299	37	Gneissic granite with mafic dykes.	Marrupa Complex	73.64	0.31	12.62	1.44	1.30	0.31	0.93	2.83	5.68	0.02	0.05	0.22	98.05
34297	251050	8472510	37	Granodi gneiss	Marrupa Complex	73.84	0.43	12.68	2.36	2.12	0.81	1.05	3.54	3.89	0.07	0.10	0.25	99.03
33479	259647	8373067	37	Syenite	Marrupa Complex	61.43	0.47	17.09	4.58	4.12	1.26	2.47	6.78	3.39	0.19	0.17	0.30	98.13
34274	262406	8476174	37	Granitic gneiss	Marrupa Complex	70.52	0.32	15.22	1.77	1.59	0.31	1.08	3.83	5.47	0.03	0.05	0.26	98.86
33502	269824	8440454	37	Granitic gneiss	Marrupa Complex	72.11	0.30	13.97	1.79	1.61	0.38	1.57	3.40	4.88	0.05	0.09	0.51	99.03
37238	270155	8700622	37	Quartzofeldspathic gneiss	Marrupa Complex	69.51	0.26	16.52	2.06	1.85	0.50	2.65	4.75	2.42	0.05	0.08	0.30	99.09
34282	271555	8510006	37	Granitic gneiss	Marrupa Complex	74.83	0.28	12.69	1.49	1.34	0.30	0.86	3.15	5.08	0.05	0.07	0.23	99.03
34284	272608	8508010	37	Granodi gneiss	Marrupa Complex	68.93	0.69	14.40	3.82	3.44	0.81	1.88	3.68	4.14	0.07	0.19	0.35	98.95
31839	274161	8647892	37	Granitic gneiss	Marrupa Complex	72.96	0.25	13.85	2.37	2.13	0.38	1.23	3.63	4.37	0.04	0.07	0.24	99.39
33508	274416	8423162	37	Gneissic mangerite	Marrupa Complex	67.22	0.78	14.88	3.62	3.26	0.77	1.42	5.21	4.20	0.16	0.24	0.13	98.64
37236	276590	8677408	37	Quartz leuco diorite	Marrupa Complex	68.84	0.46	14.92	2.77	2.49	1.02	2.46	3.60	4.14	0.07	0.12	0.21	98.62
33498	283087	8435408	37	Monzonitic granite	Marrupa Complex	78.92	0.22	11.11	1.00	0.90	0.05	0.37	2.90	4.71	<0.01	0.02	0.13	99.43
26813	284330	8425956	37	Quartz-rich granitic gneiss (602)	Marrupa Complex	73.65	0.28	13.58	2.13	1.92	0.70	2.35	4.53	1.10	0.04	0.09	0.20	98.65
33345	286120	8479996	37	Granitic gneiss	Marrupa Complex	75.45	0.11	12.23	1.68	1.51	0.02	0.52	3.20	4.96	<0.01	0.03	0.20	98.42
33251	306339	8461572	37	granitic gneiss	Marrupa Complex	74.12	0.14	14.14	1.21	1.09	0.27	1.70	4.45	2.55	0.04	0.03	0.22	98.87
38410	306368	8606984	37	Plagioclase gneiss	Marrupa Complex	67.95	0.42	14.93	4.73	4.26	0.61	2.97	3.98	2.38	0.13	0.11	0.20	98.40
33253	308221	8523726	37	granitic gneiss	Marrupa Complex	67.57	0.54	15.46	2.84	2.56	0.59	2.06	3.72	4.88	0.06	0.14	0.29	98.15
33428	319769	8498526	37	Tonalitic orthogneiss	Marrupa Complex	70.25	0.27	14.27	2.70	2.43	0.36	1.46	2.86	5.24	0.06	0.10	0.77	98.35
37273	322187	8618362	37	Granodioritic gneiss	Marrupa Complex	69.01	0.51	14.74	3.35	3.02	1.31	2.79	4.72	2.08	0.08	0.15	0.48	99.22
37274	322234	8618324	37	Microgranodioritic dyke	Marrupa Complex	69.65	0.45	14.66	2.38	2.14	0.44	1.17	3.84	5.33	0.02	0.11	0.22	98.26
37229	324095	8706898	37	Intermediate orthogneiss	Marrupa Complex	56.34	0.65	9.00	6.62	5.96	6.42	15.38	1.54	2.09	0.16	0.23	0.78	99.21
33405	326441	8518115	37	Granitic Gneiss	Marrupa Complex	71.49	0.30	14.44	1.76	1.58	0.38	1.38	3.59	5.32	0.05	0.09	0.22	99.01
37227	327696	8704212	37	LEUCOCRATIC GNEISS	Marrupa Complex	67.93	0.32	15.64	3.64	3.28	1.44	3.85	4.54	1.31	0.08	0.10	0.59	99.45
26831	328522	8423696	37	Ultramafics (harzburgite?) (701)	Marrupa Complex	47.32	0.56	6.20	10.11	9.10	17.55	15.77	0.53	0.14	0.18	0.05	0.30	98.70
26829	329549	8422945	37	Ultramafics (harzburgite?) (701)	Marrupa Complex	48.99	0.59	6.29	9.00	8.10	16.10	15.51	0.99	0.34	0.18	0.07	0.36	98.42
37235	329570	8696308	37	Charnockite	Marrupa Complex	56.34	0.90	16.66	7.65	6.89	4.03	6.41	3.57	2.10	0.14	0.37	0.27	98.45
33341	329690	8534768	37	Tonalitic gneiss	Marrupa Complex	71.91	0.17	15.31	1.68	1.51	0.39	2.81	4.63	1.36	0.04	0.08	0.26	98.64
33252	335562	8537364	37	granitic gneiss	Marrupa Complex	73.00	0.14	14.78	1.37	1.23	0.40	2.38	4.34	2.11	0.05	0.08	0.23	98.87
37239	337182	8600746	37	Amphibolite	Marrupa Complex	47.91	2.55	13.07	14.92	13.43	5.84	9.83	2.79	0.87	0.25	0.33	0.16	98.51
33408	340035	8563232	37	Granitic gneiss	Marrupa Complex	72.13	0.13	14.47	1.37	1.23	0.18	1.01	3.88	5.17	0.03	0.03	0.39	98.80
26826	340193	8417284	37	Economic, calcsilicate	Marrupa Complex	66.77	0.62	14.60	2.48	2.23	2.01	3.91	7.66	0.64	0.08	0.02	0.18	98.97
26827	340193	8417284	37	Economic, sulphidic	Marrupa Complex	69.23	0.69	13.67	3.91	3.52	<0.01	0.94	6.96	0.52	<0.01	0.05	3.05	98.96
26828	340193	8417284	37	Economic, gossan	Marrupa Complex	17.83	0.34	3.70	65.22	58.70	1.26	0.96	1.36	0.11	0.08	0.04	3.43	94.33
37268	344765	8624470	37	Granodioritic gneiss	Marrupa Complex	63.22	0.76	16.06	4.76	4.28	2.41	4.55	3.89	2.61	0.07	0.14	0.36	98.83
33202	347437	8551266	37	Granodioritic(tonalitic) migmatitic gneiss	Marrupa Complex	71.31	0.36	14.42	2.72	2.45	0.55	2.05	4.09	2.90	0.08	0.10	0.23	98.80
26821	351155	8390767	37	Gneissic bt-granite (602)	Marrupa Complex	71.65	0.25	14.09	1.86	1.67	0.32	1.32	3.71	5.17	0.01	0.10	0.25	98.73
33205	353422	8635806	37	Granite	Marrupa Complex	75.36	0.19	11.72	2.56	2.30	0.05	0.87	3.33	4.08	0.03	0.03	0.18	98.42
37226	353463	8649630	37	Migmatised granitic orthogneiss	Marrupa Complex	76.10	0.13	11.73	1.40	1.26	0.11	0.61	2.94	4.81	0.03	0.06	0.28	98.20
33207	353877	8638948	37	Quartz dioritic gneiss	Marrupa Complex	59.29	1.52	15.16	7.88	7.09	2.32	4.44	4.01	2.90	0.14	0.37	0.25	98.28
33206	353958	8637452	37	Granitic mylonite	Marrupa Complex	69.77	0.52	14.97	2.82	2.54	0.64	2.19	4.32	3.03	0.04	0.13	0.41	98.83
33204	354416	8620838	37	Tonalitic gneiss	Marrupa Complex	65.99	0.39	17.79	2.44	2.20	0.87	3.80	5.27	1.70	0.04	0.11	0.31	98.71
33343	354793	8542848	37	Granitic gneiss	Marrupa Complex	72.41	0.28	13.71	1.48	1.33	0.30	1.07	3.72	4.61	0.02	0.07	0.40	98.07
33407	355376	8513482	37	Granodioritic gneiss	Marrupa Complex	67.87	0.46	16.22	2.63	2.37	1.00	2.67	4.74	2.63	0.04	0.12	0.39	98.77
33203	357122	8569532	37	Granitic gneiss	Marrupa Complex	75.82	0.26	11.96	1.52	1.37	0.09	0.45	2.68	5.83	0.03	0.03	0.18	

S	Cl	F	Mo	Nb	Zr	Y	Sr	Rb	U	Th	Pb	Cr	V	As	Sc	Hf	Ba	Sb	Sn	Ga	Zn	Cu	Ni	Yb	Co	Ce	La	Nd	W	Cs	Ta	Pr
<0.1	<0.1	<0.1	<5	6	136	<5	63	118	<10	15	16	<10	16	<5	<10	<10	535	<10	<10	<10	20	10	<5	<15	7	30	30	<10	20	<10	<10	<10
<0.1	<0.1	0.13	<5	24	542	49	318	127	<10	9	16	15	30	<5	10	40	1750	<10	<10	10	93	16	<5	<15	12	106	45	53	10	<10	11	15
<0.1	<0.1	<0.1	<5	6	653	9	50	108	<10	9	15	<10	<10	<5	<10	49	178	<10	<10	11	40	10	<5	<15	6	28	17	17	16	<10	<10	<10
<0.1	<0.1	<0.1	<5	12	400	28	305	167	<10	54	22	20	26	<5	<10	30	1143	<10	<10	15	40	12	<5	<15	7	298	188	100	18	<10	10	37
<0.1	<0.1	0.23	<5	9	273	29	374	68	<10	8	15	<10	65	<5	13	<10	1029	<10	<10	10	62	16	6	<15	13	40	23	21	27	<10	<10	<10
<0.1	<0.1	<0.1	<5	13	112	21	125	155	<10	16	12	20	17	<5	<10	<10	762	<10	<10	10	41	<10	<5	<15	5	55	46	21	39	<10	<10	<10
<0.1	<0.1	<0.1	<5	17	123	37	112	101	<10	15	11	13	12	<5	<10	<10	816	<10	<10	15	38	<10	<5	<15	6	28	16	15	39	<10	<10	<10
<0.1	<0.1	<0.1	<5	17	437	49	374	94	<10	5	13	10	56	<5	13	18	1646	<10	<10	12	84	<10	<5	<15	12	122	64	53	25	<10	<10	<10
<0.1	<0.1	<0.1	<5	6	246	13	317	97	<10	8	11	25	23	<5	<10	<10	1620	<10	<10	11	41	<10	<5	<15	7	67	55	19	29	<10	<10	<10
<0.1	<0.1	<0.1	<5	6	122	12	250	70	<10	6	<10	21	28	<5	12	<10	1440	<10	<10	10	58	<10	<5	<15	6	28	21	10	34	<10	<10	<10
<0.1	<0.1	<0.1	<5	14	119	13	297	53	<10	7	12	20	26	<5	<10	<10	784	<10	<10	10	44	<10	<5	<15	6	25	13	<10	36	<10	<10	<10
<0.1	<0.1	<0.1	<5	18	166	40	109	127	<10	19	14	29	<10	<5	11	<10	828	<10	<10	10	43	<10	5	<15	<5	108	84	32	37	<10	<10	13
<0.1	<0.1	<0.1	<5	10	178	27	128	231	<10	30	11	11	16	<5	<10	<10	574	<10	<10	10	22	<10	<5	<15	<5	73	57	25	35	<10	<10	<10
<0.1	<0.1	<0.1	<5	14	258	54	126	80	<10	11	<10	<10	26	<5	<10	<10	795	<10	<10	12	65	<10	6	<15	6	104	51	48	35	<10	<10	10
<0.1	<0.1	<0.1	<5	13	218	43	139	108	<10	21	14	10	<10	<5	<10	<10	1236	<10	<10	11	36	<10	<5	<15	<5	183	101	61	33	<10	<10	19
<0.1	<0.1	<0.1	<5	7	154	21	244	76	<10	12	12	14	22	<5	<10	<10	1706	<10	<10	10	35	<10	<5	<15	6	68	39	22	30	<10	<10	<10
<0.1	<0.1	<0.1	<5	6	124	6	947	54	<10	<5	<10	15	27	<5	<10	14	2114	<10	<10	10	39	<10	<5	<15	<5	27	23	11	34	<10	<10	<10
<0.1	<0.1	<0.1	<5	16	169	36	93	183	<10	24	13	10	13	<5	<10	<10	640	<10	<10	10	30	<10	<5	<15	<5	88	56	26	37	<10	<10	<10
<0.1	<0.1	<0.1	<5	15	287	59	199	95	<10	13	13	21	34	<5	12	<10	1135	<10	<10	11	56	<10	5	<15	8	110	79	51	33	<10	<10	15
<0.1	<0.1	<0.1	<5	5	129	5	334	91	<10	10	16	40	19	<5	<10	<10	1655	<10	<10	11	41	<10	<5	<15	7	15	27	<10	25	<10	<10	<10
<0.1	<0.1	<0.1	<5	52	340	61	309	93	<10	9	<10	<10	13	<5	10	14	1165	<10	<10	21	80	<10	<5	<15	5	94	64	48	37	<10	<10	11
<0.1	<0.1	<0.1	<5	8	127	19	331	110	<10	7	15	<10	39	<5	<10	<10	1061	<10	<10	10	50	<10	<5	<15	7	59	34	21	34	<10	<10	<10
<0.1	<0.1	<0.1	<5	10	222	27	44	62	<10	10	<10	14	<10	<5	<10	<10	333	<10	<10	10	20	<10	<5	<15	<5	38	26	18	39	<10	<10	<10
<0.1	<0.1	<0.1	<5	9	217	16	99	169	<10	18	13	10	<10	<5	<10	<10	912	<10	<10	10	25	<10	<5	<15	<5	92	16	10	36	<10	<10	<10
<0.1	<0.1	<0.1	<5	8	310	80	9	310	<10	6	<10	23	10	<5	<10	<10	908	<10	<10	10	30	<10	<5	<15	<5	11	<10	<10	39	<10	<10	<10
<0.1	<0.1	<0.1	<5	8	314	33	386	39	<10	<5	<10	38	21	<5	<18	12	1388	<10	<10	10	84	<10	<5	<15	10	74	31	35	31	<10	<10	<10
<0.1	<0.1	<0.1	<5	12	319	42	244	113	<10	15	15	18	32	<5	<10	<10	2193	<10	<10	14	56	<10	<5	<15	5	133	85	47	29	<10	<10	13
<0.1	<0.1	<0.1	<5	228	7	497	103	<10	34	21	14	21	<5	<10	<10	3868	<10	<10	10	48	19	<5	<15	5	247	171	69	26	15	<10	24	
<0.1	<0.1	<0.1	<5	9	171	38	371	48	<10	11	16	21	47	<5	17	<10	883	<10	<10	10	58	<10	12	<15	9	66	44	27	35	<10	<10	<10
<0.1	<0.1	<0.1	<5	10	361	15	597	113	<10	39	29	12	17	<5	<10	<10	2888	<10	<10	12	47	14	<5	<15	5	204	147	68	33	<10	<10	23
<0.1	<0.1	<0.1	<5	13	125	49	272	68	<10	12	12	110	112	<5	28	<10	1063	<10	<10	10	99	<10	44	<15	17	58	28	41	19	12	<10	14
<0.1	<0.1	<0.1	<5	8	170	22	176	142	<10	18	18	<10	13	<5	<10	<10	1100	<10	<10	10	46	<10	<5	<15	<5	94	71	31	37	<10	<10	<10
<0.1	<0.1	<0.1	<5	5	74	13	338	19	<10	7	<10	16	48	<5	16	<10	389	<10	<10	11	66	<10	<5	<15	8	36	21	19	32	<10	<10	<10
<0.1	<0.1	<0.1	<5	5	33	17	108	5	<10	<5	<10	1891	243	5	61	<10	249	<10	<10	10	49	23	274	<15	55	26	<10	11	<10	<10	<10	
<0.1	<0.1	<0.1	<5	5	59	17	172	8	<10	5	13	2173	188	<5	62	<10	204	<10	<10	10	55	24	201	<15	54	12	22	23	12	<10	<10	11
<0.1	<0.1	0.14	<5	7	163	21	700	67	<10	<5	<10	96	154	<5	26	11	1162	<10	<10	10	19	34	<15	19	47	24	23	20	13	<10	<10	<10
<0.1	<0.1	<0.1	<5	5	110	6	656	26	<10	<5	<10	15	13	<5	<10	<10	1110	<10	<10	10	45	10	<5	<15	5	18	20	<10	36	<10	<10	<10
<0.1	<0.1	<0.1	<5	5	93	5	549	38	<10	<5	10	13	15	<5	<10	<10	1655	<10	<10	10	38	<10	<5	<15	<5	30						

Sample	UTM, E	UTM, N	Zone	Field name	Tectonic Unit	SiO ₂	TiO ₂	Al ₂ O ₃	Fe ₂ O ₃	FeO	MgO	CaO	Na ₂ O	K ₂ O	MnO	P ₂ O ₅	Gt _{tp}	SUM
37286	395318	8656352	37	Granitic gneiss	Marrupa Complex	65.17	0.95	15.02	4.27	3.84	1.06	2.01	3.25	5.41	0.04	0.32	0.60	98.09
37260	396411	8654206	37	Granodioritic migmatitic gneiss	Marrupa Complex	69.08	0.41	14.92	2.13	1.92	0.70	2.13	2.70	6.05	0.03	0.12	0.46	98.74
37284	397954	8700928	37	Granitic/granodioritic migmatitic gneiss	Marrupa Complex	70.96	0.35	14.37	2.28	2.05	0.91	1.91	3.30	4.14	0.03	0.13	0.32	98.70
26832	399129	8441659	37	Banded migmatite; Bt-Pl-Qtz gneiss (615)	Marrupa Complex	69.82	0.37	14.88	3.12	2.81	0.70	2.30	4.28	2.86	0.05	0.12	0.26	98.77
26802	407616	8416103	37	Granitic gneiss (614)	Marrupa Complex	69.31	0.46	14.09	3.79	3.41	0.44	1.72	3.36	4.97	0.04	0.15	0.13	98.46
38418	409347	8593708	37	Gabbro	Marrupa Complex	42.33	4.70	14.49	17.49	15.74	6.33	7.99	2.80	1.05	0.20	1.21	-0.28	98.30
33224	414058	8513166	37	Granitic gneiss	Marrupa Complex	73.68	0.06	14.47	0.68	0.61	0.06	0.66	4.33	3.81	0.12	0.01	0.47	98.35
37259	414923	8731530	37	Pyroxene-amphibolitic gneiss	Marrupa Complex	48.44	0.46	11.92	9.91	8.92	8.86	16.58	1.24	0.51	0.24	0.22	0.61	99.00
26816	418246	8414883	37	Bt-Pl-Qtz gneiss, migmatised (211)	Marrupa Complex	69.28	0.30	15.23	2.84	2.56	0.61	2.00	3.88	4.27	0.03	0.06	0.22	98.73
39299	418530	8654549	37	Migmatitic gneiss	Marrupa Complex	55.13	0.74	16.90	6.79	6.11	4.14	9.01	4.13	1.03	0.06	0.28	0.25	98.45
38417	419068	8597970	37	Granite	Marrupa Complex	68.85	0.18	15.56	1.79	1.61	0.35	2.50	4.55	2.78	0.03	0.06	0.31	96.97
38440	420673	8618820	37	Magnetite quartzite	Marrupa Complex	50.41	0.03	0.33	43.98	39.58	2.33	0.88	0.13	0.02	0.07	0.34	-0.53	98.00
38439	422942	8616110	37	Granitic gneiss	Marrupa Complex	73.81	0.09	13.69	0.91	0.82	0.10	0.56	3.45	5.66	<0.01	0.02	0.38	98.68
37293	432054	8717276	37	Granitic gneiss	Marrupa Complex	59.30	0.95	12.98	4.55	4.10	2.34	6.51	3.39	5.74	0.14	0.72	0.56	97.17
26807	459235	8433529	37	Leucogneiss (612)	Marrupa Complex	73.91	0.16	13.29	1.27	1.14	0.14	1.39	3.28	5.11	0.02	0.02	0.14	98.75
26895	284470	8396343	37	Foliated (early) Pan-African granitoid (104)	Marrupa Complex	61.41	1.30	14.78	6.64	5.98	1.20	2.93	5.27	3.37	0.21	0.54	0.54	98.18
26892	291146	8381529	37	Coarse syenitic gneiss (603)	Marrupa Complex	56.43	1.01	12.25	6.96	6.26	2.24	8.78	4.31	4.19	0.25	1.57	0.31	98.30
26893	291146	8381529	37	Coarse syenitic gneiss (603)	Marrupa Complex	62.17	0.18	17.46	2.68	2.41	0.82	4.43	6.58	3.35	0.07	0.53	0.53	98.81
26867	313991	8395322	37	Felsic gneiss (612)	Marrupa Complex	78.54	0.06	11.40	1.45	1.31	<0.01	0.30	3.42	4.47	<0.01	0.03	0.20	99.87
26868	322724	8394901	37	Leucogneiss-granulite (612)	Marrupa Complex	73.85	0.25	12.72	3.26	2.93	0.54	2.88	3.84	0.94	0.08	0.06	0.31	98.73
26889	328871	8417793	37	Biotite leucogneiss/migmatite (614)	Marrupa Complex	69.05	0.63	14.84	3.37	3.03	0.64	1.91	3.89	4.23	0.04	0.18	0.20	98.98
26888	328871	8417793	37	Biotite leucogneiss/migmatite (614)	Marrupa Complex	72.02	0.18	13.99	1.34	1.21	0.21	1.15	3.21	5.75	0.02	0.04	0.30	98.20
26865	329536	8420085	37	Migmatitic Bt gneiss (602)	Marrupa Complex	69.80	0.68	13.28	4.42	3.98	1.84	2.78	3.50	2.09	0.06	0.11	0.40	98.97
26864	343847	8411289	37	Bt gneiss (612)	Marrupa Complex	75.06	0.09	13.31	0.87	0.78	0.09	0.77	4.29	4.06	0.13	0.03	0.18	98.87
33325	493489	8577448	37	Felsic orthogneiss	Nairobi Complex	69.19	0.43	14.56	3.37	3.03	1.75	3.39	3.62	2.31	0.06	0.10	0.38	99.17
36076	515172	8600890	37	Tonalitic gneiss	Nairobi Complex	60.38	0.69	16.05	7.38	6.64	2.79	6.43	3.71	1.22	0.14	0.16	0.25	99.20
40711	515824	8656296	37	Granitic gneiss	Nairobi Complex	70.13	0.42	14.46	2.96	2.66	0.82	3.21	3.57	3.30	0.05	0.10	0.19	99.20
40651	528365	8714714	37	Granitic gneiss	Nairobi Complex	70.78	0.50	14.23	2.60	2.34	0.76	1.93	3.52	4.42	0.04	0.11	0.39	99.28
40678	630566	8532440	37	Metagabbro	Nairobi Complex	43.53	1.91	12.56	10.76	9.68	5.03	20.98	0.98	0.06	0.18	0.20	1.40	97.59
40679	631031	8532582	37	Graphite-bearing biotite gneiss	Nairobi Complex	76.04	0.47	3.09	0.52	0.47	0.24	0.61	0.78	0.31	0.01	0.05	16.80	98.91
33350	484783	8570670	37	Granodioritic gneiss	Nairobi Complex	73.40	0.26	13.83	1.68	1.51	0.36	1.61	4.49	2.69	0.04	0.09	0.26	98.71
33229	593522	8543084	37	Granitic gneiss	Meluco Complex	71.60	0.28	14.11	2.25	2.03	0.33	1.09	3.98	4.33	0.04	0.06	0.32	98.39
33237	597369	8543762	37	Granitic gneiss/foliated granite	Meluco Complex	72.47	0.21	14.48	1.30	1.17	0.24	1.19	3.77	4.69	0.02	0.05	0.15	98.56
40760	611174	8600264	37	Granitic gneiss	Meluco Complex	66.89	0.56	15.75	2.89	2.60	0.59	2.02	4.00	5.75	0.06	0.14	0.24	98.90
40672	618589	8584524	37	Granodioritic gneiss	Meluco Complex	68.71	0.36	15.10	3.43	3.09	0.44	2.35	4.88	2.95	0.06	0.10	0.33	98.72
38431	426828	8595106	37	Granitic gneiss	Xixano Complex	77.74	0.18	11.09	2.01	1.81	0.23	0.08	2.08	5.67	0.01	0.02	0.56	99.67
38434	428500	8580668	37	Granodioritic gneiss	Xixano Complex	70.25	0.32	14.69	2.67	2.40	0.37	1.35	3.94	4.51	0.05	0.13	0.19	98.47
36091	430722	8614486	37	ACID META-VOLCANIC	Xixano Complex	66.22	0.36	14.24	7.22	6.50	0.08	0.18	4.62	3.56	0.03	0.05	0.79	97.35
36090	431804	8609430	37	QUARTZO-FELDSPATHIC GNEISS	Xixano Complex	77.31	0.14	12.51	1.69	1.52	0.21	1.05	3.63	1.84	0.01	0.01	0.72	99.12
36089	432908	8565660	37	MAFIC DYKE	Xixano Complex	46.96	0.66	14.12	10.14	9.13	14.19	10.24	1.29	0.09	0.16	0.03	0.82	98.71
36093	433001	8602358	37	?????????	Xixano Complex	61.73	2.50	11.85	4.35	3.92	2.05	1.54	0.89	11.51	0.04	1.20	0.52	98.19
36092	433080	8606504	37	QUARTZO-FELDSPATHIC GNEISS	Xixano Complex	73.59	0.02	15.45	0.30	0.27	0.05	1.16	4.02	3.92	<0.01	0.01	0.50	99.03
33387	434208	8549406	37	Psammite	Xixano Complex	67.48	0.54	15.03	3.49	3.14	0.35	0.08	1.08	3.68	0.03	0.04	7.45	99.27
36082	434745	8597938	37	BASIC-INTERMEDIATE PORPHYRY	Xixano Complex	51.09	0.70	14.29	10.57	9.51	7.09	10.27	1.88	0.86	0.17	0.12	1.51	98.56
33221	437435	8538564	37	Leucogranitic gneiss	Xixano Complex	71.54	0.08	15.87	0.89	0.80	0.10	1.83	6.07	1.26	0.03	0.03	0.53	98.23
36095	438015	8573770	37	ACID META-VOLCANIC	Xixano Complex	66.53	0.48	14.56	5.60	5.04	0.17	0.50	3.92	5.60	0.05	0.07	0.70	98.18
37207	439222	8639514	37	META-RHYOLITE	Xixano Complex	76.35	0.17	11.80	1.54	1.39	0.18	0.17	2.85	5.30	0.02	0.03	0.65	99.05
33219	440079	8545636	37	Quartz, coarse grained	Xixano Complex	98.44	0.377	0.25	0.346	0.31	<0.01	0.02	<0.1	0.069	<0.01	<0.01	0.31	99.78
40717	441794	8732349	37	Tonalitic gneiss	Xixano Complex	57.57	0.79	13.90	4.11	3.70	1.93	6.32	1.74	8.30	0.09	1.06	0.31	96.10
36098	442024	8572554	37	ACID META-VOLCANIC	Xixano Complex	56.16	0.95	20.03	12.26	11.03	0.23	0.08	1.94	2.71	0.02	0.06	4.16	98.61
40755	442660	8733158	37	Amphibolitic gneiss	Xixano Complex	49.77	1.00	16.80	10.21	9.19	4.99	9.48	3.20	2.02	0.18	0.44	0.62	98.70
36100	443405	8663222	37	GRANITIC GNEISS	Xixano Complex	72.51	0.19	13.86	1.53	1.38	0.24	1.06	3.30	5.22	0.03	0.06	0.31	98.30
33402	445921	8584552	37	Paragneiss	Xixano Complex	74.44	0.22	13.12	2.98	2.68	0.48	1.48	4.42	1.20	0.04	0.05	0.54	98.98
33388	450870	8497866	37	Meta-volcanic	Xixano Complex	72.55	0.29	13.73	2.93	2.64	0.90	4.01	4.20	0.13	0.08	0.07	0.20	99.10
33339	451029	8589856	37	Leucogranite	Xixano Complex	75.22	0.16	11.88	1.49	1.34	0.13	0.31	3.42	4.76	0.02	0.02	0.47	97.89
33227	455437	8511024	37	Granodioritic gneiss	Xixano Complex	69.70	0.37	15										

S	Cl	F	Mo	Nb	Zr	Y	Sr	Rb	U	Th	Pb	Cr	V	As	Sc	Hf	Ba	Sb	Sn	Ga	Zn	Cu	Ni	Yb	Co	Ce	La	Nd	W	Cs	Ta	Pr	
<0.1	<0.1	<0.1	<5	14	663	49	456	209	<10	69	30	10	51	<5	<10	13	2628	<10	10	16	75	21	8	<15	5	628	454	226	21	16	<10	79	
<0.1	<0.1	<0.1	<5	9	151	23	440	120	<10	8	22	11	37	<5	<10	<10	2276	<10	<10	<10	29	14	<5	<15	<5	58	33	25	30	12	<10	<10	
<0.1	<0.1	<0.1	<5	5	133	5	519	114	<10	11	13	17	32	<5	<10	<10	1659	<10	<10	12	36	12	<5	<15	5	71	59	19	30	<10	<10	<10	
<0.1	<0.1	<0.1	<5	10	151	14	244	96	<10	15	22	10	27	<5	<10	<10	766	<10	<10	10	62	13	<5	<15	9	73	40	20	23	<10	<10	12	
<0.1	<0.1	<0.1	<5	21	362	35	310	199	<10	53	22	14	<10	<5	<10	<10	29	1206	<10	<10	22	69	11	<5	<15	5	281	199	81	22	<10	<10	31
<0.1	<0.1	0.23	<5	21	138	27	605	16	<10	<5	<10	22	303	<5	24	<10	512	<10	<10	14	130	67	83	<15	77	76	26	50	<10	10	20	<10	
<0.1	<0.1	<0.1	<5	55	68	33	32	463	12	21	81	12	<10	<5	10	<10	90	<10	19	34	37	<10	10	<15	<5	<10	<10	37	<10	<10	<10		
<0.1	0.10	<0.1	<5	7	34	14	474	11	<10	<5	14	531	243	<5	51	11	192	<10	<10	<10	97	<10	84	<15	39	32	22	18	10	<10	10	<10	
<0.1	<0.1	<0.1	<5	9	181	21	163	153	<10	21	17	23	13	<5	10	<10	704	<10	10	16	45	12	<5	<15	8	82	33	16	25	<10	<10	<10	
<0.1	<0.1	0.11	<5	93	21	841	6	<10	<5	<10	100	95	<5	22	14	142	<10	<10	<10	35	<10	38	<15	20	54	30	21	23	<10	<10	<10		
<0.1	<0.1	<0.1	<5	125	6	390	106	<10	6	12	13	17	<5	<10	<10	1114	<10	<10	<10	33	<10	<5	<15	5	36	34	10	37	<10	<10	<10		
<0.1	<0.1	<0.1	6	5	21	12	49	<5	<10	8	<10	76	18	<5	<10	<10	143	16	<10	<10	35	<10	<5	<15	109	139	81	122	<10	12	45	55	
<0.1	<0.1	<0.1	<5	6	96	<5	118	194	<10	40	29	23	<10	<5	<10	<10	389	<10	<10	12	23	<10	<5	<15	<5	24	18	<10	36	<10	<10	<10	
<0.1	<0.1	<0.1	<5	33	141	78	3091	128	<10	15	26	11	76	<5	15	23	6672	<10	<10	13	109	10	14	<15	5	420	142	218	11	19	10	49	
<0.1	<0.1	<0.1	<5	7	157	28	132	154	<10	17	17	<10	<10	<5	10	<10	1062	<10	<10	16	26	13	<5	<15	6	74	51	29	33	<10	<10	<10	
<0.1	<0.1	0.18	<5	61	542	60	448	61	<10	6	<10	11	22	7	14	53	922	<10	<10	21	153	12	<5	<15	10	147	59	69	10	<10	19		
<0.1	<0.1	<0.1	<5	106	235	99	516	113	<10	18	15	31	55	<5	21	<10	552	<10	<10	22	163	<10	38	<15	13	219	140	145	13	<10	16	40	
<0.1	<0.1	<0.1	<5	10	311	23	847	69	<10	5	<10	10	24	7	<10	23	535	<10	<10	29	45	13	<5	<15	11	56	26	17	28	<10	<10	10	
<0.1	<0.1	<0.1	<5	36	269	32	21	235	<10	45	<10	20	<10	<5	<10	17	65	<10	<10	24	35	15	<5	<15	5	67	35	10	30	<10	<10	<10	
<0.1	<0.1	<0.1	<5	6	109	21	138	14	<10	8	<10	18	25	7	16	<10	305	<10	<10	10	40	11	<5	<15	10	15	13	<10	33	<10	<10	<10	
<0.1	<0.1	<0.1	<5	19	347	39	399	169	<10	43	25	10	25	<5	<10	22	1070	<10	<10	20	68	13	<5	<15	7	161	92	59	28	<10	<10	25	
<0.1	<0.1	<0.1	<5	7	110	7	304	203	<10	8	28	<10	14	<5	<10	<10	1181	<10	<10	18	36	12	<5	<15	6	19	14	<10	25	<10	<10	<10	
<0.1	<0.1	<0.1	<5	8	215	19	279	70	<10	16	<10	37	74	<5	15	<10	640	<10	<10	13	54	23	9	<15	12	93	50	33	28	<10	<10	13	
<0.1	<0.1	<0.1	<5	12	85	99	59	75	<10	10	21	<10	11	6	12	<10	401	<10	<10	17	79	17	<5	<15	9	<10	<10	39	<10	<10	<10		
<0.1	<0.1	<0.1	<5	7	154	31	330	59	<10	7	<10	54	57	6	16	<10	822	<10	<10	11	49	<10	17	<15	11	34	25	17	33	<10	<10	<10	
<0.1	<0.1	<0.1	<5	6	121	36	416	28	<10	<5	12	51	123	<5	27	<10	368	<10	<10	10	81	23	7	<15	17	29	13	12	31	<10	<10	<10	
<0.1	<0.1	<0.1	<5	8	147	21	335	87	<10	19	23	<10	31	<5	14	<10	978	<10	<10	10	42	15	<5	<15	7	63	36	17	25	<10	<10	12	
<0.1	<0.1	<0.1	<5	9	191	30	260	125	<10	15	19	23	38	<5	12	<10	1090	<10	<10	12	29	27	<5	<15	9	94	60	33	29	<10	<10	16	
0.65	<0.1	<0.1	<5	17	111	18	276	5	<10	8	11	66	240	<5	38	<10	49	<10	<10	16	95	110	26	<15	37	53	<10	14	<10	12	15		
0.10	<0.1	<0.1	29	9	163	69	74	11	15	12	10	116	686	<5	<10	<10	593	<10	<10	<10	48	59	5	<15	9	26	20	12	47	<10	<10	<10	
<0.1	<0.1	<0.1	<5	10	137	34	326	159	<10	8	17	29	21	<5	10	<10	1397	<10	<10	<10	55	<10	<5	<15	5	40	30	17	39	<10	<10	<10	
<0.1	<0.1	<0.1	<5	8	196	36	110	124	<10	12	12	12	19	<10	<10	852	<10	<10	13	47	<10	<5	<15	5	40	29	21	38	11	<10	<10		
<0.1	<0.1	0.18	<5	5	161	13	1156	97	11	23	50	15	10	<5	<10	<10	2890	<10	<10	14	54	10	<5	<15	5	107	66	25	31	<10	<10	<10	
<0.1	<0.1	<0.1	<5	19	369	38	344	119	<10	14	26	<10	16	5	13	32	2137	<10	<10	19	61	14	<5	<15	8	106	49	42	25	13	<10	<10	<10
<0.1	<0.1	<0.1	<5	17	206	35	184	67	<10	10	19	23	17	<5	13	<10	760	<10	<10	18	98	<10	<5	<15	10	47	33	29	28	<10	<10	11	
<0.1	<0.1	<0.1	<5	92	678	76	12	223	<10	21	10	16	<10	<5	<10	29	86	<10	11	22	56	<10	6	<15	<5	104	39	37	44	11	11	<10	
<0.1	<0.1	0.14	<5	26	273	14	291	146	<10	21	19	18	12	<5	<10	<10	1416	<10	<10	17	85	<10	<5	<15	<5	102	67	36	28	13	<10	<10	
<0.1	<0.1	<0.1	<5	94	1287	53	112	63	<10	13	<10	18	<5	<10	35	1842	<10	<10	23	64	17	<5	<15	12	148	80	80	20	<10	<10	14		
<0.1	<0.1	<0.1	<5	5	100	6	155	33</																									

Sample	UTM, E	UTM, N	Zone	Field name	Tectonic Unit	SiO ₂	TiO ₂	Al ₂ O ₃	Fe ₂ O ₃	FeO	MgO	CaO	Na ₂ O	K ₂ O	MnO	P ₂ O ₅	Gt _{tp}	SUM
38442	468044	8605158	37	Silisified metagabbro	Xixano Complex	41.46	1.24	16.00	12.48	11.23	5.07	16.57	1.19	0.17	0.16	0.11	3.71	98.15
40752	468780	8732418	37	Quartz-feldspar gneiss	Xixano Complex	77.35	0.12	11.66	1.48	1.33	0.02	0.49	2.81	5.22	0.02	0.02	0.24	99.43
38411	472925	8731708	37	Diorite	Xixano Complex	57.78	0.72	16.15	7.97	7.17	4.28	7.30	2.76	1.13	0.14	0.18	0.45	98.84
33338	473318	8606276	37	Intermediate metavolcanite?	Xixano Complex	51.67	0.64	17.37	10.66	9.59	5.43	9.66	3.08	0.28	0.19	0.11	0.02	99.09
33417	475693	8574100	37	Tonalite	Xixano Complex	72.65	0.12	14.86	0.87	0.78	0.20	1.46	4.26	3.64	0.02	0.03	0.16	98.28
33420	476043	8528294	37	Granitic gneiss	Xixano Complex	73.78	0.27	11.59	3.51	3.16	0.06	0.20	4.13	4.70	0.06	0.03	0.03	98.38
33215	478212	8542704	37	Tonalite, mus/bio	Xixano Complex	73.33	0.11	15.06	0.32	0.29	0.15	0.99	3.54	4.61	0.02	0.03	0.47	98.65
33216	478217	8543012	37	Graphite schist/gneiss	Xixano Complex	70.73	0.258	5.29	0.547	0.49	0.21	0.04	<0.1	1.516	0.018	0.015	20.65	99.35
33337	479899	8607586	37	Ferruginous quartzite	Xixano Complex	42.53	0.16	16.68	13.60	12.24	1.64	9.83	0.10	0.05	12.56	0.34	-0.28	97.20
33336	480501	8608718	37	Metasediment	Xixano Complex	54.87	0.52	11.73	5.10	4.59	5.73	15.32	2.92	1.73	0.18	0.11	0.91	99.12
33414	495263	8476986	37	Amphibolite	Xixano Complex	47.36	0.24	15.55	7.67	6.90	10.20	16.27	0.68	0.06	0.15	<0.01	0.38	98.58
33429	496853	8525208	37	Metadiabas	Xixano Complex	44.65	0.74	16.35	11.20	10.08	4.29	19.86	0.57	0.31	0.21	0.20	1.04	99.43
33430	498017	8524454	37	Granitic orthogneiss	Xixano Complex	73.92	0.13	13.71	1.33	1.20	0.18	1.21	3.41	4.66	0.02	0.04	0.22	98.82
33431	502408	8520338	37	Orthopyroxene-bearing metagabbro	Xixano Complex	50.37	1.06	9.58	8.24	7.42	10.57	15.53	1.90	0.38	0.16	0.16	0.56	98.51
40652	503236	8734434	37	Amphibolite	Xixano Complex	47.84	1.06	14.29	13.04	11.74	8.06	11.87	1.31	0.18	0.20	0.09	0.54	98.47
40748	508748	8752896	37	Amphibolitic gneiss	Xixano Complex	43.19	0.70	18.73	14.45	13.01	6.17	13.21	1.32	0.52	0.21	0.02	0.59	99.11
40747	510296	8752896	37	Marble	Xixano Complex	2.23	0.01	0.00	0.07	0.06	19.00	33.34	<0.1	0.015	0.005	0.06		
40663	513384	8741392	37	Granitic gneiss	Xixano Complex	68.79	0.41	14.95	2.65	2.39	0.42	1.68	3.41	5.29	0.03	0.11	0.90	98.65
40662	514560	8747978	37	Marble	Xixano Complex	14.26	0.00	0.00	0.07	0.06	11.81	37.57	<0.1	0.013	0.013	0.15		
40746	517936	8753162	37	Granite	Xixano Complex	73.03	0.15	14.18	1.33	1.20	0.22	1.12	3.59	4.88	0.02	0.06	0.68	99.28
40664	520875	8729630	37	Tonalitic gneiss	Xixano Complex	48.11	0.71	22.79	5.20	4.68	2.86	13.73	2.91	0.49	0.14	0.10	1.33	98.37
40653	523577	8751122	37	Marble	Xixano Complex	7.58	0.01	0.00	0.07	0.06	8.22	44.32	<0.1	0.038	0.020	0.17		
40745	523662	8754440	37	Amphibolitic gneiss	Xixano Complex	41.29	1.43	19.72	11.24	10.12	3.74	20.74	0.28	0.28	0.18	0.19	0.29	99.38
33259	435294	8518053	37	amphibolite	Xixano Complex	39.78	1.19	16.61	16.02	14.42	7.85	13.64	1.74	0.38	0.22	0.10	1.07	98.59
33258	435426	8518300	37	amphibolite	Xixano Complex	48.38	0.64	14.87	12.39	11.15	8.86	13.34	0.92	0.04	0.19	0.05	-0.02	99.65
33275	443652	8539964	37	granulite	Xixano Complex	72.08	0.29	11.89	6.07	5.46	0.82	3.43	3.06	0.38	0.12	0.05	0.20	98.40
33274	443739	8539932	37	Grt granulite	Xixano Complex	70.47	0.56	12.62	6.12	5.51	1.15	1.96	4.34	0.77	0.16	0.02	0.49	98.66
33276	444146	8543073	37	Graphite gneiss	Xixano Complex	71.46	0.66	10.82	3.07	2.76	0.40	0.16	0.56	2.21	<0.01	0.04	9.34	98.72
33348	461810	8512658	37	Granite	Xixano Complex	71.70	0.21	14.30	1.55	1.40	0.21	1.12	3.99	4.61	0.06	0.05	0.30	98.10
33347	467131	8520606	37	Felsic metavolcanite	Xixano Complex	74.57	0.16	11.78	2.53	2.28	0.07	0.38	4.23	3.64	0.01	0.02	0.34	97.72
33355	471365	8512334	37	Amphibolite	Xixano Complex	48.45	2.53	12.13	15.78	14.20	5.86	10.54	2.09	0.15	0.25	0.20	0.69	98.66
33273	473075	8542389	37	Quartzofeldspathic gneiss	Xixano Complex	75.18	0.13	11.43	1.27	1.14	0.05	0.04	0.36	9.59	<0.01	0.03	0.46	98.55
31952	215070	8602610	37	Granitic gneiss with quartz rich bands	Muaquia Complex	87.92	0.02	5.71	0.61	0.55	0.01	0.01	2.23	1.84	0.02	0.01	0.34	98.73
31999	227601	8572845	37	Biotite-paragneiss	Muaquia Complex	74.49	0.29	13.30	1.32	1.19	0.47	0.23	3.85	4.30	0.01	0.04	0.78	99.08
32000	227814	8575975	37	Kyanite-quartzite	Muaquia Complex	59.90	0.56	35.87	1.74	1.57	0.14	0.04	<0.1	0.19	<0.01	0.16	0.62	99.22
31980	228310	8572518	37	Kyanite-muscovite-garnet-quartzite	Muaquia Complex	71.38	1.84	24.79	0.38	0.34	0.11	0.02	<0.1	0.02	0.01	0.10	0.23	98.92
31836	243905	8627086	37	Biotite gneiss	Muaquia Complex	70.30	0.32	15.47	2.38	2.14	0.76	2.43	4.43	2.87	0.06	0.11	0.48	99.61
34283	260955	8518266	37	Granitic gneiss	Muaquia Complex	71.21	0.55	13.35	3.55	3.20	0.62	0.51	4.88	3.72	0.01	0.10	0.24	98.75
34276	268760	8515792	37	Granitic gneiss	Muaquia Complex	75.52	0.24	12.25	1.77	1.59	0.38	0.14	4.39	3.37	<0.01	0.05	0.35	98.46
34278	279870	8518225	37	Granitic gneiss	Muaquia Complex	72.50	0.20	14.34	1.49	1.34	0.21	0.99	4.44	3.89	0.03	0.03	0.36	98.47
36056	289779	8549678	37	Pyroxenite	Muaquia Complex	48.00	0.66	8.83	10.05	9.05	14.03	14.72	1.09	0.28	0.18	0.04	0.59	98.47
36059	290009	8552672	37	Enderbite?	Muaquia Complex	44.93	0.09	24.23	4.98	4.48	8.26	15.77	0.94	0.14	0.08	0.01	0.56	99.99
37262	303868	8567982	37	Amphibolite	Muaquia Complex	66.62	0.59	14.36	4.58	4.12	1.97	2.16	4.19	1.73	0.04	0.15	2.36	98.75
38412	314057	8545036	37	Granite	Muaquia Complex	78.26	0.15	11.96	1.39	1.25	0.11	1.52	5.88	0.11	0.02	0.02	0.16	99.58
33255	332105	8564327	37	amphibolite	Muaquia Complex	49.72	0.89	18.87	7.99	7.19	4.84	12.17	3.31	0.33	0.11	0.03	0.59	98.85
33256	332105	8564327	37	amphibolite	Muaquia Complex	55.81	0.41	16.09	4.04	3.64	5.07	12.44	4.40	0.21	0.11	0.03	0.26	98.87
33257	325810	8578127	37	granitic-gneiss	Muaquia Complex	66.39	0.47	16.48	2.87	2.58	0.79	2.47	4.68	3.53	0.06	0.12	0.34	98.19
31796	241388	8606286	37	mafic granulitic gneiss	M'Sawize Complex	53.48	0.90	17.79	9.17	8.25	4.18	8.12	4.09	1.16	0.19	0.17	0.02	99.26
37246	246484	8545976	37	Metagabbro	M'Sawize Complex	63.52	0.77	12.64	5.22	4.70	3.75	7.34	4.38	0.43	0.06	0.07	0.31	98.49
31978	248255	8588574	37	Tonalite	M'Sawize Complex	59.46	0.39	16.67	3.34	3.01	3.47	8.89	6.34	0.42	0.05	0.01	0.13	99.16
37245	249453	8548646	37	Metagabbro	M'Sawize Complex	56.94	0.72	11.09	16.03	14.43	4.50	7.52	2.02	0.32	0.21	0.15	-0.25	99.26
37244	249779	8549028	37	Microgabbro	M'Sawize Complex	49.46	0.59	16.60	10.06	9.05	7.60	12.13	1.88	0.39	0.16	0.07	0.51	99.46
37243	249874	8549332	37	Metagabbro	M'Sawize Complex	45.04	1.05	13.36	15.76	14.18	8.22	10.54	2.42	0.75	0.17	0.11	0.63	98.03
36073	527463	8599738	37	Intermediate dyke?	Lalamo Complex	48.52	0.33	18.02	7.79	7.01	9.54	11.63	2.25	0.15	0.13	0.01	0.02	98.41
38430	551032	8568752	37	Tonalitic gneiss	Lalamo Complex	67.24	0.46	16.64	3.02	2.72	1.47	3.49	4.56	2.08	0.05	0.13	0.32	99.47
40787	553182	8685354	37	Arenitic paragneiss	Lalamo Complex	75.73	0.20	11.77	1.99	1.79	0.03	0.62	2.97	4.99	0.03	0.01	0.23	98.56
40790	555366	8692462																

S	Cl	F	Mo	Nb	Zr	Y	Sr	Rb	U	Th	Pb	Cr	V	As	Sc	Hf	Ba	Sb	Sn	Ga	Zn	Cu	Ni	Yb	Co	Ce	La	Nd	W	Cs	Ta	Pr
4.10	<0.1	<0.1	<5	7	86	22	240	<5	<10	<5	13	123	204	<5	35	<10	129	<10	12	17	125	36	39	<15	50	<10	10	<10	13	<10	16	<10
<0.1	<0.1	<0.1	<5	<5	180	10	56	57	<10	13	10	<10	6	<10	<10	1304	<10	<10	<10	32	11	<5	<15	6	60	28	19	28	<10	<10	12	
<0.1	<0.1	<0.1	<5	6	103	26	276	34	<10	5	<10	54	153	<5	28	<10	386	<10	<10	10	82	14	11	<15	21	50	16	21	28	<10	<10	<10
<0.1	<0.1	<0.1	<5	5	71	20	269	<5	<10	<5	<10	56	213	<5	38	<10	101	<10	10	14	84	23	8	<15	34	<10	<10	25	<10	12	10	
<0.1	<0.1	<0.1	<5	<5	72	10	878	91	<10	<5	26	20	<10	<5	<10	<10	1327	<10	<10	14	42	<10	<5	<15	18	23	<10	39	<10	<10	<10	
<0.1	<0.1	<0.1	<5	26	734	95	10	135	<10	18	16	17	<10	<5	<10	14	136	<10	<10	19	115	<10	5	<15	5	143	98	69	31	<10	<10	16
<0.1	<0.1	<0.1	<5	6	54	12	394	96	<10	7	40	11	<10	<5	<10	<10	2050	<10	<10	15	59	<10	<5	<15	17	13	<10	38	<10	<10	<10	
<0.1	<0.1	<0.1	15	<5	94	36	10	42	<10	7	<10	601	1138	<5	15	<10	637	<10	<10	10	18	21	8	<15	6	<10	17	<10	49	<10	<10	<10
<0.1	<0.1	1.08	<5	5	133	46	11	5	<10	5	<10	214	253	<5	16	<10	70	<10	<10	24	106	<10	8	19	15	17	<10	<10	25	20		
<0.1	<0.1	<0.1	<5	16	264	57	162	53	<10	13	15	55	56	<5	20	<10	442	<10	<10	13	64	11	24	<15	8	64	36	36	25	<10	<10	11
<0.1	<0.1	0.15	<5	<5	17	6	362	<5	<10	<5	<10	374	141	6	62	<10	101	<10	<10	10	51	<10	63	<15	33	<10	<10	28	<10	<10	<10	
<0.1	<0.1	0.4	39	<5	48	16	203	5	<10	<5	<10	290	230	5	42	<10	479	<10	<10	16	73	28	106	<15	47	21	<10	14	<10	<10	12	<10
<0.1	<0.1	<0.1	<5	7	142	25	158	145	<10	20	27	11	13	<5	<10	<10	1315	<10	<10	11	35	<10	<5	<15	<5	52	38	22	33	<10	<10	<10
<0.1	<0.1	0.26	<5	8	84	34	382	<5	<10	<5	<10	438	227	<5	68	<10	172	<10	<10	10	74	<10	100	<15	35	47	109	73	17	<10	11	23
0.10	0.16	<0.1	<5	5	58	26	117	6	<10	5	<10	332	294	<5	50	<10	54	<10	<10	97	52	61	<15	59	<10	<10	<10	<10	<10	<10	<10	
<0.1	<0.1	<0.1	<5	21	6	379	5	<10	<5	<10	45	613	<5	48	<10	137	<10	<10	16	82	124	<5	<15	54	<10	<10	<10	<10	<10	<10	13	14
<0.1	<0.1	<0.1	<5	<5	17	<5	75	<5	<10	<5	<10	<10	<10	<5	32	<10	39	<10	<10	25	<10	<5	<15	<5	<10	<10	<10	<10	<10	<10	<10	
<0.1	<0.1	<0.1	<5	18	313	27	161	168	<10	31	22	20	16	<5	<10	15	939	<10	<10	17	60	12	<5	<15	9	146	98	60	22	<10	<10	17
0.43	<0.1	<0.1	<5	<5	23	9	62	6	<10	6	2262	12	<10	<5	35	<10	35	22	<10	<10	7252	<10	<5	<15	<5	<10	<10	<10	<10	<10	<10	
<0.1	<0.1	<0.1	<5	7	176	<5	195	177	<10	66	35	20	10	<5	<10	<10	943	<10	<10	10	34	14	<5	<15	6	128	91	31	28	<10	<10	12
<0.1	<0.1	<0.1	<5	5	119	25	484	6	<10	8	20	234	113	<5	30	<10	174	<10	<10	18	104	14	65	<15	27	<10	<10	11	19	<10	<10	<10
<0.1	<0.1	<0.1	<5	19	5	51	5	<10	5	<10	<10	<10	<5	39	<10	40	<10	<10	<10	39	<10	<5	<15	<5	<10	<10	<10	<10	<10	<10	<10	
<0.1	<0.1	<0.1	<5	6	178	44	1973	5	<10	5	<10	245	186	<5	41	<10	52	<10	<10	21	30	12	19	<15	21	49	20	31	<10	<10	12	17
<0.1	0.40	0.64	<5	5	33	25	514	<5	<10	<5	12	108	425	7	50	<10	148	13	<10	13	96	<10	217	<15	83	<10	16	<10	<10	11	<10	
<0.1	<0.1	0.21	<5	<5	40	18	123	<5	<10	<5	<10	169	278	<5	41	<10	35	<10	<10	67	<10	66	<15	50	<10	<10	13	11	<10	<10	<10	
<0.1	<0.1	<0.1	<5	<5	220	90	146	<5	<10	7	<10	<10	<10	<5	18	<10	176	<10	<10	15	95	<10	<5	<15	7	36	16	26	36	<10	<10	<10
<0.1	<0.1	<0.1	<5	9	211	39	115	<5	<10	<5	<10	19	<10	<5	12	<10	357	<10	<10	17	100	10	<5	<15	10	<10	<10	32	<10	<10	<10	
<0.1	<0.1	<0.1	43	17	171	11	92	88	<10	5	<10	206	1738	6	<10	<10	1888	<10	<10	71	36	18	<15	8	<10	14	<10	39	<10	<10	<10	
<0.1	0.1	0.1	5	26	168	69	122	253	13	31	30	14	13	<5	<10	<10	580	<10	<10	13	64	<10	<5	<15	5	98	86	51	39	<10	<10	18
<0.1	<0.1	<0.1	<5	34	351	186	29	44	<10	15	<10	19	<10	<5	<10	<10	1149	<10	<10	23	20	<10	9	<15	5	191	113	107	45	<10	<10	24
<0.1	<0.1	0.45	<5	6	146	54	188	<5	<10	<5	<10	52	441	<5	54	11	111	<10	<10	12	115	13	24	<15	58	18	17	25	<10	<10	16	<10
<0.1	<0.1	0.18	<5	34	276	61	22	210	<10	18	22	11	<10	64	<10	<10	1017	<10	<10	12	8	<10	5	<15	<5	34	34	14	30	<10	<10	<10
<0.1	<0.1	<0.1	<5	17	474	5	<5	71	<10	10	<10	13	<10	<5	<10	<10	<10	<10	<10	38	<10	<5	<15	<5	<10	<10	22	<10	<10	<10		
<0.1	<0.1	<0.1	<5	14	148	17	79	104	<10	20	<10	27	13	<5	11	<10	919	<10	<10	10	16	10	7	<15	6	<10	11	10	31	<10	<10	<10
<0.1	<0.1	<0.1	<5	10	214	5	35	<5	<10	6	<10	54	24	<5	<10	<10	64	<10	<10	27	<5	10	<5	<15	9	14	17	11	29	<10	<10	<10
<0.1	<0.1	<0.1	<5	21	684	10	32	<5	<10	7	<10	73	47	<13	<10	18	107	<10	<10	10	5	10	<5	<15	6	11	<10	<10	29	<10	<10	<10
<0.1	<0.1	<0.1	<5	6	113	9	578	75	<10	13	13	17	46	<5	16	<10	1092	<10	<10	15	50	34	<5	<15	10	45	31	17	27	<10	<10	<10
<0.1	<0.1	0.1	8	13	361	65	44	81	<10	12	<10	25	17	<5	11	<10	695	<10	<10	19	<10	5	<15	7	82	50	40	36	<10	<10	<10	
<0.1	<0.1	<0.1	<5</																													

Sample	UTM, E	UTM, N	Zone	Field name	Tectonic Unit	SiO ₂	TiO ₂	Al ₂ O ₃	Fe ₂ O ₃	FeO	MgO	CaO	Na ₂ O	K ₂ O	MnO	P ₂ O ₅	Gt _{lap}	SUM
40669	574059	8654400	37	Quartz	Lalamo Complex	99.48	0.00	0.01	0.00	0.00 <0.01	0.03	<0.1	<0.01	<0.01	<0.01	0.05	99.47	
33239	577317	8548844	37	Amphibolite	Lalamo Complex	46.80	0.81	14.15	10.22	9.20	7.89	16.21	1.27	0.45	0.40	0.07	0.29	98.55
33238	580578	8551342	37	Quartz	Lalamo Complex	99.51	<0.01	<0.01	0.024	0.02 <0.01	0.01	<0.1	<0.01	<0.01	<0.01	0.04	99.56	
33330	585257	8559576	37	Dyke	Lalamo Complex	71.95	0.27	14.92	1.44	1.30	0.34	1.30	3.78	4.61	0.03	0.06	0.47	99.17
33329	585257	8559576	37	Mica gneiss	Lalamo Complex	73.00	0.17	13.75	1.38	1.24	0.42	1.95	3.27	3.80	0.02	0.05	0.22	98.04
40720	589143	8661328	37	Ultramafic rock	Lalamo Complex	36.15	0.04	1.82	13.41	12.07	33.78	0.04	<0.1	0.01	0.10	0.02	12.30	97.58
40721	591998	8635413	37	Amphibolite	Lalamo Complex	49.93	0.66	16.65	10.21	9.19	6.29	10.42	3.41	0.32	0.25	0.10	0.46	98.70
33327	593749	8542508	37	Tonalitic gneiss?	Lalamo Complex	66.30	0.39	16.83	2.62	2.36	1.36	4.10	4.59	1.71	0.05	0.14	0.32	98.42
38415	601327	8623420	37	Biotite gneiss	Lalamo Complex	64.30	0.72	15.76	4.97	4.47	1.43	3.39	4.35	3.25	0.09	0.21	0.51	98.99
38414	603959	8623394	37	Granite	Lalamo Complex	67.22	0.87	14.80	3.24	2.92	0.79	1.57	3.47	5.35	0.03	0.22	0.42	97.97
40758	606223	8611490	37	Granitic gneiss	Lalamo Complex	67.25	0.83	14.95	3.86	3.47	0.83	2.09	3.80	4.44	0.04	0.23	0.64	98.96
33230	608377	8561868	37	Graphite gneiss	Lalamo Complex	65.34	0.209	2.18	0.826	0.74	0.48	0.03	<0.1	0.363	0.011	0.010	26.73	96.23
33231	608377	8561868	37	Graphite gneiss	Lalamo Complex	66.06	0.151	2.35	0.168	0.15	0.11	0.59	0.34	0.099	<0.01	0.064	26.01	95.94
37247	615084	8620978	37	Mafic gneiss	Lalamo Complex	52.74	0.45	9.18	8.65	7.79	9.81	15.36	1.64	0.32	0.44	0.10	0.37	99.05
40730	630695	8548839	37	Ultramafic rock	Lalamo Complex	45.09	0.03	0.59	10.24	9.22	30.11	0.04	<0.1	0.01	0.09	0.02	11.98	98.19
40759	631213	8545948	37	Talc schist	Lalamo Complex	57.92	0.04	1.31	4.97	4.47	28.69	0.05	<0.1	0.01	0.06	0.03	4.87	97.89
40763	633555	8533112	37	Chlorite gneiss	Lalamo Complex	41.73	0.08	11.11	9.98	8.98	24.97	4.45	0.33	0.05	0.17	0.02	5.41	98.28
40762	634551	8535488	37	Amphibolitic gneiss	Lalamo Complex	50.22	1.34	14.04	12.31	11.08	5.89	10.83	2.71	0.86	0.17	0.11	0.39	98.87
40675	634769	8547124	37	Granitic gneiss	Lalamo Complex	74.13	0.13	14.66	1.11	1.00	0.14	1.28	4.57	3.85	0.03	0.04	0.24	100.18
40674	637239	8549076	37	Granodiorite	Lalamo Complex	76.42	0.19	12.61	1.20	1.08	0.25	1.34	3.68	3.65	0.02	0.03	0.24	99.62
40673	637239	8549076	37	Quartz diorite	Lalamo Complex	65.87	0.52	16.11	3.62	3.26	1.85	5.15	4.22	1.25	0.06	0.09	0.46	99.21
33212	496595	8539366	37	Quartz, coarse grained	Montepuez Complex	99.67	0.035	0.18	0.165	0.15	<0.01	<0.01	<0.1	0.077	<0.01	<0.01	0.06	100.18
33243	502181	8552008	37	Granodioritic gneiss	Montepuez Complex	75.46	0.32	12.62	1.82	1.64	0.34	1.37	4.34	2.20	0.06	0.05	0.32	98.90
33222	504094	8512728	37	Granitic gneiss	Montepuez Complex	73.29	0.18	12.43	1.54	1.39	0.15	0.65	3.14	4.74	0.03	0.03	0.35	96.53
33223	512542	8514412	37	Banded hbl-gneiss	Montepuez Complex	59.24	0.40	14.24	4.89	4.40	2.70	11.52	2.73	1.65	0.16	0.09	0.43	98.04
33224	513150	8513668	37	Quartz-feldspathic gneiss.	Montepuez Complex	96.75	0.043	1.22	0.272	0.24	0.06	0.03	<0.1	0.495	<0.01	<0.01	0.39	99.30
38428	514523	8551754	37	Amphibolite	Montepuez Complex	51.63	0.64	11.84	7.80	7.02	6.84	14.23	2.49	0.34	0.17	0.12	2.62	98.72
33335	520952	8555494	37	Paragneiss. Metaarkose(?)	Montepuez Complex	75.82	0.11	12.28	1.00	0.90	0.12	0.51	2.64	5.14	0.02	0.02	0.42	98.07
33236	524518	8501782	37	Quartz-dioritic gneiss	Montepuez Complex	60.15	0.59	14.10	4.50	4.05	3.81	8.65	1.87	4.57	0.08	0.16	0.39	98.87
33332	565441	8552836	37	Granitic/tonalitic gneiss	Montepuez Complex	74.17	0.18	13.24	1.46	1.31	0.21	1.14	3.41	4.28	0.03	0.04	0.25	98.40
33299	594457	8528665	37	granitic gneiss	Montepuez Complex	73.62	0.20	14.08	1.71	1.54	0.49	2.30	3.76	2.56	0.03	0.05	0.21	99.02
40774	610336	8529262	37	Graphite gneiss	Montepuez Complex	69.58	1.07	8.57	2.48	2.23	0.05	1.46	1.88	0.66	<0.01	0.16	13.32	99.23
40769	613700	8520540	37	Tonalitic gneiss	Montepuez Complex	66.68	0.42	16.40	4.49	4.04	1.23	5.03	4.01	0.38	0.14	0.14	0.14	99.05
40680	617024	8528262	37	Minerais rara	Montepuez Complex	30.66	0.60	17.80	5.95	5.36	2.22	12.44	<0.1	0.04	<0.01	0.01	2.25	71.50
9155																		
40764	619423	8527248	37	Marble	Montepuez Complex	1.77	0.03	0.14	0.21	0.19	0.81	53.91	<0.1	0.040	0.005	0.01		
40729	637611	8526796	37	Metagabbro	Montepuez Complex	48.54	0.83	17.64	6.96	6.26	7.94	13.03	2.19	0.15	0.14	0.32	1.28	99.01
40782	645465	8516668	37	Graphite gneiss	Montepuez Complex	75.07	0.59	5.81	0.98	0.88	0.04	0.22	0.89	3.09	<0.01	0.08	11.49	98.26
33575	798906	8214662	36	Amphibolite/metagabbro	Ocua Complex	52.46	2.27	16.81	8.14	7.33	3.41	6.27	4.44	3.46	0.11	0.87	0.13	98.38
33583	799366	8206097	36	2px granulites +/- garnet	Ocua Complex	50.72	1.89	14.05	15.08	13.57	1.73	6.69	2.62	5.09	0.22	0.58	0.02	98.69
33587	799366	8206097	36	Felsic/intermediate granulites/charnockites	Ocua Complex	59.45	0.64	13.22	7.90	7.11	1.46	6.06	3.12	6.44	0.15	0.20	0.54	99.19
33584	800010	8213567	36	2px granulites +/- garnet	Ocua Complex	62.92	0.64	15.11	6.40	5.76	1.86	5.75	3.66	1.05	0.13	0.16	0.51	98.18
33588	804705	8222661	36	Felsic/intermediate granulites/charnockites	Ocua Complex	60.49	1.87	15.43	3.09	2.78	1.05	5.55	4.96	5.26	0.08	0.29	0.75	98.82
33585	809285	8226662	36	2px granulites +/- garnet	Ocua Complex	45.45	0.79	15.00	17.56	15.80	8.39	9.37	1.47	0.34	0.25	0.05	-0.36	98.32
26811	370941	8387034	37	Granitic gneiss (105)	Ocua Complex	65.40	0.68	14.76	5.89	5.30	0.55	2.11	3.91	4.47	0.12	0.17	0.08	98.14
26810	486474	8437474	37	Felsic granulite - mylonitic (401)	Ocua Complex	71.60	0.44	13.30	2.94	2.65	0.35	1.99	3.24	4.09	0.05	0.10	0.19	98.30
33340	545000	8490408	37	Granodioritic orthogneiss	Ocua Complex	66.86	0.24	16.36	3.21	2.89	0.83	5.71	3.90	0.53	0.08	0.10	0.18	98.01
33314	584918	8504618	37	Grt amphibolite	Ocua Complex	56.87	1.12	16.41	7.28	6.55	3.69	6.03	3.74	2.72	0.11	0.28	0.18	98.43
33245	585277	8506126	37	Amphibolite	Ocua Complex	49.19	2.04	14.78	13.57	12.21	3.62	9.75	2.68	0.32	0.23	0.33	-0.10	99.11
33247	585277	8506126	37	Amphibolite	Ocua Complex	54.48	1.43	14.65	10.05	9.05	4.79	8.65	3.24	0.70	0.18	0.20	0.41	98.80
33248	585277	8506126	37	Silisified amphibolite	Ocua Complex	61.56	0.98	13.24	9.65	8.69	4.04	4.75	3.47	0.50	0.23	0.12	0.13	98.67
33298	596463	8510768	37	Gt gneiss	Ocua Complex	71.31	0.36	13.30	5.08	4.57	0.91	4.18	3.44	0.36	0.10	0.07	0.07	99.17
33307	608008	8506110	37	Grt amphibolite	Ocua Complex	55.73	1.32	16.64	8.21	7.39	3.51	6.70	3.67	1.72	0.11	0.45	0.51	98.56
33304	608375	8511931	37	diorite gneiss	Ocua Complex	57.74	0.67	14.24	4.28	3.85	2.86	5.28	2.35	8.46	0.07	0.80	0.16	96.91
33399	608426	8509552	37	Quartz paragneiss	Ocua Complex	65.15	0.60	16.46	4.82	4.34	1.60	4.64	3.84	1.33	0.07	0.16	0.12	98.78
33305	608605	8508344	37	Grt amphibolite	Ocua Complex	58.96	1.40	17.02	10.05	9.05	3.75	3.12	2.72	1.95	0.13	0.24	-0.27	99.08
33311	608733	8506279	37	Grt amphibol														

S	Cl	F	Mo	Nb	Zr	Y	Sr	Rb	U	Th	Pb	Cr	V	As	Sc	Hf	Ba	Sb	Sn	Ga	Zn	Cs	Ni	Yb	Co	Ce	La	Nd	W	Cs	Ta	Pr				
<0.1	<0.1	0.1	<5	<5	18	<5	<5	<5	<10	8	<10	11	<10	<10	28	<10	<10	<10	11	11	<5	<15	8	<10	<10	<10	44	<10	<10	<10						
<0.1	<0.1	0.31	<5	<5	50	20	180	7	<10	<5	<10	610	220	<5	40	<10	108	<10	<10	13	72	10	226	<15	47	<10	<10	<10	<10	<10	<10					
<0.1	<0.1	<0.1	<5	<5	20	<5	<5	<10	5	<10	<10	<5	<10	<10	<10	<10	<10	<10	<10	<10	11	<10	<5	<15	<5	<10	<10	44	<10	<10	<10					
<0.1	<0.1	<0.1	<5	<5	161	<5	386	88	<10	15	19	10	18	<5	<10	<10	1865	<10	<10	13	41	<10	<5	<15	<5	51	39	15	35	<10	<10	<10				
<0.1	<0.1	<0.1	<5	<5	94	<5	285	67	<10	7	<10	10	22	<5	<10	<10	1827	<10	<10	<10	26	<10	<5	<15	<5	33	18	10	34	<10	<10	<10				
<0.1	<0.1	<0.1	<5	<5	17	<5	7	<5	<10	5	<10	5520	72	5	<10	<10	43	<10	<10	49	124	6109	<15	173	<10	<10	<10	<10	<10	<10	<10					
<0.1	<0.1	<0.1	<5	<5	46	16	265	5	<10	7	<10	188	234	<5	37	<10	74	<10	<10	11	101	<10	10	<15	43	17	12	<10	13	<10	<10	12				
<0.1	<0.1	<0.1	<5	<5	103	8	566	41	<10	<5	<10	30	42	<5	<10	<10	707	<10	<10	<10	40	14	7	<15	8	28	24	11	32	<10	<10	<10				
<0.1	<0.1	0.1	<5	9	309	44	200	94	<10	7	<10	15	48	<5	20	<10	783	<10	<10	11	61	<10	5	<15	12	50	33	25	31	<10	<10	<10				
<0.1	<0.1	0.23	<5	7	541	14	800	97	<10	15	23	13	39	<5	<10	23	3892	<10	<10	15	80	<10	<5	<15	<5	237	161	78	23	18	<10	24				
<0.1	<0.1	<0.1	<5	15	612	48	316	90	<10	16	15	<10	43	<5	10	70	1703	<10	<10	<10	90	19	<5	<15	6	169	92	64	23	10	<10	15				
0.10	<0.1	<0.1	57	<5	79	54	17	17	<10	6	<10	720	5119	<5	20	<10	406	<10	<10	<10	348	21	68	<15	7	<10	12	<10	53	<10	<10	<10				
<0.1	<0.1	<0.1	6	7	53	68	49	<5	<10	<5	<10	173	812	<5	14	<10	75	<10	<10	<10	536	34	104	<15	8	39	54	30	53	<10	<10	<10				
<0.1	<0.1	<0.1	<5	5	209	69	156	<5	<10	<5	<10	35	54	<5	25	<10	89	<10	<10	<10	146	<10	14	<15	23	45	22	41	20	<10	<10	<10				
<0.1	<0.1	<0.1	<5	<5	18	<5	<5	<5	<10	6	<10	4661	35	<5	<10	<10	32	<10	<10	<10	46	14	3262	<15	113	<10	<10	<10	<10	<10	<10	<10				
<0.1	<0.1	<0.1	<5	<5	18	<5	6	<5	<10	6	<10	2968	31	5	<10	<10	77	<10	<10	<10	52	18	1739	<15	61	<10	<10	<10	<10	<10	<10	<10				
<0.1	<0.1	<0.1	<5	<5	20	8	28	<5	<10	7	<10	783	33	5	16	<10	51	<10	<10	<10	83	18	1019	<15	90	<10	<10	<10	<10	<10	<10	<10				
<0.1	<0.1	<0.1	<5	<5	83	26	215	10	<10	<5	<10	236	287	5	46	<10	94	<10	<10	<10	894	<10	<10	14	46	<10	<5	<15	8	33	12	<10	31	<10	<10	<10
<0.1	<0.1	<0.1	<5	8	114	7	209	94	<10	10	27	12	<10	<5	<10	<10	894	<10	<10	<10	26	11	<5	<15	8	38	28	12	36	<10	<10	<10				
<0.1	<0.1	<0.1	<5	6	112	6	170	87	<10	11	21	<10	13	<5	<10	<10	1140	<10	<10	<10	212	<10	118	35	130	22	23	44	<5	98370	25182	27376	<10	52	50	
<0.1	<0.1	<0.1	8	<5	22	<5	872	<5	<10	<5	12	<10	<10	<5	36	<10	98	<10	<10	<10	16	<10	<5	<15	<5	<10	<10	<10	<10	<10	<10	<10	<10	<10		
<0.1	<0.1	<0.1	<5	<5	29	18	464	<5	<10	<5	<10	321	115	<5	46	<10	123	<10	<10	<10	53	94	123	<15	29	<10	<10	<10	<10	<10	<10	<10	<10	<10	<10	
0.50	<0.1	<0.1	51	13	169	27	174	54	17	18	17	90	176	8	13	<10	1635	<10	<10	<10	20	99	27	<15	10	25	34	18	40	<10	<10	<10	<10	<10		
<0.1	<0.1	0.21	<5	26	425	28	1437	82	<10	<5	23	45	138	<5	16	43	1665	11	<10	19	110	29	8	<15	21	134	65	67	<10	15	13	18				
<0.1	<0.1	<0.1	<5	30	200	56	393	94	<10	<5	<10	24	<10	<5	19	<10	2079	10	<10	21	237	11	18	<15	26	134	46	82	<10	<10	23	12				
<0.1	<0.1	<0.1	<5	21	893	21	399	196	<10	12	20	12	<10	<5	<10	72	1062	<10	<10	17	150	15	<5	<15	11	92	29	35	<10	<10	16	12				
<0.1	<0.1	<0.1	<5	6	27	18	542	<5	<10	5	13	19	83	<5	22	<10	503	<10	<10	<10	57	29	<5	<15	16	42	26	<10	15	<10	11	11				
<0.1	<0.1	<0.1	<5	72	102	49	1510	93	<10	5	14	<10	41	<5	10	<10	2025	<10	<10	<10	67	13	<5	<15	8	138	65	71	<10	<10	<10	21				
<0.1	<0.1	<0.1	<5	5	30	18	110	<5	<10	<5	<10	48	474	<5	60	<10	53	<10	<10	<10	120	22	11	<15	76	25	<10	10	<10	23	<10					
<0.1	<0.1	<0.1	<5	85	565	87	135	115	<10	16	14	<10	26	<5	15	66	856	<10	<10	<10	20	107	11	<5	9	143	92	64	22	<10	<10	17				
<0.1	<0.1	<0.1	5	7	247	26	374	94	<10	6	12	<10	27	<5	11	<10	2237	<10	<10	<10	14	50	22	<5	<15	9	69	35	25	30	<10	<10	<10			
<0.1	<0.1	<0.1	<5	40	6	944	<5	<10	<5	<10	27	<5	14	<10	218	<10	<10	<10	43	<10	<5	<15	5	12	<10	10	33	<10	<10	<10						
<0.1	<0.1	0.18	5	7	214	25	782	49	<10	<5	12	80	133	<5	19	19	905	<10	<10	<10	79	26	22	<15	22	56	23	19	19	<10	<10	<10				
0.15	<0.1	0.31	<5	16	107	46	184	<5	<10	<5	<10	118	280	<5	46	<10	76	<10	<10	<10	93	38	36	<15	50	24	<10	28	18	<10	21	16				
0.36	<0.1	0.31	<5	7	84	37	335	<5	<10	<5	<10	165	237	<5	36	<10	309	<10	<10	<10	13	112	85	51	<15	36	33	<10	20	21	<10	<10	<10			
0.19	<0.1	0.13	<5	8	152	43	239	<5	<10	6	<10	185	170	<5	29	<10	247	<10	<10	<10	81	66	34	<15	29	22	15	19	25	<10	<10	<10				
<0.1	<0.1	<0.1	<5	100	34	152	<5	<10	<5	<10	42	51	<5	21	<10	145	<10	<10	<10	44	<10	<5	<15	10	<10	13	12	35	<10	<10	<10					
<0.1	<0.1	0.22																																		

Sample	UTM, E	UTM, N	Zone	Field name	Tectonic Unit	75.34	0.26	12.45	1.02	0.92	0.17	0.81	3.22	4.84	0.02	0.04	0.30	98.48
						SiO ₂	TiO ₂	Al ₂ O ₃	Fe ₂ O ₃	FeOt	MgO	CaO	Na ₂ O	K ₂ O	MnO	P ₂ O ₅	Gt,lap	SUM
33359	552667	8491220	37	Granitic gneiss	Ocua Complex	75.34	0.26	12.45	1.02	0.92	0.17	0.81	3.22	4.84	0.02	0.04	0.30	98.48
33358	568407	8490192	37	Dioritic gneiss	Ocua Complex	56.88	0.87	14.73	5.05	4.55	2.34	5.88	2.55	7.83	0.09	0.80	0.23	97.24
33370	606452	8515446	37	Amphibolitic gneiss	Ocua Complex	47.59	1.22	16.24	11.15	10.04	8.24	10.99	2.44	0.49	0.18	0.13	0.26	98.93
31824	686270	8619140	36	Tremolite-rock	Ponta Messuli C.	55.10	0.04	1.30	13.23	11.91	24.49	0.86	<0.1	0.03	0.28	0.02	2.41	97.73
38427	686905	8633817	36	Amphibolite	Ponta Messuli C.	49.25	1.30	11.56	12.72	11.45	9.09	14.15	0.71	0.31	0.22	0.11	0.72	100.16
36068	717251	8710574	36	Metadiorite, porphyric	Ponta Messuli C.	62.77	0.82	16.38	5.57	5.01	2.95	4.26	2.57	2.12	0.08	0.08	0.71	98.31
31779	691660	8657448	36	quartz syenite	Txitonga Group	64.80	0.86	14.95	4.66	4.19	1.34	2.16	2.29	5.87	0.05	0.42	0.97	98.36
31902	719100	8679307	36	Quartz-muscovite-feldspar schist (sandstone)	Txitonga Group	51.43	0.84	23.71	8.62	7.76	2.16	0.04	0.21	6.26	0.09	0.08	4.14	97.58
38413	724557	8679988	36	Banded Iron Formation	Txitonga Group	71.24	<0.01	0.20	25.68	23.11	0.07	0.29	0.11	0.01	0.06	0.07	0.44	98.19
31900	724567	8701402	36	Quartz-muscovite schist	Txitonga Group	53.37	1.21	22.19	10.50	9.45	0.87	0.01	<0.1	5.97	0.12	0.04	5.07	99.40
31901	727675	8702265	36	Arkosic metasandstone	Txitonga Group	70.73	0.80	12.54	3.97	3.57	1.10	1.24	2.84	3.11	0.09	0.17	2.01	98.60
31815	730031	8708594	36	banded iron formation	Txitonga Group	17.79	2.34	19.04	49.23	44.31	0.73	0.20	<0.1	3.04	0.10	0.07	4.52	97.03
31899	731363	8717206	36	Sillimanite-muscovite schist	Txitonga Group	45.00	1.06	28.89	13.13	11.82	0.36	0.02	<0.1	2.53	0.03	0.03	7.96	99.05
31818	732056	8705434	36	syenite	Txitonga Group	75.87	0.18	12.39	1.52	1.37	0.25	1.21	1.95	5.07	0.03	0.03	1.54	100.03
31819	732766	8705176	36	amphibolite	Txitonga Group	53.41	3.01	12.17	15.90	14.31	3.59	9.13	1.17	0.17	0.30	0.33	0.21	99.38
31858	739344	8713876	36	Epidote-chlorite schist	Txitonga Group	56.51	1.05	20.17	10.38	9.34	2.01	0.09	0.78	3.63	0.12	0.06	3.83	98.65
31856	739549	8714130	36	Undeformed microgabbro	Txitonga Group	47.32	2.90	13.85	15.19	13.67	5.77	9.43	1.86	0.26	0.24	0.34	1.22	98.38
31855	739549	8714130	36	Deformed and altered microgabbro	Txitonga Group	47.02	1.57	16.67	18.10	16.29	8.28	1.15	0.90	0.41	0.17	0.14	5.05	99.45
31857	739683	8714016	36	Mylonitic, altered microgabbro	Txitonga Group	50.45	1.11	22.22	13.15	11.84	3.20	0.17	0.89	3.81	0.13	0.06	4.10	99.28
31325	710235	8517380	36	alkali granite	Niassa Suite	63.82	0.46	18.00	2.57	2.31	0.57	1.87	4.92	5.62	0.04	0.14	0.39	98.39
31323	710492	8519070	36	alkali syenite	Niassa Suite	65.63	0.50	17.42	2.12	1.91	0.40	0.72	5.07	6.72	0.04	0.07	0.37	99.06
31324	710585	8518325	36	alkali granite	Niassa Suite	71.11	0.34	14.42	2.04	1.84	0.40	1.24	3.74	5.15	0.04	0.10	0.32	98.90
31246	746558	8502248	36	Massive coarse-granitic syenite	Niassa Suite	62.46	0.98	16.76	4.06	3.65	0.86	1.75	4.54	6.66	0.11	0.28	0.21	98.66
31257	752010	8483378	36	Microgranite dyke	Niassa Suite	69.32	0.42	13.80	2.63	2.37	0.33	0.67	3.45	5.73	0.03	0.11	0.83	97.33
31258	753045	8494484	36	Biotite-quartz-syenite	Niassa Suite	60.86	0.98	17.28	4.00	3.60	1.03	1.80	4.48	6.92	0.09	0.29	0.37	98.10
31218	757796	8475807	36	Quartz syenite/granite	Niassa Suite	77.54	0.13	11.58	0.95	0.86	0.08	0.69	3.00	4.51	0.01	0.02	0.34	98.85
31219	761314	8474877	36	Quartz syenite/granite,	Niassa Suite	65.22	0.45	17.66	1.70	1.53	0.29	0.79	4.75	7.72	0.03	0.05	0.29	98.96
31225	763225	8462871	36	Granite, fine to medium grained	Niassa Suite	70.92	0.47	13.55	2.23	2.01	0.43	0.86	3.85	5.08	0.07	0.10	0.56	98.10
31226	765611	8469264	36	Syenite?, red, fine to medium grained.	Niassa Suite	73.86	0.19	12.39	2.83	2.55	0.08	0.50	2.39	5.77	0.07	0.02	0.14	98.23
31260	768529	8482664	36	Granite	Niassa Suite	61.78	0.66	17.94	4.12	3.71	0.83	2.73	4.78	5.06	0.09	0.29	0.34	98.61
33504	769452	8447609	36	Granite	Niassa Suite	71.16	0.32	13.45	2.97	2.67	0.31	1.09	3.17	5.44	0.08	0.14	0.29	98.41
33505	771238	8434430	36	Biotite granite	Niassa Suite	63.73	0.79	16.51	3.52	3.17	0.72	1.72	4.03	6.47	0.12	0.18	0.26	98.05
33496	771524	8429229	36	Syenite / monzonite	Niassa Suite	65.82	0.64	15.93	3.06	2.75	0.51	0.51	4.18	6.97	0.07	0.14	0.29	98.11
33497	251353	8355546	37	Biotitic granite	Malema suite	64.15	1.10	14.87	5.88	5.29	1.15	2.91	3.05	4.32	0.05	0.34	0.30	98.13
33501	251609	8369522	37	Monzonitic-dioritic rocks	Malema suite	58.84	1.18	16.02	7.59	6.83	0.99	2.86	4.78	4.94	0.18	0.37	0.12	97.87
33500	251609	8369522	37	Late granite	Malema suite	66.82	0.46	15.50	3.67	3.30	0.37	1.47	4.46	5.63	0.08	0.11	0.06	98.62
33511	257967	8349173	37	Biotite-granite	Malema suite	63.00	0.73	14.97	6.58	5.92	0.53	2.36	3.41	6.17	0.10	0.15	0.06	98.08
33495	262752	8450224	37	Dolerite	Malema suite	52.22	0.84	14.34	11.27	10.14	6.66	10.16	1.99	0.82	0.18	0.10	0.95	99.54
33509	277501	8359213	37	Charnockite	Malema suite	58.30	1.05	18.07	6.17	5.55	0.71	3.98	4.14	5.13	0.12	0.35	0.04	98.04
26841	312041	8376426	37	Coarse-grained syenite (101)	Malema suite	61.62	0.72	18.87	3.34	3.01	0.44	2.30	6.65	4.35	0.12	0.22	0.07	98.70
26852	409312	8404279	37	Banded gneiss (211)	Malema suite	52.44	2.79	14.35	11.46	10.31	3.62	6.00	3.59	3.02	0.15	1.18	0.16	98.74
26815	417903	8405591	37	Gneissic qtz-diorite (205)	Malema suite	54.69	2.10	15.70	9.06	8.15	3.06	6.22	3.60	2.70	0.11	0.74	0.26	98.24
26805	445674	8426659	37	Granitic gneiss (105)	Malema suite	65.91	0.78	15.15	4.28	3.85	0.95	2.35	3.69	4.84	0.02	0.20	0.21	98.39
26885	315669	8349314	37	Charnockite (106)	Malema suite	62.18	0.92	16.69	4.24	3.82	0.76	1.91	5.98	4.82	0.12	0.36	0.14	98.09
26886	320871	8367730	37	Pink Pan African granite/syenite (102)	Malema suite	68.32	0.44	13.48	4.82	4.34	0.27	1.47	2.96	6.07	0.06	0.07	0.23	98.19
26861	374602	8395926	37	granite gneiss / Bt gneiss (105)	Malema suite	62.59	0.60	16.15	4.49	4.04	1.94	5.27	4.48	1.88	0.05	0.20	0.91	98.56
26859	387949	8404885	37	Granite gneiss (105)	Malema suite	64.00	0.84	14.59	6.57	5.91	0.65	2.37	3.37	5.24	0.10	0.23	0.10	98.06
31997	733103	8625759	36	Nef syenite	Neoprot intr.	51.29	0.81	20.20	5.87	5.28	0.42	3.53	7.52	4.99	0.26	0.13	3.15	98.18
31940	754484	8630700	36	Granitic rock with weak fabric	Neoprot intr.	76.98	0.03	12.18	1.12	1.01	0.03	0.15	4.70	3.84	<0.01	0.03	0.35	99.41
31941	754550	8632004	36	Metadioritic rock	Neoprot intr.	54.55	2.14	14.70	10.71	9.64	2.68	5.79	3.58	2.37	0.19	0.62	1.07	98.40
37237	275920	8680606	37	Granite	Neoprot intr.	71.05	0.34	14.57	2.43	2.19	0.34	1.00	4.50	4.56	0.08	0.12	0.25	99.23
31837	282755	8660808	37	Monzonitic rock	Neoprot intr.	58.12	0.09	19.17	5.63	5.07	<0.01	0.74	8.25	4.34	0.37	0.14	1.41	98.24
37231	287536	8664690	37	Monzonite	Neoprot intr.	60.52	0.15	18.76	5.30	4.77	0.01	0.96	7.32	5.21	0.24	0.05	0.50	99.02
37230	349074	8668162	37	Hornblende granodiorite	Neoprot intr.	59.18	1.14	14.74	4.57	4.11	1.83	5.05	3.51	5.38	0.07	0.98	0.74	97.18
37266	363075	8																

S	Ci	F	Mo	Nb	Zr	Y	Sr	Rb	U	Th	Pb	Cr	V	As	Sc	Hf	Ba	Sb	Sn	Ga	Zn	Cu	Ni	Yb	Co	Ce	La	Nd	W	Cs	Ta	Pr	
<0.1	<0.1	<0.1	<0.1	<5	5	129	7	94	73	<10	11	<10	12	<10	<5	<10	<10	887	<10	<10	<10	23	<10	<5	<15	<5	47	35	21	38	<10	<10	<10
<0.1	<0.1	0.42	<5	<5	94	32	3385	217	<10	<5	16	20	81	<5	15	35	6182	<10	<10	<10	69	14	16	<15	8	99	45	49	11	25	11	<10	
<0.1	<0.1	0.28	<5	5	75	27	307	<5	<10	<5	<10	147	242	<5	41	11	150	<10	<10	11	85	38	76	<15	53	<10	11	<10	17	10	<10	<10	
<0.1	<0.1	0.29	<5	5	12	5	13	<5	<10	11	<10	3048	66	<5	31	<10	78	<10	<10	<10	148	<10	450	<15	92	<10	22	<10	13	<10	<10	<10	
<0.1	<0.1	<0.1	<5	5	82	17	132	6	<10	<5	<10	843	187	<5	35	<10	156	<10	<10	<10	102	<10	305	16	66	<10	<10	<10	<10	<10	<10	<10	
<0.1	<0.1	0.11	<5	11	199	15	422	118	<10	37	20	84	90	<5	25	<10	735	<10	<10	10	70	31	51	<15	18	126	72	53	31	<10	<10	18	
<0.1	<0.1	0.13	<5	21	485	20	300	193	<10	82	50	23	68	<5	10	14	1804	<10	<10	17	67	72	11	<15	10	229	104	95	15	14	<10	22	
<0.1	<0.1	0.38	<5	12	156	31	70	455	<10	23	20	208	151	<5	21	<10	735	<10	<10	27	158	27	86	<15	28	77	49	37	34	<10	<10	11	
<0.1	<0.1	<0.1	<5	<5	22	5	7	<5	<10	9	435	23	39	<5	<10	12	149	11	<10	<10	289	317	5	<15	52	<10	<10	12	<10	18	<10		
<0.1	<0.1	0.52	<5	18	180	20	34	250	<10	25	26	259	176	<5	24	<10	703	<10	12	30	57	23	70	<15	21	70	16	24	<10	<10	<10		
<0.1	<0.1	0.13	<5	16	195	253	180	103	<10	21	15	52	74	<5	16	10	803	<10	<10	11	55	18	27	17	14	75	116	64	34	<10	<10	18	
<0.1	<0.1	0.41	<5	12	275	5	158	113	<10	17	<10	1261	1030	<5	47	31	373	<10	<10	101	271	<10	478	<15	240	143	35	<10	<10	54	<10		
<0.1	<0.1	0.12	<5	19	152	14	16	126	<10	24	25	330	210	<5	34	13	232	<10	13	31	94	168	99	<15	28	28	31	30	12	<10	<10	<10	
<0.1	<0.1	<0.1	<5	23	185	62	78	144	<10	32	12	26	10	<5	12	<10	557	<10	<10	11	38	<10	<5	<15	6	97	66	44	32	<10	<10	10	
<0.1	<0.1	0.41	<5	15	201	39	292	13	<10	7	23	16	422	<5	44	10	48	<10	<10	16	150	11	31	<15	60	87	33	45	<10	<10	16	<10	
<0.1	<0.1	<0.1	<5	11	209	30	169	92	<10	26	16	230	147	<5	29	<10	1369	<10	<10	26	106	<10	98	<15	34	72	182	94	22	<10	<10	30	
<0.1	<0.1	0.28	<5	15	216	38	252	<5	<10	8	<10	135	375	<5	34	<10	45	<10	<10	15	120	51	61	<15	59	41	16	32	<10	<10	10		
<0.1	<0.1	0.15	<5	11	79	13	94	12	<10	<5	<10	306	383	<5	31	<10	127	<10	<10	25	100	<10	98	<15	89	<10	16	17	<10	<10	<10		
<0.1	<0.1	<0.1	<5	12	189	12	159	96	<10	24	13	256	190	<5	21	<10	1387	<10	<10	33	109	14	116	<15	47	96	69	50	12	<10	<10	10	
<0.1	<0.1	<0.1	<5	16	444	29	1019	139	<10	17	40	<10	22	<5	11	14	4115	<10	<10	22	54	15	<5	<15	5	286	221	121	11	11	<10	35	
<0.1	<0.1	0.11	<5	27	677	82	263	119	<10	26	36	12	15	<5	12	11	2104	<10	<10	19	61	13	<5	<15	<5	468	289	210	18	<10	<10	51	
<0.1	<0.1	<0.1	<5	22	199	10	468	245	<10	44	43	21	20	<5	11	<10	1660	<10	<10	22	38	13	<5	<15	7	121	84	30	22	<10	<10	16	
<0.1	<0.1	<0.1	<5	28	1421	48	28	95	<10	14	29	15	11	<5	12	26	344	<10	<10	18	87	<10	<5	<15	<5	404	222	166	<10	<10	44		
<0.1	<0.1	0.11	6	64	589	82	87	226	<10	40	39	14	<10	<5	11	<10	1028	<10	<10	25	65	12	<5	<15	5	344	231	165	19	10	<10	41	
<0.1	<0.1	<0.1	<5	23	1122	37	105	111	<10	12	22	<10	13	<5	13	27	1171	<10	<10	17	76	14	<5	<15	6	169	97	90	<10	<10	19		
<0.1	<0.1	<0.1	<5	5	104	5	217	71	<10	10	14	17	15	<5	10	<10	1006	<10	<10	10	23	12	<5	<15	<5	36	33	18	26	<10	<10	10	
<0.1	<0.1	<0.1	<5	34	430	297	57	123	<10	12	28	11	<10	<5	10	<10	279	<10	<10	19	53	<10	12	<15	<5	306	255	311	34	<10	<10	61	
<0.1	<0.1	0.18	16	49	399	77	223	209	<10	24	34	19	14	<5	11	12	1074	<10	<10	16	92	12	<5	<15	<5	295	200	142	17	<10	<10	36	
<0.1	<0.1	<0.1	<5	10	349	23	27	103	<10	14	16	21	<10	<5	10	<10	672	<10	<10	16	52	11	<5	<15	6	57	34	26	22	<10	<10	10	
<0.1	<0.1	<0.1	18	29	633	41	854	108	<10	7	23	<10	22	<5	11	19	3817	<10	<10	21	98	13	<5	<15	7	136	78	60	<10	16	<10	<10	
<0.1	<0.1	0.12	<5	54	276	92	137	187	<10	19	26	13	14	<5	<10	<10	627	<10	<10	19	100	<10	6	<15	<5	223	126	105	35	<10	<10	32	
<0.1	<0.1	0.16	<5	54	911	78	194	150	<10	12	29	13	10	<5	12	23	2958	<10	<10	24	150	<10	5	<15	<5	412	215	169	24	15	<10	40	
<0.1	<0.1	<0.1	<5	46	845	62	23	126	<10	22	20	13	<10	<5	13	23	183	<10	10	19	85	<10	7	<15	<5	769	391	280	30	<10	<10	75	
<0.1	<0.1	0.32	<5	47	857	69	307	199	<10	41	15	15	46	<5	<10	24	1279	<10	<10	19	89	21	7	<15	11	424	219	159	24	<10	<10	48	
<0.1	<0.1	0.15	<5	64	544	59	463	95	<10	<5	14	<10	13	<5	15	20	2589	<10	<10	20	129	<10	5	<15	7	194	74	86	22	<10	12	24	
<0.1	<0.1	0.12	8	47	456	47	195	126	<10	21	14	15	<10	<5	<10	<10	942	<10	<10	19	65	<10	5	<15	5	177	105	70	31	<10	<10	18	
<0.1	0.15	0.22	<5	66	1044	95	176	130	<10	<5	17	29	10	<5	16	36	1226	<10	<10	23	110	<10	6	<15	7	185	66	118	21	<10	<10	18	
<0.1	<0.1	<0.1	<5	7	105	30	154	26	<10	7	<10	100	228	5	38	<10	487	<10	<10	10	76	107	63	<15	45	31	20	18	18	<10	<10	13	
<0.1	<0.1	0.26	<5	24																													